APPLICATIONS OF SCINTILLATION COUNTERS TO FAST NEUTRON SPECTROSCOPY.

by

D.J.SILVERLEAF

DEPARTMENT OF NATURAL PHILOSOPHY,

UNIVERSITY OF GLASGOW.

PRESENTED AS A THESIS FOR THE DEGREE OF DOCTOR OF PHILOSOPHY IN THE UNIVERSITY OF GLASGOW.

DECEMBER 1957.

ProQuest LLC.
789 East Eisenhower Parkway
P.O. Box 1346
Ann Arbor, MI 48106 – 1346

APPLICATIONS OF SCINTILLATION COUNTERS TO FAST NEUTRON SPECTROSCOPY.

Contents.

PREFACE.

This thesis contains an account of work performed during the period October 1950 to July 1954 on the development and application of scintillation counters to measurements of neutrons in the range of energy 1 to 20 Mev.

The first part of the thesis consists mainly of a review of the experiments in which useful information may be obtained from measurements of neutrons in the approximate energy range 1 to 20 Mev. Discussions of these experiments lead to an evaluation of the properties of an ideal fast neutron spectrometer suitable for obtaining new information. Finally, the possible approaches to the problem of measuring the energies of fast neutrons are discussed. References to material drawn from the literature for this part are cited throughout.

In Part II some of the properties of organic scintillators and the related apparatus are discussed briefly. Preliminary experiments which were conducted in order to improve the performance of the scintillators when used to detect fast neutrons are described. The results are given of later experiments in which new information was acquired about the response of organic scintillators to protons and electrons. The work described in this Part of the thesis was my own apart from general collaboration in the later experiments with Mr.J. Shields.

In Part III various attempts to use single scintillation counters as neutron spectrometers are described. The analysis of the expected performance of both the Single Scattering Spectrometer and the Edge Effect Spectrometer was carried out by me, as was the analysis of the results. The early experimental work on the Single Scattering Spectrometer was performed by me but the results quoted were obtained later in collaboration with Mr. J. Shields. The leading idea of the Edge Effect Spectrometer is due to Mr. R. Giles; I performed the preliminary experiments with it and assisted Mr. J. Shields in taking later measurements.

In Part IV some possible approaches to the use of two scintillation counters simultaneously for the measurement of neutron energies are discussed. The experimental work on the Double Scattering Pulse Height Spectrometer was performed in collaboration with Mr. J. Shields; the idea, the analysis and the discussion of the results of this were my own. The basic idea of the Time-of-Flight Spectrometer, which has proved to be the most successful of the scintillation counter arrangements for measuring neutron energies, is my own; the final design of this spectrometer and the testing of it were also carried out alone; Mr. J. Shields assisted me in taking the final measurements.

In Part V the conclusions reached throughout the thesis are summarised and the relative merits of the various spectrometers assessed with particular reference as to what extent they may prove suitable for experiments which had previously been outwith the scope of existing techniques.

Appendix A consists of a critical review of the previous techniques used to perform the experiments discussed in Part I.

In Appendix B the 50 kv H.T. Set used to supply a source of D-D and D-T neutrons for test purposes is described. This Set was constructed by me at the beginning of the research programme from a temporary arrangement used by Dr. J.G. Rutherglen for testing ion sources. In this work I was advised by Mr. R.Giles.

In Appendix C some of the electronic equipment which I built and tested for use with the scintillation counters is described. Mr. R. Giles designed the units for use in pulse height work whilst the fast coincidence units were my own adaptations of published circuits.

Acknowledgements.

I have pleasure in thanking Professor P. I. Dee not only for his interest in the work but also for his insistence, from my earliest undergraduate days, on logical thought and expression

which has been largely responsible for my appreciation of physics.

My thanks are due also to Mr. R. Giles for his advice during the first year of this research and to Mr. J. Shields who assisted me in taking many of the measurements during the remainder of the time.

I take this opportunity to thank my friends in the Department for many fruitful discussions and I am grateful for the help (and instruction) of the technical staffs under Mr. J.T. Lloyd and Mr. T. Pollok and of the workshop staff.

During the course of this research I received financial assistance from the D.S.I.R. and the Faculty of Science.

D.J.S.

I. THE FIELD OF STUDY.

1. INTRODUCTION.

This part of the thesis consists essentially of a review of the experiments in which useful information may be obtained from measurements of fast neutrons in the approximate range of energies 1 to 20 Mev. Such experiments fall into two main groups.

Fast neutrons arise as products of artificial nuclear reactions. They may be produced in the bombardment of nuclei by charged particles or by γ-rays. (Fast neutrons which occur as the result of fission of very heavy nuclei are beyond the scope of the present work.) Measurements of the neutrons emitted in these reactions make up the first group of experiments which is condidered. The second group of experiments which is considered is that in which fast neutrons interact with matter. The scattered neutrons are frequently in the same energy range and measurements of these neutrons are of great theoretical significance.

In both the cases in which neutrons are the emitted and the incident particles, the possible experiments and the extent to which they have been performed are discussed. (The techniques which have been used to obtain these results are mentioned but description of these techniques is confined to Appendix A.) The theoretical significance of the results is given for each type of experiment and conclusions are drawn as to what further experiments are required and as to the extent to which the obtaining of such information has previously been precluded by the lack of suitable techniques. References are given to typical work in each type of experiment; references are also given to relevant review articles, which are extremely limited in number, where further references to the work may be found.

Conclusions common to the various types of experiment are then summarised and the properties of a fast neutron spectrometer

capable of obtaining all the required information are deduced. A brief discussion of possible approaches to the problem of measuring the energies of fast neutrons concludes this part of the thesis.

2. NEUTRONS AS EMITTED PARTICLES.

(i). The neutrons emitted in the bombardment of light nuclei by charged particles.

(a). General.

The general purpose of measurements of the neutrons emitted in the bombardment of light nuclei is to establish the positions and other properties of the excited states of the nuclei concerned. Such information is required for checking theoretical models of nuclei and finding relationships in the level structures of related nuclei. In the particular case of deuteron-induced reactions, knowledge may be gained of the stripping process which in turn may lead to a better understanding of the nature of the force between neutrons and protons.

(b). Methods and Results.

The observations which may usefully be made in such reactions are as follows:

(A). The total yield of neutrons as a function of the energy of the incident radiation.

(B). The distribution in energy of the emitted neutrons when the energy of the incident radiation is kept constant.

(C). The angular distribution of neutrons of a given energy relative to a fixed direction.

(D). The correlation of the energies of the neutrons with the energies of γ-rays or charged particles emitted simultaneously. (Decay schemes)

(E). The angular correlation of the neutrons and their associated γ-rays or charged particles.

The above list is in order of logical consideration; it is

also in order of increasing experimental difficulty. Consequently progress has been uneven, ranging from virtually complete knowledge for type (A) to no data of significance for type (E). Exhaustive references to all work in this field prior to 1951 may be found in the review article by HORNYAK et al (1951). References to subsequent work which is typical of recent developments are cited below.

(A). The measurement of excitation functions requires simple detection devices which are insensitive to, or can discriminate against, γ -rays and which need not be able to distinguish between neutrons of different energies. B and BF_3 counters and the radioactive foil technique have been extensively used for such measurements and are adequate for the task.

In general, the excitation curves are found not to be constant functions of the incident energy and, in some cases, resonances in the yield are observed at certain bombarding energies.

(B). Straightforward measurements of the energies of the emitted neutrons have also been extensively made. Early measurements were made mainly with cloud chambers (See LIVINGSTON and BETHE 1937). The most accurate results have been obtained with photographic plates. A complete bibliography of all experiments up till 1953 on the determination of neutron spectra using photographic plates has been given by ROSEN (1953). Ionization chambers (HOLT, 1954) and proportional counters (WORTH, 1950; GILES, 1953) have also been used. The most significant ommissions in such data are in the measurement of neutron groups of low intensity: this has been due to the low detection efficiencies of the available spectrometers.

(C). Some studies have been made of angular distributions, mainly with photographic plates, but much useful information has still to be obtained.

(D) and (E). Until now it has been impossible to examine either decay schemes or angular correlations between neutrons and γ-rays since the available techniques have suffered not only from the disadvantage of a low detection efficiency but also from a slow (or even infinitely long) resolving time.

(c). Interpretation and Conclusions.

Compound nucleus theory.

The well-known hypothesis of the compound nucleus (BOHR, 1936) has served to explain much of the information obtained from measurements of the type (A) to (E) above. The compound nucleus theory leads to particularly simple interpretations of such information.

(A). The total yield of neutrons is related to the formation of excited states of the compound nucleus consisting of the target nucleus + bombarding particle. For high excitation energies where the compound nucleus has closely spaced levels the yield is related to the level density; for low excitation energies the yield is related to the probability of forming individual levels of the compound nucleus: resonances in the yield are observed when the sum of the kinetic energy of the incident particle and its binding energy in the compound nucleus is equal to the excitation energy levels of the compound nucleus. Conversely, the observation of resonances and their widths leads to the establishment of the positions and partial widths of the levels of the compound nucleus.

(B). The energies of the emitted neutrons are related to the formation of the residual nucleus in its ground state or one of its excited states. Measurement of the energies of the neutrons thus leads to the establishment of the positions of the levels of the residual nucleus. The intensity of each neutron group leads to a knowledge of the partial width of each level of the residual nucleus.

(C). The angular distribution of the neutrons is determined by the quantum numbers of angular momentum and parity associated with the levels of the nuclei involved. In general, knowledge of the angular distribution leads to possible sets of values for these quantum numbers; absolute values may be determined by combination with measurements of the type (D) to (E).

(D) and (E). The possible modes of decay of the excited states of the residual nucleus and the angular correlation of the neutrons with their associated radiations are also determined by the quantum numbers of angular momentum, spin and parity of the nuclear levels which are involved. Conversely, a knowledge of the decay scheme and of the angular correlations may be interpreted in terms of these quantum numbers.

From the measurements on neutrons (outlined above) that have been made, and with a knowledge of similar measurements on other radiations emitted in the bombardment of light nuclei, it has been possible to build up an extensive knowledge of the positions of most of the bound levels in light nuclei. The other properties of relatively few of these levels are known. It follows from this discussion that the knowledge of angular distributions must be extended and that decay schemes and angular correlations must be examined. Such measurements have been beyond the scope of the available techniques but are attainable using techniques developed in the course of the present work. With the knowledge obtained it may be hoped to gain a complete picture of the positions and other properties of all the bound levels of light nuclei.

Deuteron-induced reactions - stripping.

Bombardment of light nuclei by deuterons is a particular case of the reactions discussed above. Precisely the same observations may be made and, for many reactions, the interpretation of these observations is the same. However, results have been obtained

which are not explicable on the assumption that the deuteron as an entity forms a compound nucleus with the target nucleus. The possibility that the interaction of the deuteron with the target nucleus can take other forms follows from its low binding energy, unsymmetrical charge distribution and finite size.

It is possible for the deuteron to be disintegrated by the Coulomb field of the target nucleus. (OPPENHEIMER, 1935). This process is not of interest in the present context since the cross-section for its occurrence is only comparable with those for the other possible processes for deuterons of energy greater than 10 Mev and for nuclei of high Z. The other possible processes are the formation of a compound nucleus by the absorption of one or other constituent of the deuteron whilst its partner misses the target nucleus altogether. This is known as the stripping process (OPPENHEIMER, 1935a). This process leads to different energies and angular distributions and correlations of the outgoing neutrons from those to be expected on the basis of normal compound nucleus theory.

At high deuteron energies, where the effect of the Coulomb repulsion between the nucleus and the deuteron may be neglected the theory of deuteron-stripping developed by SERBER (1947) gives an explanation of the anomalous angular distributions and high energies of the neutrons found by ROBERTS (1947) in the bombardment of nuclei by deuterons of 15 Mev.

At low deuteron energies normal compound nucleus formation would be expected to predominate; stripping, if it takes place at all, would be expected to favour neutron absorption and repulsion of the proton by the Coulomb field. However, angular distributions of neutrons obtained using deuterons of the order of 1 Mev (SWARZ, 1952; HOLT, 1954; WARD and GRANT, 1954) cannot be explained solely on the basis of one theory or the other. Several attempts have been made to predict the mechanism of the reaction at low deuteron energies using mixtures of compound nucleus formation and

stripping theory (PEASLEE, 1948; BUTLER, 1950; HUBY, 1952). However, there is insufficient experimental evidence at present to determine how these reactions do proceed. Knowledge of this process will help in understanding the nature of the force between protons and neutrons. Further measurements of angular distributions are required and decisive information would be obtained from angular correlations between neutrons and their associated γ-rays. The same technical difficulties arise here as those discussed above: it is expected that the spectrometers described later will prove capable of measuring the $n - \gamma$ angular correlations.

(ii) ($\gamma - n$) reactions.

(a). General.

The main object of neutron measurements in ($\gamma - n$) reactions is to provide sufficient information to check the validity of the many different theoretical models which have been proposed to explain the mechanism of the photodisintegration process. Measurements of the products of the photodisintegration of the deuteron, in particular, are helpful in understanding the nature of the force between protons and neutrons.

At present the only point firmly agreed by both experiment and theory is the predominance of electric dipole absorption in the medium energy region. Whilst the characteristic 'giant resonances' of photodisintegration processes have now been found with elements throughout the periodic table, other results are limited and clouded by the continuous energy distribution of the γ-ray sources used in many investigations. The wide variety of theoretical models proposed can nearly all be made to fit the experimental information that exists although they differ widely in fundamental assumptions. Much more experimental data are required before discrimination between these models can be made and the photodisintegration process be put on a sound theoretical

basis.

(b). Methods and Results.

The measurements which are of interest in (γ - n) reactions are;

(A). The reaction threshold and the neutron yield as a function of γ -energy.

(B). The energies of the emitted neutrons at fixed γ - energies.

(C). The angular distributions of the total neutron yield and of neutrons of given energies.

The experimental work has been extremely difficult due to the lack of mono-energetic γ -sources of continuously variable energy. For the (n - γ) reaction to proceed it is necessary for the γ-energy to be equal to or greater than the binding energy of the neutron in the nucleus. For all nuclei, except deuterium and beryllium this energy is about 6 or 8 Mev; for deuterium it is 2.2 Mev and for beryllium it is 1.6 Mev. The available γ-sources are the natural γ-emitters, some γ-emitting artificially produced isotopes, the 17 Mev γ-rays from the reaction $Li^7(p,\gamma)2\alpha$ and synchrotrons. The first two types of sources are all of low energy and limited in their applicability to deuterium and beryllium; the lithium γ-rays are obviously of limited use and the γ-rays from synchrotrons, although variable in energy, have a continuous distribution of energies. This latter difficulty has been overcome to some extent by ingenious variations but nevertheless it has made the assessment of results extremely difficult.

References to some typical work are given below;

(A). Measurements of the (γ - n) threshold for many elements have been made by observing the γ-ray energy when, as is frequently the case, the target nucleus becomes unstable against β^+ or β^- emission following the emission of a neutron. This technique has been extended by KATZ (1950; 51) to obtain

excitation functions by measuring the variation in the activity of the target nucleus as a function of incident γ-ray energy. Such methods which do not involve direct observation of the neutrons are not of present interest.

For all nuclei investigated the neutron yield has been found to increase rapidly between 10 and 20 Mev γ-ray energy and to have a broad 'giant resonance' at about 20 Mev. (BALDWIN, 1948; McELHINNEY, 1949) It appears that the γ-ray energy at which the maximum cross-section occurs increases as the mass of the target nucleus decreases (PERLMAN, 1948; STRAUCH, 1951). Many measurements have been made of the absolute (γ - n) cross-section using 17 Mev γ-rays from the Li(p, γ) reaction (WALKER, 1950).

Direct observation of thresholds and yields may be made using counters which do not measure the neutron energies: a BF_3 counter encased in paraffin is suitable for this purpose.

(B). Measurements of neutron energies have been made using cloud chambers and photographic plates. The reactions D(γ, n)p and Be^9(γ, n)Be^8 have been extensively studied using natural γ-rays: these range from the earliest measurements by CHADWICK and GOLDHABER (1935) and by FEATHER (1935) to typical recent work by RUSSELL et al (1948). Measurements on other elements are nearly all of doubtful accuracy (due to the γ-ray source) but it has been established that, in general, most of the neutrons emitted have a continuous energy distribution whilst a small percentage of the neutrons are grouped together at a much higher energy (POSS, 1950).

(C). The angular distribution of the products of the D(γ, n)p reaction have been measured, but with low accuracy, by FULLER (1949; 1950) for γ-ray energies between 4 and 20 Mev. Measurements of the angular distributions of the total neutron yield in other elements have shown that the distribution is isotropic for most of the neutrons (PRICE, 1950) though there are indications that the high energy group has an anisotropic

distribution.

Whilst there are certain advantages in using a radioactive foil technique for measurements of yield, and photographic plates and cloud chambers for the measurement of neutron energies and angular distributions when the observations must, necessarily, be made with an intense γ-ray background, these methods are extremely tedious. Adaptations of the scintillation methods described later might prove useful for all such measurements.

(c). Interpretation and Conclusions.

Theoretical studies of the photodisintegration effect have been mainly concerned with explaining the mechanism of the reaction. All the original work on the subject was based on the assumption that the reaction proceeded by the formation of a normal Bohr compound nucleus which was in a highly excited state following the absorption of a γ-ray.

Considerations of the contributions of the electric dipole, magnetic dipole and electric quadrupole radiation to the cross-section for the formation of the compound nucleus led to the expectation of a strong maximum at about 20 Mev γ-ray energy, the major effect at this energy being due to electric dipole absorption. This was in good agreement with the experimental results. However, consideration of the 'evaporation' of particles from such an excited compound nucleus did not lead to complete prediction of the observed data. In particular, the compound nucleus model predicts that neutrons will be much more likely to be emitted than protons (due to the Coulomb barrier) whereas this is not in agreement with the experimental results(HIRZEL and WAFFLER, 1947).

HIRZEL and WAFFLER (1947) and COURANT (1948) suggested an alternative mechanism for the process in which the incident quantum interacts directly with a nucleon at the nuclear surface. A recent development of this idea by WILKINSON (1954) success-

fully predicts all the data obtained so far: the giant resonances, the relative magnitudes of the (γ , n) and (γ , p) cross-sections and the emission of small groups of protons and neutrons of high energy. However, there are not sufficient experimental data to check his predictions on the angular distributions.

The particular case of the photodisintegration of the deuteron is of great importance in view of the possibility that a knowledge of this process may lead to a better understanding of the nature of the $n - p$ force. Again, it is the angular distribution of the products of the reaction which is of most interest: RARITA (1941, a, b) has pointed out that the angular distribution of the products of the reaction D(γ , n)p is more sensitive to the force law than the total cross-section for the reaction.

The theoretical studies of the photodisintegration process are much more prolific than the experimental work. It is hoped that the spectrometers described later may help in reducing this lack of balance by allowing further experiments to be performed more easily.

3. NEUTRONS AS INCIDENT PARTICLES.

(i). The interaction of neutrons with matter.

(a). The possible interactions.

If a thin sheet of material is placed in the path of a beam of neutrons, then some of the neutrons are removed from, or scattered out of, the beam. The attenuation of the beam of neutrons is attributed to a variety of causes: the relative importance of each cause is found to depend on the energy of the neutrons and on the atomic number of the scatterer or absorber.

The possible processes which lead to an attenuation of the neutron flux are radiative capture of the neutrons, (n , γ), and elastic scattering of the neutrons, (n , n), both of which are possible for neutrons of all energies and for all absorbers, and inelastic scattering, (n , n'), (n , $2n$), etc, and neutron-induced

reactions such as (n, p) and (n, α) reactions. Another possibility which is, as yet, not of great enterest for neutrons in the range of energies 1 to 20 Mev is polarization scattering of the neutrons.

This review is concerned with experiments in which useful information may be obtained from measurements of neutrons with energies between 1 and 20 Mev and, accordingly, the discussion is limited to elastic and inelastic scattering experiments. Many measurements of neutrons in this energy range may be made in these experiments and useful information may be acquired about sizes of nuclei, positions and properties of energy levels of nuclei not otherwise accessible and the general theory of nuclear reactions. Further, the elastic scattering of neutrons by protons is of interest in the development of techniques for the measurement of fast neutrons.

(b). Neutron sources.

One of the major difficulties in the past in the performance of neutron scattering experiments has been the lack of suitable sources of monoenergetic neutrons of continuously variable energy. Recently this difficulty has been largely overcome and large fluxes of neutrons over most of the range 1 to 20 Mev can now be obtained, many of them with a 1 Mev HT Set, although the complete range can only be obtained with a Van der Graaf Set of about 8 Mev.

A comprehensive review of the possible sources of neutrons and their characteristics has been given by HANSON, TASCHEK and WILLIAMS (1949). McKIBBEN (1946) has given nomograms for the relationship between the energy of the bombarding particle and the energy and angle of emission of the emitted neutrons.

The most useful exothermic reactions are $D(d,n)He^3$ (the D-D reaction) and $H^3(d,n)He^4$ (the D-T reaction), both of which give large yields at as little as 50 Kev bombarding energy. The D-D

reaction gives neutrons from 2.5 to 3.0 Mev at low bombarding energies when advantage is taken of the variation of energy with angle of emission. The D-T reaction gives neutrons of 13 to 20 Mev.

The lower end of the energy range may be obtained using the endothermic reactions $H^3(p,n)He^3$, threshold = -1.019 Mev., and $Li^7(p,n)Be^7$, threshold = -1.8882 Mev, although the latter reaction is not truly monoenergetic for neutrons of more than 700 Kev as the Be^7 may be formed in its first excited state, 430 Kev, which leads to the emission of lower energy neutrons.

(ii). Elastic scattering.

(a). General.

When neutrons are scattered elastically by a nucleus the total kinetic energy of the incident neutron and the target nucleus is conserved. It follows that, except for the very lightest nuclei, the energies of the scattered neutrons will differ very little from the incident energy and will be substantially independent of the angle of scattering. The main interest in elastic scattering lies in measurements of the angular distributions of the scattered neutrons and their relation to nuclear sizes.

(b). Methods and Results.

In most of the work on elastic scattering of fast neutrons the detection device has been required only to distinguish the elastically scattered neutrons from the less energetic inelastically scattered neutrons and to record their intensity. Threshold detectors have proved suitable for this purpose in a limited number of cases. AMALDI and his collaborators (1947) used this technique in their investigation of the angular distribution of 14 Mev neutrons from the D-T reaction scattered by lead. They observed distinct maxima and minima in the differential cross-section at small scattering angles. The theoretical importance of these results is considered below.

Other workers have examined similar angular distributions using 14 Mev neutrons (ELLIOT, 1955; COON, 1955) and D-D neutrons have also been used (REDMOND and RICAMO, 1952; WHITEHEAD and SNOWDON, 1953, 1954). Photographic plates have also been used in these experiments.

WALT and BARSCHALL (1954) have used a proportional counter which was suitably biassed to exclude inelastically scattered neutrons, to measure the angular distribution of 1 Mev neutrons scattered by 28 intermediate and heavy nuclei.

The results of many experiments on (n-p) scattering using neutrons in the energy range 1 to 20 Mev are summarised here for use in the later discussion of techniques:

(A). The n-p scattering cross-section is large (See Fig.II.12.1.).

(B). There are no competing reactions.

(C). There are no resonances in the cross-section.

(D). The scattering is spherically symmetrical in centre-of-mass coordinates.

Although the techniques already used in elastic scattering measurements could be usefully employed in the further measurements required, the scintillation counters described later are capable of performing these measurements more easily.

(c). Interpretation and Conclusions.

The major point that calls for explanation in elastic acattering is the appearance of maxima and minima in the differential scattering cross-section at small scattering angles. This arises when the quantum mechanical wavelength associated with the incident neutrons is small compared with the nuclear radius. The situation is then analogous to optical diffraction by a black object.

The diffraction pattern obtained may be related quantitatively to λ, the neutron wavelength and R, the radius of the

nucleus. From the value of R obtained the constant, K, in the equation $R = KA^{1/3}$ which relates the nuclear radius and mass number, may be determined. The equation $R = KA^{1/3}$ arises in various nuclear models, the value of the constant depending upon which model is used. Such measurements are useful therefore in checking the validity of the models. The results of AMALDI (1947) referred to above were in excellent agreement with a theoretical calculation of the differential cross-section computed in this way (HAUSER and FESHBACH, 1952). It should be noted that this diffraction scattering is confined to very small angles, of the order of $\lambda\!\!\!^{-}/_{R}$.

More measurements of this type are required: in order to perform all such experiemtns well it would be necessary to have a neutron detector which is capable of examining the intensity of neutrons of a given energy in a background of neutrons of different energies. Further, the detector must be capable of fine angular variation. Until the development of the techniques described later, detectors capable of performing these functions over a wide range of energies have not existed.

(iii). Inelastic scattering.

(a). General.

In the inelastic scattering of a fast neutron, the neutron is absorbed by a target nucleus and re-emitted with less than its original energy. The energy acquired by the (original) target nucleus is then usually emitted as γ -radiation. Thus, in contrast with elastic scattering, kinetic energy is not conserved.

The reaction can proceed only if the incident neutron has sufficient energy to raise the target nucleus to its first excited state. If the energy of the incident neutron is increased so that there is sufficient energy available for the target nucleus to be in its first excited state and also to supply the

binding energy of a neutron in the target nucleus then the (n, 2n)reaction becomes possible. Very approximately, over most of the periodic table, the (n, n′) reaction takes place with neutrons of up to 10 Mev and the (n, 2n) reaction with neutrons of up to 18 Mev. As the neutron energy is increased further the (n, 3n) reaction becomes possible.

Levels in light nuclei may be examined in this way but probably the main interest of the process is in intermediate and heavy nuclei where several of the lowest lying levels are usually contained within a few Mev and cannot, in general, be excited in any other way. Thus observation of inelastically scattered neutrons can lead to an extension of the number of the nuclei for which the position and properties of some of the excited states are known.

(b). Methods and Results.

The measurements which are of interest in the inelastic scattering of neutrons are almost identical with those enumerated in the section dealing with the emission of neutrons in the bombardment of light nuclei by charged particles. The same measuring devices have been used and much the same difficulties and limitations encountered. The measurements which may be made are:

(A). The yield of inelastically scattered neutrons as a function of neutron energy.

(B). The energies of the emitted neutrons for a given incident neutron energy.

(C). The angular distribution of the emitted neutrons.

(D). The energy and angular correlations of the neutrons and their associated γ -rays.

Each of these types of experiments is considered briefly below:

(A). Measurement of the yields in inelastic scattering is not

quite as straightforward as in the experiments described earlier. It is necessary to count the neutrons in a background of the primary and elastically scattered neutrons which are of higher energy. In practice, the yield has usually been measured by the reverse procedure: that is, the number of neutrons observed by a detector which does not respond to neutrons of energy less than the primary energy, or the energy of the elastically scattered neutrons, is recorded without, and with, the scatterer in position. The difference is , in many cases, a good approximation to the inelastic yield. Radioactive threshold detectors have been mainly used for this type of experiment (PHILIPS, DAVIS and GRAVES, 1952).

The yield has also been derived from measurements on the total scattering cross-section - which is relatively easy to measure (HUGHES and HARVEY, 1955) - and the integral of the differential elastic scattering cross-section described in the previous section.

(B). Measurements of the energies of inelastically scattered neutrons have been made using all of the available detection devices. Such measurements have not been very extensive and a great deal of information is still required.

The earliest measurements were obtained using cloud chambers (AUGER, 1933). This technique has also been used more recently to measure the scattering of D-D neutrons from magnesium and a neutron group was resolved which corresponded to inelastic scattering from a level at 1.30 Mev in magnesium (LITTLE, LONG and MANDEVILLE, 1946). One advantage of the technique is that the scattering material may sometimes be contained in the chamber and the energies of the scattered neutrons may be computed from measurements of the energies of the recoiling target nuclei: this has been done with the scattering of D-T neutrons by oxygen (CONNER, 1953).

Photographic plates have been most used in these studies:

reference may again be made to the review article by ROSEN (1953). Most of the work has been performed with 14 Mev neutrons from the D-T reaction: scattering from individual levels would not usually be expected with neutrons of this energy but degradation of the energies of the neutrons scattered from the continuum of levels has been observed (GRAVES and ROSEN, 1953). Some work on the inelastic scattering of lower energy neutrons from individual levels has also been performed in this way and the positions of levels of intermediate nuclei estimated (STELSON and PRESTON, 1952; JENNINGS et al, 1955). The accuracy of the determination of the positions of the levels has been increased by combination with the results of SEPARATE observations of the γ-rays emitted (GRIFFITHS, 1955). Plates loaded with the scattering material have also been used (ALLAN, 1954). (The 'loading' of photographic plates is discussed later in the appropriate section of the appendix on techniques)

Measurements of the inelastic scattering of neutrons of the order of 1 Mev by uranium have been made using a proportional counter filled with He^3 (BATCHELOR, 1955).

Contemporary applications of scintillation counters to these measurements (POOLE, 1952, 1953; ELIOT et al, 1954) are discussed later in relation to the developments described in the main body of the thesis.

(C). Work on angular distributions has been extremely limited: in the measurements of neutron energies by STELSON and PRESTON (1952) and JENNINGS et al (1955), cited above, the angular distributions of the neutron groups found were also obtained.

(D). No correlations between scattered neutrons and their associated γ-rays have been reported; this has (again) been due to the lack of suitable techniques.

(c). Interpretation and Conclusions.

As in the section on the emission of neutrons in the bombardment of light nuclei most of the experimental results can be

explained on the assumption of the formation of a compound nucleus. The interpretations of results of the type (A) to (D) are exactly analogous to those given in that section except that in simple inelastic scattering the target and residual nucleus are the same.

The information obtained depends on the energy of the incident neutrons and on the target nucleus. With light nuclei and heavy nuclei near a closed shell the properties of individual levels may still be established provided that the neutron energy is not too great. In inelastic scattering by heavy nuclei the information obtained may be used in statistical approaches to the properties of a continuum of overlapping levels.

The validity of the details of most of the theoretical approaches to the problem may only be checked with experimental information about angular distributions and correlations. The techniques developed during this work should help to make this information available.

4. SUMMARY OF CONCLUSIONS: PROPERTIES OF AN IDEAL SPECTROMETER.

From the brief review of the state of the experimental data and the theoretical interpretation of those results certain general conclusions may be drawn which apply to all the different types of experiment.

The measurement of neutron fluxes, both relative and absolute has been well covered and further results could be obtained using the techniques used in previous work; improved techniques could facilitate further results being obtained more quickly and more easily. Determinations of neutron energies have also been extensively made, the major drawback has been the length of time involved in getting results; again, an electronic technique of high detection efficiency would be useful for further work. The same considerations apply to angular distributions, although the labour involved in obtaining these with the techniques used in the past is even greater than in straightforward determinations of neutron spectra; this accounts for the small amount of experimental

evidence available. Determinations of correlations between neutrons and γ-rays, or other associated particles, has been beyond the capacity of the existing techniques; the validity of many theoretical considerations can only be checked by such measurements and, in many cases, progress in understanding the processes involved remains impossible without them.

A spectrometer which would be capable of making all of the required measurements would possess the following characteristics:

(A). A high efficiency for the detection of neutrons.

(B). (i). A response proportional to the energy of the neutrons incident upon it.

(ii). The capacity to resolve groups of neutrons whose energies differ by 0.1 Mev.

(C). A fast response to the passage of a neutron (short resolving time).

(D). Insensitivity to γ-radiation (or, at least, the capacity to distinguish between neutrons and γ-rays).

It is of interest to obtain some particular values for the performance characteristics outlined above. These may be obtained to an order of magnitude by considering a typical (d-n) reaction initiated with a 1 Mev H.T. Set:

A typical such reaction yields about 10^8 neutrons and γ-rays emitted simultaneously per second.

A good γ-ray spectrometer has a total detection efficiency of the order of $\underline{10}^{-3}$ per γ-ray emitted by the source and a resolving time of the order of $\underline{10}^{-8}$ seconds.

If the resolving time of the neutron spectrometer can also be arranged to be of the order of $\underline{10}^{-8}$ seconds then the random coincidence rate is of the order of 1 per second.

Hence the minimum real coincidence rate allowable (which is of the order of the random rate) is 1 per second.

Thus the neutron spectrometer must have a total detection

efficiency of the order of 10^{-5} per neutron emitted by the source.

5. PRINCIPLES OF THE SPECTROSCOPIC METHODS.

(i). General.

Since neutrons have no charge they can be detected only by the effects of the secondary radiations to which they give rise. For the measurement of the energies of fast neutrons the interactions of interest, of which the first is the most important, are elastic collisions with nuclei (usually protons) and nuclear reactions in which charged particles or γ-rays are produced. (In this section the possible means of utilising these interactions are considered in general terms.)

(ii). Elastic Collisions.

(a). Reduction to thermal velocities.

In principle, the energy of a neutron may be determined by allowing it to be reduced to thermal velocities by successive elastic collisions in a scattering medium. Theoretically this might be done where the scattering medium is hydrogen contained in an infinite cloud chamber; the energies of all the recoil protons could then be measured and the sum would give the energy of the neutron. The method assumes practical possibilities with the use of a dense scattering medium such as a scintillation counter. A difficulty which arises, however, is that it may not be possible to measure the energy of the recoiling protons directly, but only a function of their energy. If the function is non-linear in energy the resolution obtainable will depend upon the number of collisions required to reduce each neutron to thermal velocities.

(b). Single scattering.

The scattering material may be arranged so that neutrons which are scattered in it are scattered once and once only. It is then necessary to consider the mechanics of individual collisions and find the distribution in energy of the recoiling nuclei.

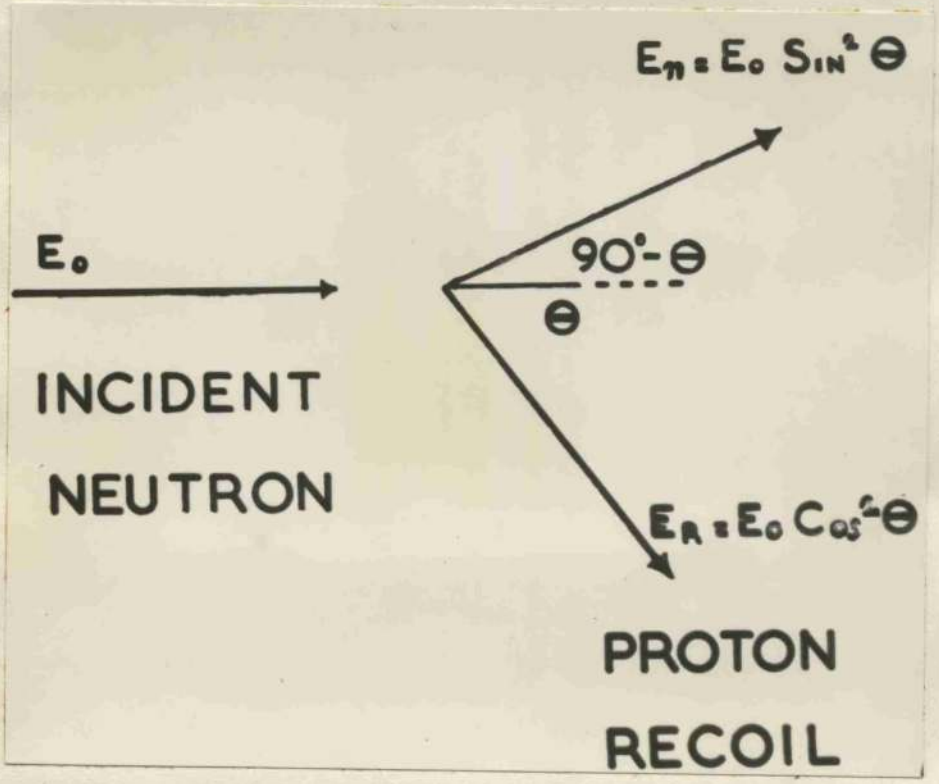

FIG.I.5.1. NEUTRON-PROTON COLLISION DIAGRAM.

Consider a neutron which has an elastic collision with a nucleus R, of mass number A. If the neutron has energy E_o and R is scattered at an angle θ to the original line of flight of the neutron, Fig.I.5.1, then the energy of R is given by

$$E_R = \frac{4A}{(1+A)^2} E_o \cos^2\theta, \quad (0 \leq \theta \leq 90^\circ) \qquad \text{I.5.1.}$$

from considerations of momentum and energy. The recoil energy is a maximum for head-on collision, that is $\theta = 0$, and is given by

$$E_{R(max)} = \frac{4A}{(1+A)^2} E_o \qquad \text{I.5.2.}$$

The recoil energy increases as A decreases and thus the maximum recoil energy available is when R is a proton, in which case

$$E_{R(max)} = E_o \qquad \text{I.5.3.}$$

That is, the proton acquires all the energy of the neutron.

Now consider a monoenergetic flux of neutrons, energy E_o, incident upon a hydrogenous material. Let $\phi(E_o)$ of these neutrons be scattered once, and once only, in the medium. Since in the centre-of-mass system (n-p) scattering is isotropic (for neutrons in the energy range 1 to 20 Mev) and in the laboratory system the energies of the recoiling protons are proportional to $\cos^2\theta$, it may readily be shown that the number of recoiling protons (corresponding to single n-p scattering) with energies in the range E_p to $E_p + dE_p$ is given by

$$N(E_p)\,dE_p = \frac{\phi(E_o)}{E_o}\,dE_p \qquad \text{I.5.4.}$$

for $E_p \leq E_o$; $N(E_p)dE_p = 0$ for $E_p > E_o$.
This is simply the rectangular distribution of Fig.I.5.2(a). If two groups of neutrons are present in the flux the distribution has the form shown in Fig.I.5.2(b).

In principle, then, the energy of a monoenergetic flux of neutrons may be found by measuring the energies of a large number of recoil protons; this might be done, for example, by measuring

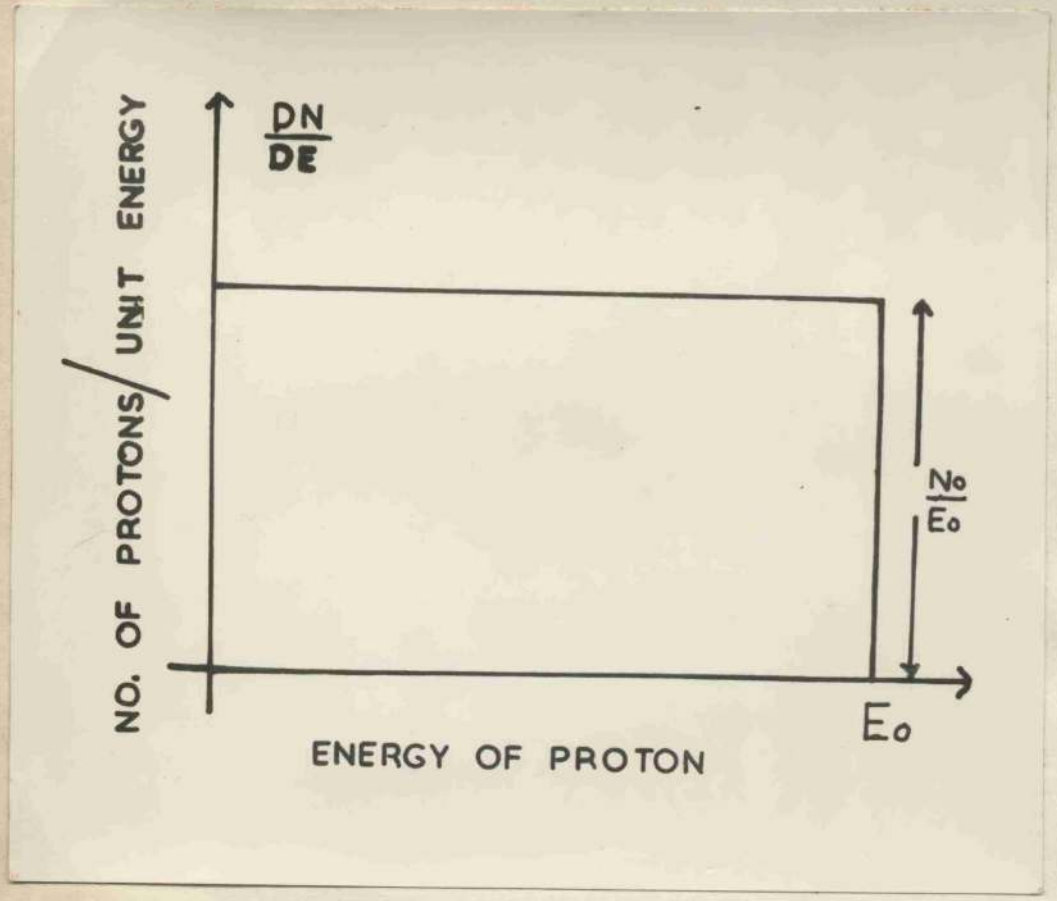

FIG.I.5.2(a)

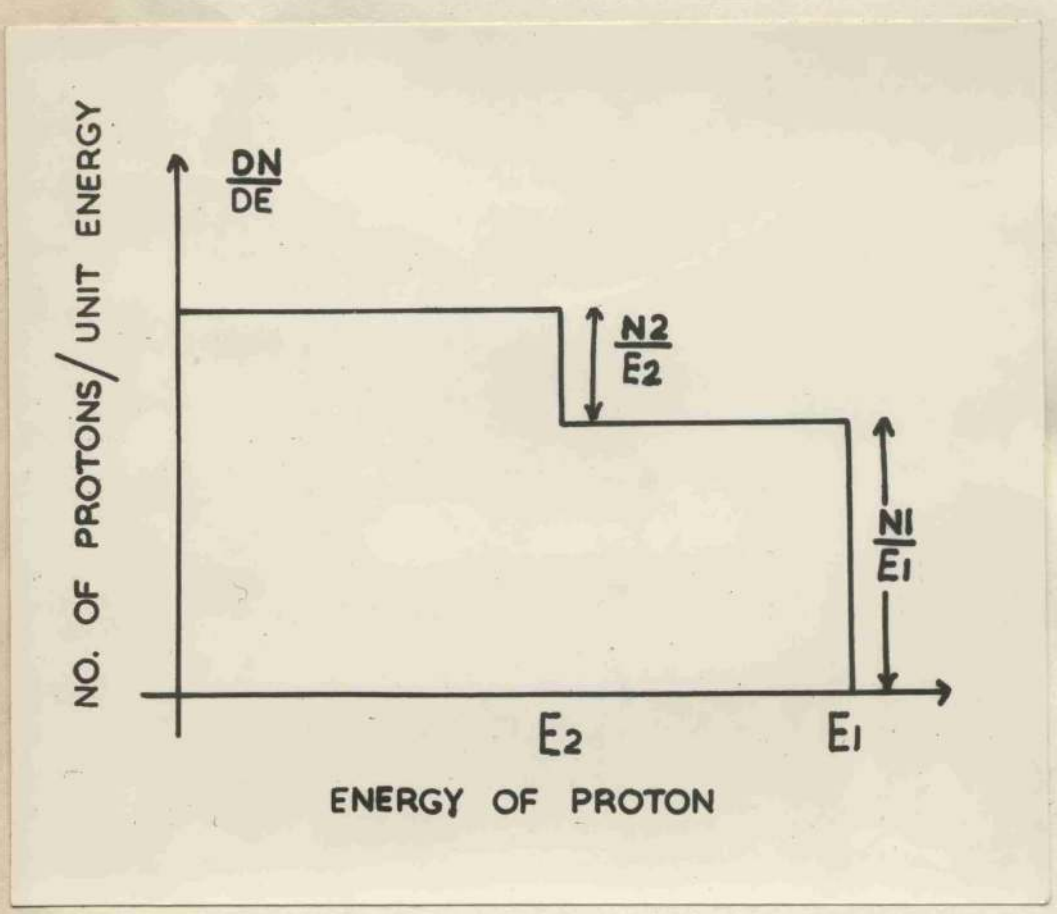

FIG.I.5.2(b)

ENERGY DISTRIBUTIONS OF RECOIL PROTONS FROM SINGLE SCATTERING EVENTS.

the pulses from a (suitably shaped) hydrogen filled ionization chamber irradiated by the neutron flux. The curve obtained by differentiating the measured distribution would then be a line corresponding to the energy of the neutrons. In practice, however, in the example quoted the distribution will be seriously affected by wall and geometrical factors. For a known geometry it may be possible to correct for these factors; however, the resolution obtained in this way may be inadequate for many experiments.

(c). Selection of recoils at a given angle.

The above method of determining neutron energies from single scattering by protons has the disadvantage that a monoenergetic flux of neutrons gives rise to a continuous distribution of proton energies. This disadvantage may be overcome in a variety of ways. Using photographic plates or cloud chambers, only recoils within a definite angular interval may be measured; using proportional or scintillation counters, mechanical collimation may be introduced. Further, the neutrons may be scattered from one (scintillation) counter into another; the energy of a neutron may be found by measuring the pulse size in the first counter only when the neutron is scattered in the second counter. Evidently the geometrical resolution obtainable in this way depends on the sizes and orientation of the counters and the source of neutrons, and may be increased indefinitely with a corresponding loss in efficiency of detection. The practical limit to the energy resolution is determined by statistical factors, which are discussed later.

(d). Time-of-flight.

No measurement of the energy of the recoiling protons is necessary in methods in which the time of flight of a neutron between two elastic collisions is found. With a suitable, known geometry there is a unique relationship between the energy of the neutrons and time. Low detection efficiencies made this approach impracticable before the advent of the scintillation counter.

Reported attempts to use this method utilizing scintillation counters have also had low detection efficiencies: details of a suitable arrangement which has high detection efficiency whilst obtaining adequate energy resolution are given in Part IV.

In experiments with pulsed sources, or in reactions in which γ-rays or charged particles are known to be emitted simultaneously with neutrons, the time of flight of the neutrons to a single scattering medium may be found.

(iii). Nuclear Reactions.

(a). Measurement of the energies of the products of the reaction.

The energies of neutrons may be found by measuring the energies of the (charged particle) products of a nuclear disintegration initiated by the neutrons. The energy of the neutron is then given by

$$E_n = \sum_{ALL\ F} E_F - Q \qquad \text{I.5.5.}$$

where E_F is the energy of a product of the reaction and Q is the energy evolved in the reaction. An important special case of this method is where the products of the reaction are a proton and a relatively massive nucleus; provided that the reaction leads to the ground state of the resultant heavier nucleus then the proton carries away the major part of the energy available and a measurement of its energy alone may be sufficient to determine the energy of the neutron to high degree of accuracy. Suitable reactions are extremely limited in number.

(b). Threshold Detectors.

It is possible to determine whether neutrons with energy greater than Q are present in a neutron flux by measuring the yield of product particles (either instantaneous or delayed) from neutron-induced reactions which have a negative Q value. A series of such reactions with different Q values may be used to determine a spectrum. The method is rather crude and suitable reactions are, again, limited in number.

II. PRELIMINARY CONSIDERATIONS AND EXPERIMENTS ON SCINTILLATION COUNTERS.

1. NEUTRON-INDUCED SCINTILLATIONS: GENERAL.

The discovery that certain hydrogenous organic compounds fluoresce under neutron bombardment (BELL, 1948; HOFSTADTER, 1948) at once led to the possibility that such materials might be applied to the problems of fast neutron spectroscopy. The fluorescence process was attributed mainly to the scattering of the neutrons by protons in the scintillators. The translation of proton energy into visible radiation is a complicated process for which no universally accepted explanation has been given. In practice, it is sufficient to know that a fraction of the kinetic energy of the protons is converted into visible or ultra-violet radiation. The value of this fraction is the conversion efficiency of the scintillator; it depends on the constitution of the scintillator and is a function of the proton energy. (It is sometimes also important to know the form of this function.) The radiation may be detected by a photomultiplier and the integrated current pulses from the photomultiplier give a measure of the proton energies.

There are two immediate advantages over previous techniques in the application of fluorescent materials to the measurement of neutron energies. Firstly, the high detection efficiencies that can be attained since large, almost translucent volumes of scintillator may be placed in the path of the neutrons. Secondly, the very fast resolving times that can be attained, which are a consequence of the short duration of the light pulses that are emitted. The main disadvantages of scintillators for this work are firstly, the non-linear response of organic scintillators to protons as a function of proton energy; secondly, the low conversion efficiency of organic scintillators for protons, which leads to intrinsically poor energy resolution at low energies; and thirdly, the high sensitivity of organic scintillators to γ-

FIG.II.2.1. FINAL ARRANGEMENT OF SCINTILLATOR AND PHOTOMULTIPLIER.

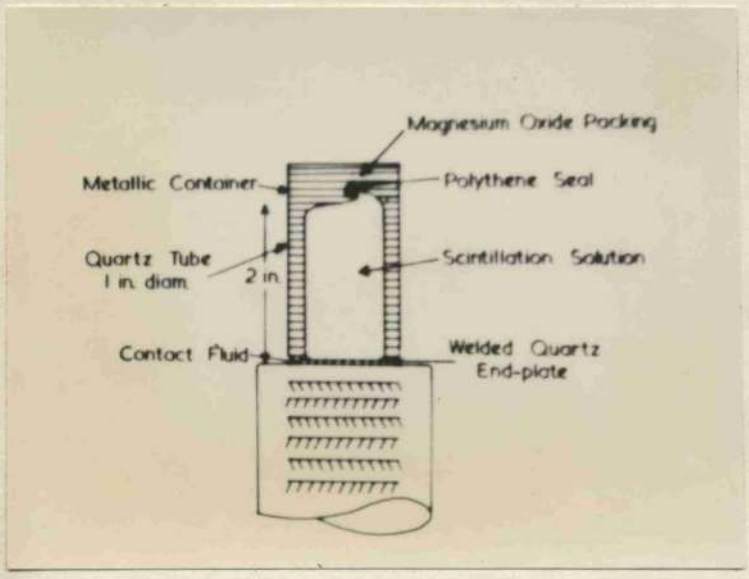

FIG.II.2.2. DETAILS OF ASSEMBLY OF LIQUID SCINTILLATION CELL.

rays, which give rise to light pulses through the formation of photo-, Compton and pair electrons in the scintillators. This last disadvantage is aggravated by the fact that the conversion efficiency of the scintillators for electrons is greater than it is for protons.

In the remainder of this part of the thesis some of the properties of organic scintillators and the related apparatus are discussed briefly. Preliminary experiments which were conducted in order to improve the performance of the scintillators are described. No systematic study of liquid scintillators in general was carried out but these experiments were directed towards reducing to a minimum the limitations which these scintillators suffer for work on fast neutrons and to finding a suitable arrangement for the counters as a whole.

The results of experiments to determine the response of liquid organic scintillators to bombardment by protons and by electrons are given: no other measurements have been reported of the functional relationship between light output and incident particle energy for this type of scintillator. These results were derived from later experiments which are described in Part IV of the thesis.

2. THE FINAL EXPERIMENTAL ARRANGEMENT FOR SCINTILLATION COUNTERS.

In the final arrangements of scintillation counters that were used, the scintillators were packed and mounted on photomultipliers in the manner which is shown in Fig.II.2.1. Details of the packing and mounting are illustrated in Fig.II.2.2. The choice of materials and their arrangement (described immediately below) followed from the experiments and considerations discussed in the following sections.

The scintillator used was a solution of 0.5 gm/l terphenyl + 0.1 gm/l anthranilic acid in purified xylene. (This is referred to as terphenyl in xylene hereafter.) This was poured in through the

narrow orifice of the welded quartz cell with a hypodermic syringe. The cell was sealed with polythene. It was then placed in a metal container so that one (flat) face was exposed and the space between the cell and the metal container was packed with dry magnesium oxide powder. The exposed face of the cell was placed on the photocathode of a photomultiplier: optical contact between the cell and the multiplier was made with silicone oil. The whole arrangement of cell and multiplier was surrounded by a light-tight metal box.

This type of arrangement was used to obtain all the results given for work on neutrons. Where more complicated shapes of counter were used, as, for example, a portion of a spherical shell, a plastic light-guide was machined to fit the cell and a flat surface on the light-guide lay on the photocathode.

3. LIQUID, CRYSTAL AND PLASTIC SCINTILLATORS.

Organic scintillators may be prepared in three forms: liquid, crystal and plastic; all three types have similar properties. However, there are certain differences which led to the choice of liquid scintillators for most of the work described here.

Plastic scintillators have only become available recently and could not be used in any of the work described. However, the properties of plastic scintillators that have been investigated (SWANK and BUCK, 1953, 1955; HARRISON,1954) indicate that their behaviour is in almost all respects similar to that of liquid scintillators and they may well replace liquid scintillators in many future applications.

The important differences between liquid and crystal scintillators are outlined now:

(a). Conversion Efficiency: The most efficient crystal scintillator is anthracene; the best readily obtainable liquid scintillator is a solution of terphenyl + anthranilic acid in xylene. Their respective conversion efficiencies for protons are of the order of 4% and 2%.

(b). Response Time: The duration of a light pulse in anthracene is of the order of 5×10^{-7} secs, the corresponding time for stilbene (which has a conversion efficiency of the same order as the best liquid scintillators) is of the order of 5×10^{-8} secs; the time for all liquid scintillators is of the order of 10^{-9} secs.

(c). Geometrical Properties: Crystal volumes are limited; it is hard to grow anthracene crystals larger than about one cubic inch. Also it is very difficult to work crystals into unusual shapes. Liquid scintillators may be prepared in large volumes and used to fill translucent containers which have previously been worked into desired shapes.

Although liquid scintillators have lower conversion efficiencies than crystal scintillators, their faster response and the ease with which they may be prepared in large volumes of almost any shape make them more suitable for use in fast neutron spectrometers. This will become evident when the design of the spectrometers is discussed in detail later.

4. PULSE HEIGHT MEASUREMENTS AND TIME MEASUREMENTS.

The properties required of a scintillation counter depend on whether it is to be used for pulse height or time measurements. Time measurements require only that the pulses from the counter be fast and, to facilitate the associated electronic work, large. The second of these requirements is axiomatic in pulse height analysis if good resolution is to be obtained; furthermore, in many pulse height spectrometers it is desirable to have fast pulses in order to be able to use a coincidence device, either as an integral part of the spectrometer or as part of the arrangement to perform additional experiments. Pulses from the counter must also satisfy other requirements if pulse height analysis is employed.

The following discussion is primarily concerned with the points to be observed in obtaining good pulse height resolution

but the conclusions are also applicable to counters used for time measurements. The special arrangements used for obtaining pulses for use in the millimicrosecond range are discussed in the description of the time-of-flight spectrometer in Part IV.

5. FACTORS AFFECTING PULSE HEIGHT RESOLUTION.

The energy resolution obtainable with scintillation counters used with pulse height analysis depends on several factors. Of these factors the most important are statistical fluctuations, non-uniform light collection and the variation of the conversion efficiency of the scintillators as a function of the energy of recoil protons. Discussion of the effect of the last of these factors is delayed since the importance of the effect depends strongly on the particular design of each spectrometer under consideration.

(a) Statistical fluctuations.

Ideally, all recoil protons of a given energy in a scintillator would give rise to pulses of the same size at the multiplier output. In practice, even under conditions of perfect light collection, this does not occur. A pulse corresponding to a proton of a given energy in the scintillator is affected by statistical fluctuations in the conversion efficiencies of the scintillator and the photocathode and in the number of photoelectrons collected and amplified by the dynode system of the multiplier. Consequently, protons of a given energy in the scintillator give rise to a distribution of pulses which are spread about a mean value. It has been shown experimentally (GARLICK and WRIGHT, 1952) that this distribution is approximately gaussian, where the full width, Γ, at half maximum height of the distribution is proportional to the square root of the mean pulse height, L.

The resolution of this gaussian curve may be defined to be R, where

$$R = \Gamma/L \qquad \text{II.5.1.}$$

Since the statistical fluctuations determine the ultimate resolution that may be obtained under otherwise ideal conditions, it is of interest to calculate values of R for typical organic scintillators and typical photomultipliers. R may be calculated easily to an order of magnitude if a simplifying assumption is made. The assumption is that the resolution is given by twice the fractional root mean square deviation on the number, N , of photoelectrons collected on the first dynode of the multiplier. That is,

$$R = 2N^{-\frac{1}{2}} \qquad \text{II.5.2.}$$

The assumption is reasonable since the number of particles concerned in the scintillation-multiplication process is a minimum at this stage. The emission spectra of most organic scintillators are in the region of 4000° A so that about 3 ev are required to produce a photon. Thus for a proton of E Mev,

$$N = \frac{E C_s C_p C_f}{3} \times 10^6 \qquad \text{II.5.3.}$$

where C_s and C_p are the conversion efficiencies of the scintillator and the photocathode, and C_f is the fraction of the photoelectrons produced at the photocathode which are focussed on the first dynode. For anthracene, the best organic scintillator, C_s is $\sim 4\%$. For most E.M.I. photomultipliers C_p and C_f are $\sim 5\%$ and $\sim 60\%$ respectively. For 14 Mev and 2.5 Mev protons (which arise as head-on recoils from collisions with neutrons of 14 Mev and 2.5 Mev) R is calculated to be $\sim 2.5\%$ and $\sim 6.5\%$. For stilbene and the best liquid and plastic scintillators, with $C_s \sim 2\%$, the corresponding values of R are $\sim 3.8\%$ and $\sim 9\%$.

These (ideal) values set the lowest limits attainable with any spectrometer employing pulse height analysis: they compare unfavourably with values obtained in practice using photographic plates and, at the lower energy, are at the limit of usefulness for acquiring new information. Provided that no other overriding consideration precludes the choice, it is always desirable

to choose to work with the scintillator with the largest C_s: this led to the choice of terphenyl in xylene since anthracene was precluded for reasons outlined earlier. Again, C_p should be as large as possible. The possible values of C_p are restricted by the photocathodes which can be manufactured. However, the effective value of C_p may be increased by shifting the emission spectra of the scintillators (by additional solutes) to the region in which the photocathodes are most sensitive. Experiments in which it was attempted to do this are described below.

A detailed account of statistical fluctuations in scintillation counters has recently been given by BREITENBERGER (1955).

(b) Non-uniform Light Collection.

The above considerations of statistical fluctuations have assumed that the light collection from all parts of the scintillator is uniform. In fact, the optical path to the photocathode of light originating at any point in the scintillator will depend on the position of the point of origin of the light. Absorption of light takes place all along the optical pathe since the transmission coefficient neither of the scintillator nor of the container wall nor the reflection coefficient of practical materials is unity at the wavelength of the light emitted by the scintillator. Thus further variation is introduced into the pulses corresponding to protons of a given energy when the recoils are formed at all points in the scintillator. The effect is averaged over the whole scintillator and increases the width of the gaussian distribution of pulses corresponding to proton recoils of the same energy.

Measurements of the transmission coefficients were made and the results are given below. (The absorption lengths of toluene, o-, m-, and p-Xylene to their own radiations have also been measured by HARRISON (1952): he gives the respective values as 40.9, 27.4, 18.5 and 11.5 cm.) The magnitude of this effect depends, of course, on the size and shape of the scintillation

counter. For small counters ($\sim 2cm^3$) made with the best materials the effect is negligible. From the values of the transmission coefficients it follows that the resolution would be completely destroyed in a large scintillator ($\sim 20cm^3$) viewed in the conventional manner with one photomultiplier. As a rough check a cylindrical scintillator, 6" long and 1" in diameter, viewed through one end was irradiated with a small source at both ends: pulses from the end remote from the photocathode were approximately a factor of two smaller than those from the end adjacent to the photocathode.

SHIELDS (1953) has conducted a similar experiment in a more refined manner using a collimated beam of γ-rays. He contrived to get a fairly uniform - but reduced - response from all parts of the scintillator by using a poor reflector at one end of the cylinder and a good reflector at the other end. More elaborate arrangements, in which it is attempted not to sacrifice any light, have been used (HARRISON et al, 1954). The scintillator was viewed at several points by different multipliers and their outputs summed. This procedure is costly and it is difficult and laborious to adjust all the multipliers to have the same effective gain. CURRAN (1953) has suggested that the problem of light collection from large scintillators may be more easily solved by making large photocathodes (possibly re-entrant in shape) and having more elaborate focussing arrangements for the collections of electrons. He points out that the major difficulty would probably be to achieve uniform sensitivity over large cathode areas.

The experiments on spectral shifting mentioned earlier were also of interest in this connection: all the transmission coefficients and reflection coefficients (measured) were nearer unity for wavelengths in the region of maximum sensitivity of the photocathode.

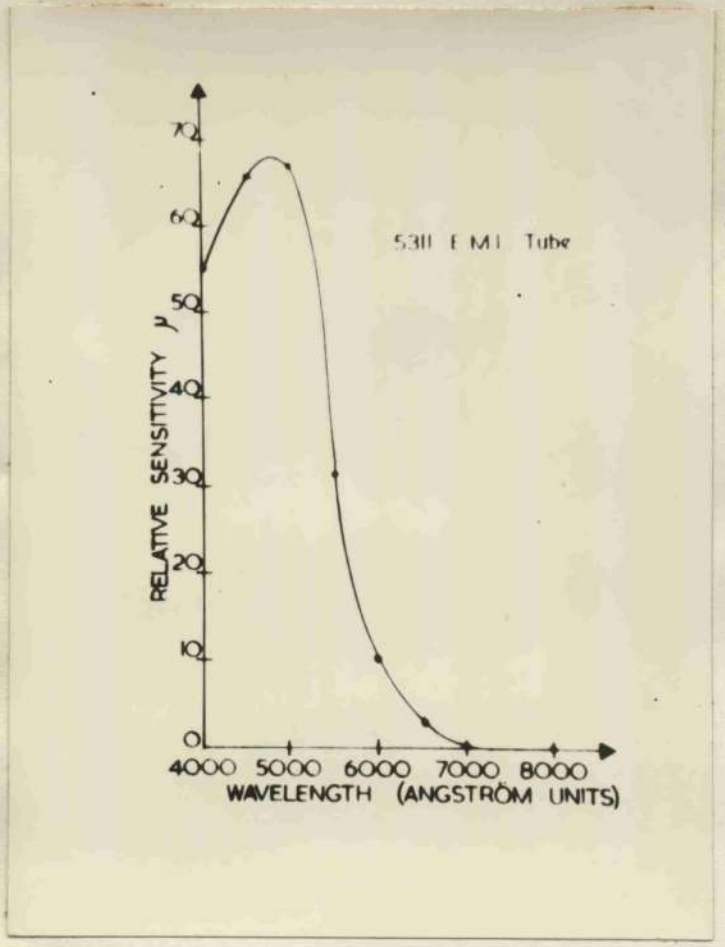

FIG.II.7.1. SPECTRAL RESPONSE CURVE OF PHOTOCATHODE.

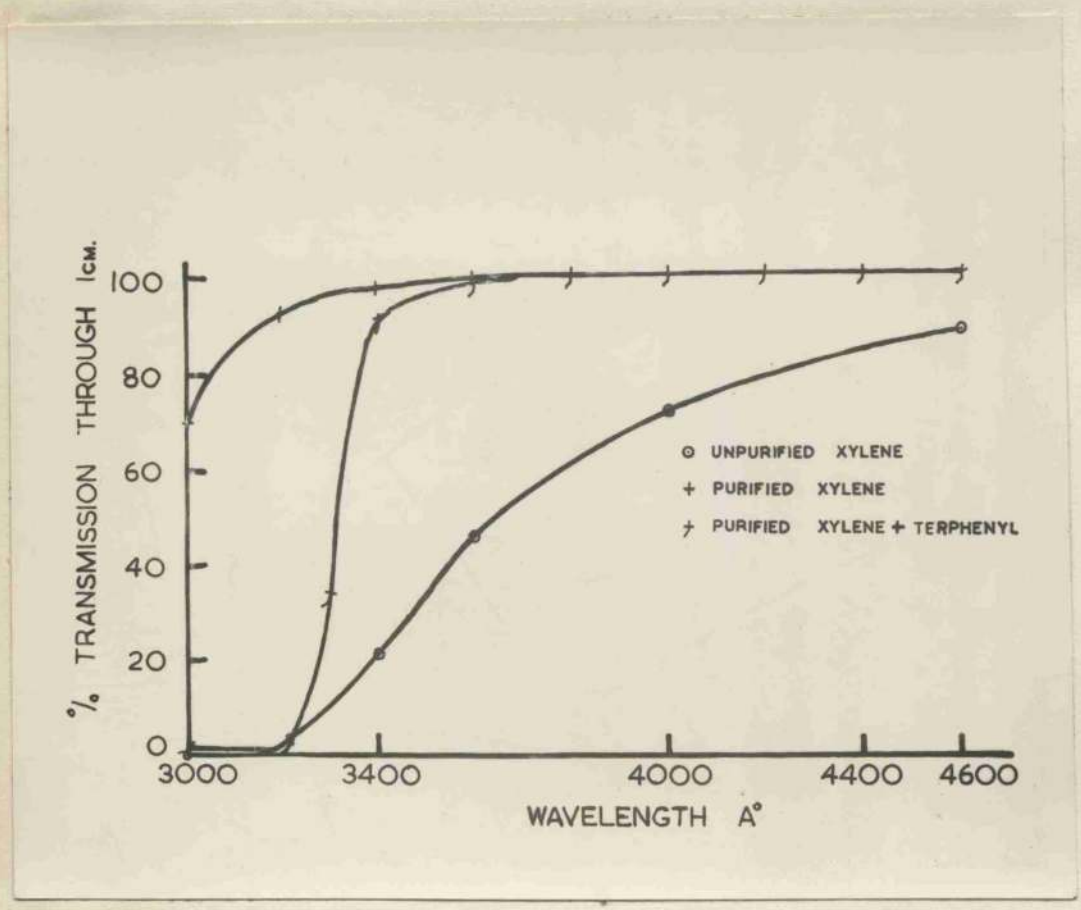

FIG.II.8.1. TRANSMISSION CURVES OF LIQUIDS USED IN SCINTILLATION COUNTERS.

6. EMISSION SPECTRUM OF THE SCINTILLATOR.

KALLMANN and FURST(1950) have investigated the scintillation properties of a large number of solutions. Many of the solutes that they tested are not available in this country. However, terphenyl in xylene, which is available, has a conversion efficiency of 90% of the best solution listed. KALLMANN gives the emission spectrum of terphenyl in xylene as lying in the region 3250 A^{o} - 4000 A^{o}.

7. THE PHOTOCATHODE SENSITIVITY.

The spectral response curve of the photocathode of the E.M.I. 5311 photomultiplier is shown in Fig.II.7.1. Other types of E.M.I. photomultipliers were also used in this work and their response curves were very similar, with maximum sensitivity in the same region (about 5000 A^{o}). This region is well to the visible side of the emission spectrum of the scintillator: this suggested some of the later experiments.

8. ABSORPTION EXPERIMENTS.

(a). The Scintillator.

The absorption spectrum of the scintillator over the region 4000 - 5000 A^{o} was measured with a Beckmann Spectraphotometer. The scintillator was found to absorb strongly in the region of the emission spectrum. Most of the absorption was attributed to chemical impurities in the xylene.

Subsequently the xylene was purified. This was done by removing the sulphur with concentrated sulphuric acid, neutralising, washing and finally distilling. The absorption spectra of the purified xylene and of purified xylene + terphenyl were also measured. A marked improvement in transmission over the region of the emission spectrum of the scintillator was found (Fig.II.8.1). Further experiments on the response of the scintillator to γ-rays showed large increases in pulse height(incr-

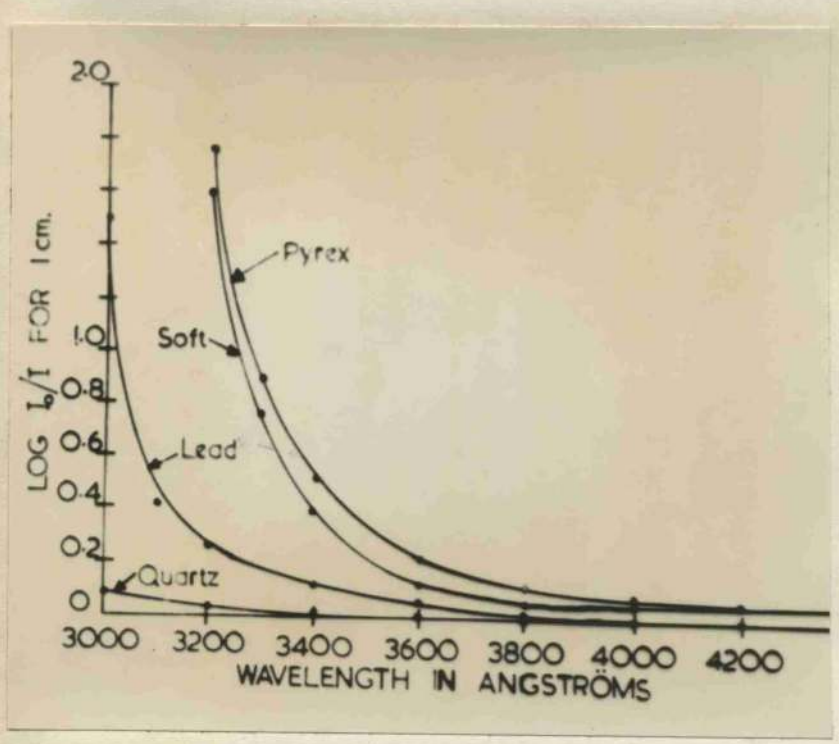

FIG.II.8.2. TRANSMISSION CURVES OF VARIOUS GLASSES.

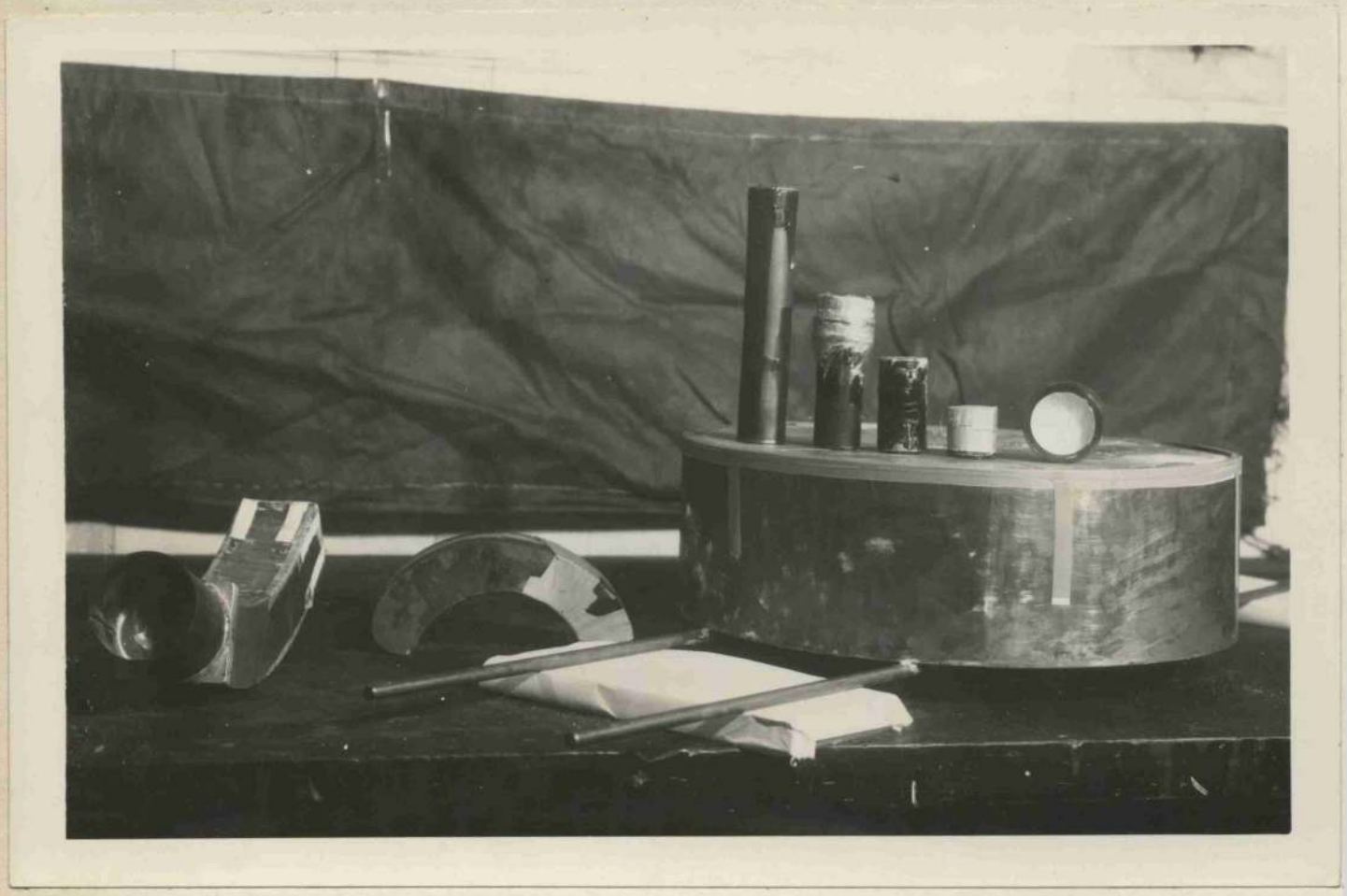

FIG.II.8.3. SOME SCINTILLATION CELLS.

easing with increasing volume of scintillator) when purified xylene was used instead of unpurified xylene as the solvent.

(b). The Containers.

The absorption spectra of some of the readily obtainable glasses and plastics and of quartz were also measured. Some of the results are shown in Fig.II.8.2.

As quartz is very difficult to work cells were constructed from some of the glasses and plastics which absorbed least in the relevant wavebands. None of these cells was satisfactory. The plastic cells gave excellent results initially but deteriorated rapidly: it was suspected that the plastic wall was soluble to a small extent in the xylene. (Very small traces of impurity are sufficient to quench the fluorescence.) Later, a block of plastic material was immersed in the scintillator for several months and a visible amount ofthe block was found to have dissolved. The glass containers all gave a poor response.

Cells were made from quartz tubing with flat quartz plates cemented on the ends. These, too, deteriorated with time, presumably by dissolving the cement. Finally, cells made by welding the quartz were found to give a good performance which remained constant over periods of the order of a year.

Fig.II.8.3. is a photograph of some of the cells used: the large cylindrical box, on which some smaller counters are resting, contains a portion of a sperical shell of radius 25cm.

(c). Contact Fluids.

It was found necessary to make optical contact between the base of the scintillation counter and the glass wall of the photomultiplier on which the photosensitive material is deposited. A gain of a factor of two in pulse height was obtained when the air-gap between these two surfaces was filled with a suitable contact fluid.

The absorption spectra of liquid paraffin, glycerine and

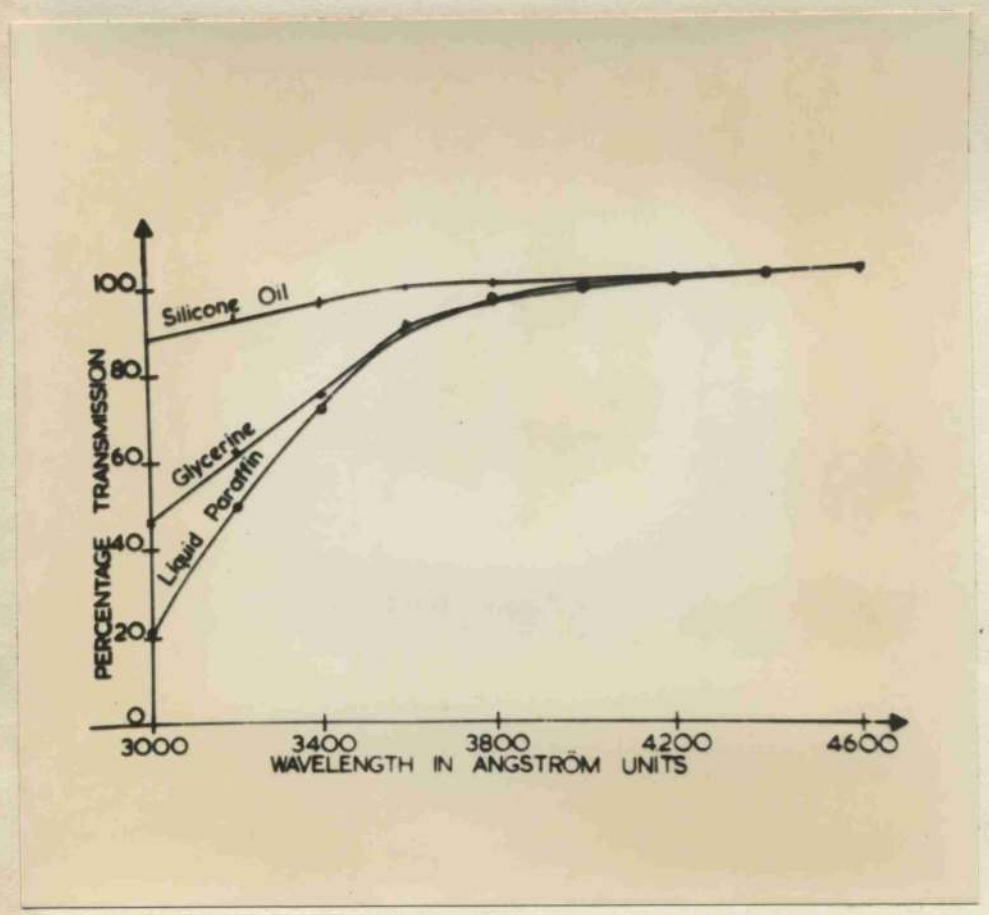

FIG.II.8.4. TRANSMISSION CURVES OF OPTICAL CONTACT FLUIDS.

WAVELENGTH (A°)	3500	4000	4500	5000	5500	6000
REFLECTION COEFFICIENT (%)	96	97.2	98	98.6	99.1	99.7

TABLE II.9.1. THE REFLECTION COEFFICIENT OF MAGNESIUM OXIDE (after BENFORD).

silicone oil were measured, Fig.II.8.4. Silicone oil was chosen as it had the best transmission properties and the additional advantages of low electrical conductivity and high viscosity.

9. REFLECTION EXPERIMENTS.

It was hoped that the difficulties associated with the choice of a suitable material for the container wall might have been overcome by making the container from an opaque but highly reflecting material. Experiments using polished metal containers and glazed white porcelain were, however, unsuccessful.

It was then necessary to find a suitable reflecting material with which to surround the container. The best listed material was magnesium oxide powder. Its reflection coefficient at various wavelengths according to BENFORD (1938) is shown in Table II.9.1.

A special white paint based on titanium oxide and prepared by a local manufacturer was, however, claimed to be a more efficient reflector than magnesium oxide. Experiments to compare the powder and the paint showed that the claims for the paint could not be substantiated. This was probably due to the fact that the binding material of the paint made good optical contact with the container. Consequently there was a greater loss in the amount of light reflected by total internal reflection than when magnesium oxide was used.

It was found that the best results were obtained when the magnesium oxide powder was used in a very dry and very fine state.

10. EXPERIMENTS ON THE DISPLACEMENT OF THE EMISSION SPECTRUM OF THE SCINTILLATOR.

It became clear from the data and the results of the preceding sections that if the terphenyl radiation could be shifted into the region 4500 A^{o} to 5000 A^{o} then

(i) The uniformity of light collection would be improved since the transmission coefficients of the scintillator, the container

Material.	Table II.10.1	Table II.10.2
	Intrinsic Scintillator	Spectral Shifter
	BIAS setting VOLTS	BIAS setting VOLTS
p-terphenyl	40	40
1:2 benzanthracene	6	9
3 hydroxyanthracene	4	4
3 acetoxyanthracene	7	8
3 methoxyanthracene	12	11
fluoranthene	11	8
chrysene	5	24
2 nitroanthene	0	0
dimethoxy 1:2 benzanthracene	11	10
2 aminochrysene	15	11
1 methoxyphenanthrene	16	30
4 methoxyphenanthrene	11	25
anthranalic acid	27	33
α -naphthalamine	32	27
11 methoxyfluoranthene	7	11
4 methoxyfluoranthene	22	18
3,4 dimethylfluoranthene	16	14
1,9 aphenylanthracene	24	31
9 phenylanthracene	25	25
pentaphene	5	9
pyrene	5	15
perylene	19	21
triphenelene	8	/

and the contact fluid and the reflection coefficient of magnesium oxide are nearer unity in this region than in the ultra-violet region.

(ii) It might be possible to increase the effective energy transfer of the scintillator since the photocathode is more sensitive in this region, provided that the terphenyl radiation is not quenched in the process of shifting the spectrum.

Organic materials soluble in xylene and known to absorb in the ultra-violet region and to fluoresce in the visible spectrum were supplied by a group engaged in fluorescence studies in the Chemistry department in this University. These materials were tested as intrinsic scintillators and then as additional solutes in the manner described below.

(a) Intrinsic scintillators.

Solutions of 1 gm/l of the materials under test were made up in xylene. 1 cc of the solution was put in a flat-bottomed speciment bottle of 1" internal diameter which was placed on the photocathode with optical contact fluid. No attempt was made to collect light by reflection. The specimens were irradiated with a Co^{60} γ-ray source held at a fixed distance. The voltage on the photomultiplier and the amplification of the pulses were kept constant and the counting rate was recorded after the pulses had passed through a discriminator. The comparison was made by adjusting the discriminator voltage level so that the counting rate was the same for each sample. A solution of 1 gm/l terphenyl in xylene was included and the counting rate chosen so that the discriminator level for this solution was 40.

It was found that none of the materials tested was as efficient a scintillator as terphenyl (Table II.10.1.) Since the emission spectra of all the materials tested except terphenyl were known to be in the region of maximum sensitivity of the photocathode it followed that they were even poorer scintillators than

the results suggest.

(b). Additional solutes.

These tests were carried out in exactly the same way as those just described. In this case the materials were added in the concentration of 0.2 gm/l to a solution of 4 gm/l terphenyl in xylene. Comparison was made with a solution of 4 gm/l of terphenyl in xylene again normalised at a discriminator setting of 40.

These results are also shown in Table II.10.1. From them it followed that all the materials tested had a quenching effect on the scintillator process in terphenyl in xylene. However, although less light was produced when these additional solutes were present it was reasonable to assume that the light which was produced was in the region of 5000 A^{o}. Thus, if light emitted in directions other than towards the photocathode were also collected by reflection, an overall gain might be achieved since there would be less loss along the optical path.

Accordingly, solutions were made up of 5 gm/l terphenyl in xylene and of 5 gm/l terphenyl in xylene plus varying concentrations of anthranilic acid. Anthranilic acid had been found to have the least quenching effect. These were put into cylindrical cells 1" in diameter and $2\frac{1}{2}$" long and surrounded by magnesium oxide in the manner described in II.2. These were irradiated with Co^{60} γ-rays and the maximum pulse heights measured. The best result was obtained with an additional concentration of 0.1 gm/l anthranilic acid: pulses from this solution were approximately 50% greater than from unadulterated terphenyl in xylene. Further experiments, similar to those mentioned in II.5.b, on the variation of pulse height along a long scintillator showed that the light collection was more uniform when the additional solute was present. This solution, 5 gm/l terphenyl + 0.1 gm/l anthranilic acid in xylene was used in all the work described later.

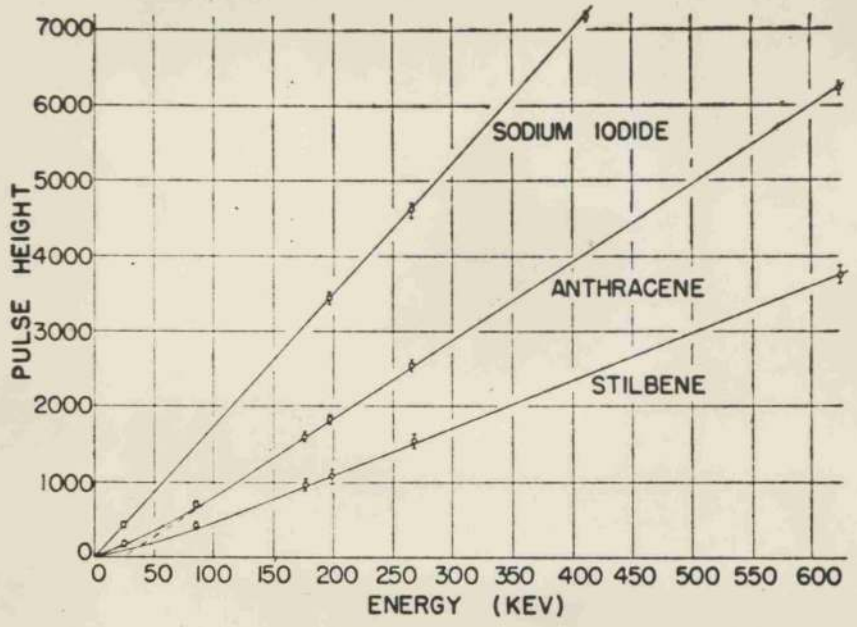

FIG.II.11.1. PULSE HEIGHT v ENERGY FOR ELECTRONS IN CRYSTAL SCINTILLATORS (after TAYLOR et al).

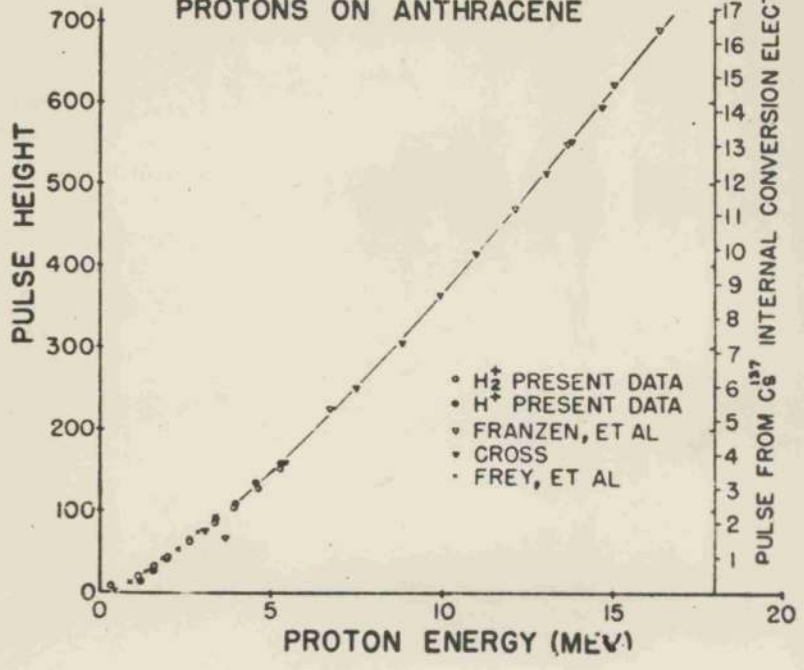

FIG.II.11.2. PULSE HEIGHT v ENERGY FOR PROTONS IN ANTHRACENE (after TAYLOR et al).

11. RESPONSE OF THE SCINTILLATORS TO PROTONS AND ELECTRONS.

In order to estimate the performance of many designs of fast neutron spectrometers it is necessary to know the variation of the conversion efficiency of the scintillator as a function of proton energy. Also, for test purposes, it is often convenient to use γ-rays: this involves knowing the variation of the conversion efficiency as a function of electron energy.

The variation in the light output from anthracene crystals as a function of the energy of electrons and protons incident upon the crystals has been investigated several times (FRANZEN et al, 1950; FREY et al, 1951; TAYLOR et al, 1951). All the results agree well and have been plotted, with their own results, by TAYLOR et al. They are shown in Figs.II.11.1 and 2. The relation is linear for electrons of more than 100 kev. For protons the curves may be used directly. However, it is found, to a fair approximation that their results are fitted by

$$L \propto E^{1.3} \qquad \text{II.11.1.}$$

where L is the light output and E the energy of the incident particle, for values of E up to about 14 Mev. Thereafter L tends to a linear function of E.

There is little published data on the response of other organic scintillators to ionizing particles. The response of stilbene to protons (TAYLOR et al) is approximately of the same form as anthracene. The response of terphenyl in xylene to α-particles has been investigated by HARRISON (1952). He compares his results with a theoretical expression due to BIRKS (1951). This expression states that

$$\frac{dL}{dr} = \frac{A\frac{dE}{dr}}{1+B\frac{dE}{dr}} \qquad \text{II.11.2.}$$

where A and B are constants and

$\frac{dL}{dr}$ = light output per unit path length.

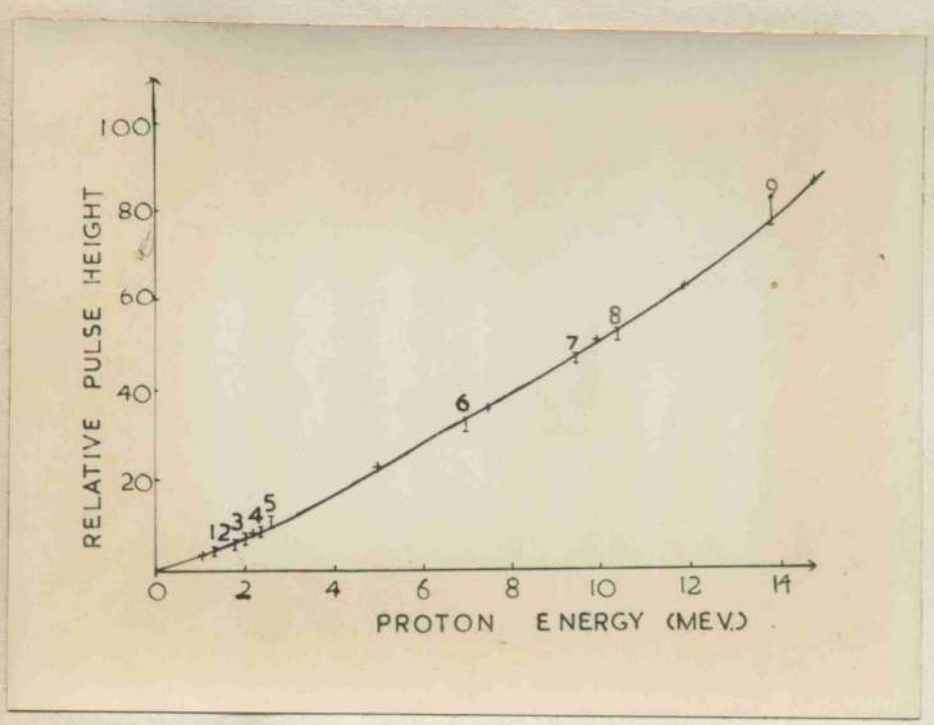

1. Double scattering of D-D neutrons at $\theta = 45^{o}$.
2. $\theta = 56^{o}$.
3. $\theta = 64^{o}$.
4. $\theta = 77^{o}$.
5. D-D neutrons single counter edge.
6. Double scattering of D-T neutrons at $\theta = 45^{o}$.
7. $\theta = 56^{o}$.
8. $\theta = 60^{o}$.
9. D-T neutrons single counter edge.

+ points are the results of TAYLOR et al for anthracene normalised.

FIG.II.11.3. PULSE HEIGHT v ENERGY FOR PROTONS IN TERPHENYL IN XYLENE.

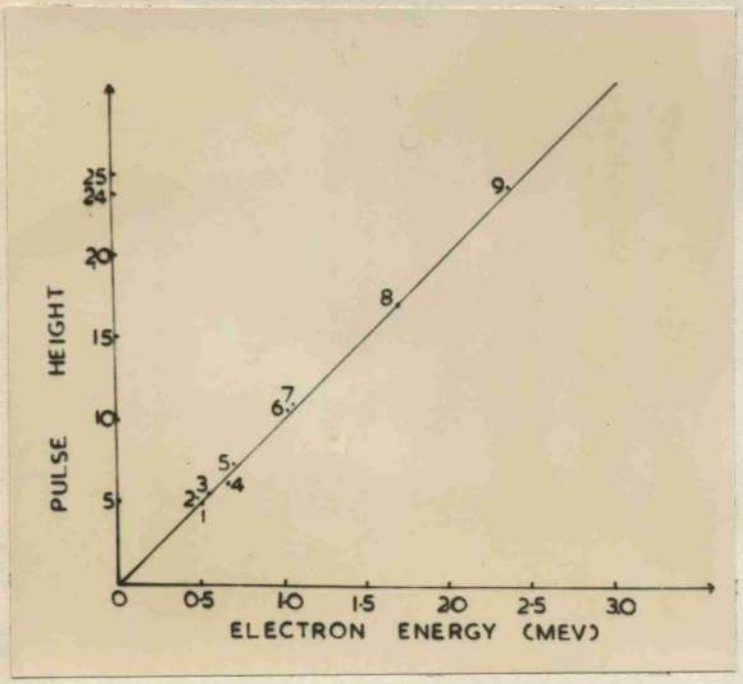

1. Na^{22} at 0.5 Mev.
2. Co^{60} 1.17 Mev at 56^{o}
3. Co^{60} 1.34 Mev at 56^{o}
4. Cs^{137}
5. Na^{22} 1.28 Mev at 52^{o}
6. Na^{22} Compton Edge.
7. Co^{60} Compton Edge.
8. ThC" 2.62 Mev at 52^{o}
9. ThC" Compton Edge.

FIG.II.11.4. PULSE HEIGHT v ENERGY FOR ELECTRONS IN TERPHENYL IN XYLENE.

and $\frac{dE}{dr}$ = loss of energy per unit path length.

HARRISON found good agreement between his experimental results and BIRKS' calculated values of the constants. HARRISON also calculated, using the appropriate values of the constants, that the non-linearity of the response to protons of terphenyl in xylene (at the optimum concentration of 5 gm/l) would be approximately the same as for anthracene.

(a). Experimental Determination of the Response of Terphenyl in Xylene.

No data has previously been published to verify these calculations. However, the response of this liquid to protons was investigated indirectly in experiments on the scattering of neutrons which are discussed later. It was found that by applying a suitable normalising factor, to allow for the different conversion efficiencies, the results thus obtained for terphenyl in xylene could be plotted as a good fit to the results of TAYLOR et al for anthracene. The results, plotted in this way, are shown in Fig.II.11.3.

The response of terphenyl in xylene to electrons was also measured indirectly in experiments on the scattering of γ-rays. The response was found to be linear over the region investigated (0.5 Mev to 3 Mev). These results are shown in Fig.II.11.4.

The keys to Figs.II.11.3 and 4 refer to the experiments from which each point was obtained: explanation of the nomenclature is given in the later description of the experiments (Section IV.2(v)).

12. DETECTION EFFICIENCY OF THE SCINTILLATOR.

(a) Neutrons.

If the neutrons of energy E fall upon a thickness l of scintillator, then the fraction of neutrons incident upon the scintillator which are scattered once by protons is readily found.

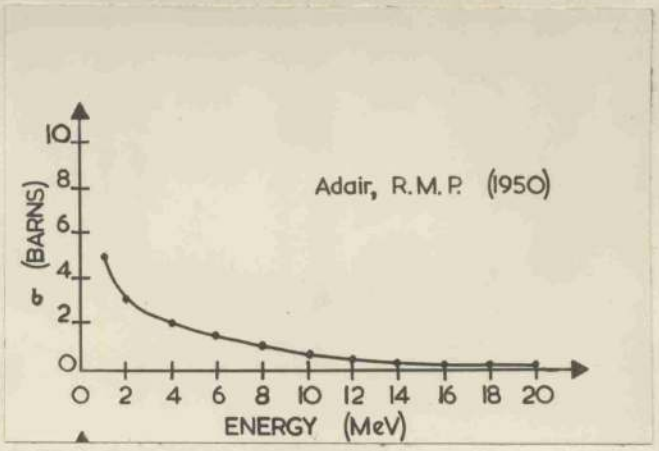

FIG.II.12.1. NEUTRON-PROTON SCATTERING CROSS-SECTION.

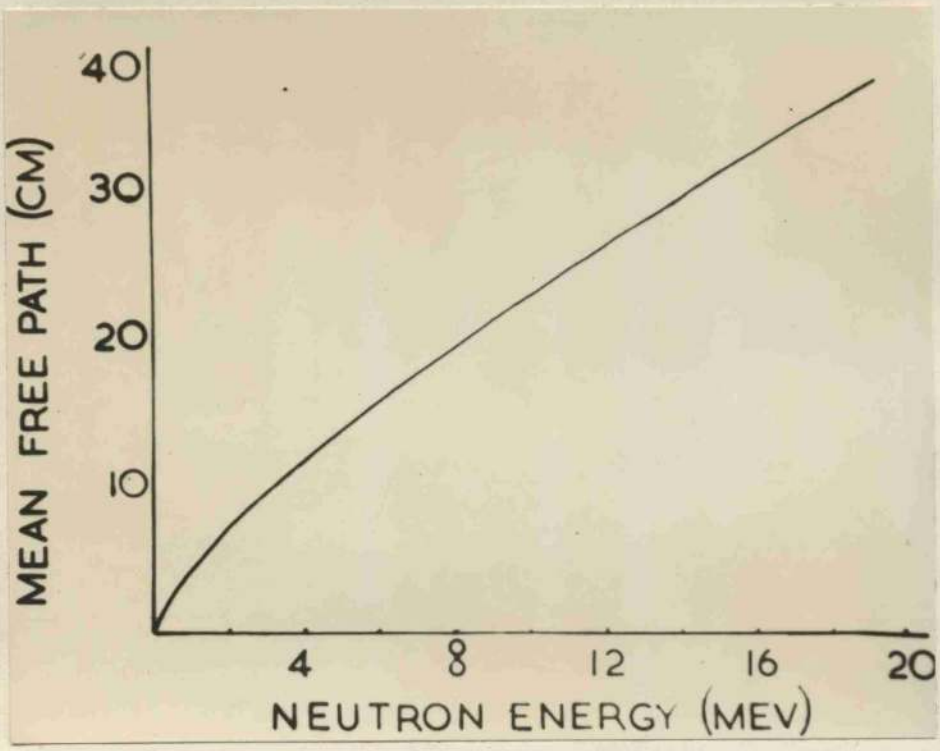

FIG.II.12.2. MEAN FREE PATH OF NEUTRONS IN XYLENE.

If the n-p scattering cross-section corresponding to E is σ, and the number of hydrogen nuclei per unit volume of the scintillator is n, then the fraction scattered once is given by

$$\varepsilon = 1 - e^{-n\sigma l} \qquad \text{II.12.1.}$$

ε is the neutron detection efficiency of the scintillator. For a scintillator whose thickness is small compared with the neutron mean free path λ ($= 1/n\sigma$) the efficiency is given by

$$\varepsilon = l/\lambda \qquad \text{II.12.2.}$$

The mean free path in xylene (which was calculated from the values of σ for protons given by ADAIR, 1950, Fig.II.12.1.) as a function of neutron energy is shown in Fig.II.12.2. Fig.II.12.3. gives ε as a function of scintillator thickness for several values of neutron energy.

The values of λ and ε shown are valid to within a few per cent for most organic scintillators since the number of hydrogen nuclei per unit volume is approximately constant for these materials. It follows that extremely high detection efficiencies, of the order of 20% or 30% may be obtained over the range of neutron energies 1 to 20 Mev with a few centimetres of organic scintillator.

(b) γ-rays.

The detection efficiency of the scintillator for γ-rays, ε_γ, defined in the same way as for neutrons, is also of importance in estimating the response of neutron spectrometers to γ-rays.

$$\varepsilon_\gamma = 1 - e^{-\mu_l l} \qquad \text{II.12.3.}$$

where μ_l is the total linear absorption coefficient in the scintillator. Fig.II.12.4 shows the linear absorption coefficients of xylene for Compton scattering and pair production for γ-rays up to 10 Mev: Compton scattering is the predominant effect at these energies. The curves were derived from the data on lead given by HEITLER (1936). is plotted as a function of γ-ray

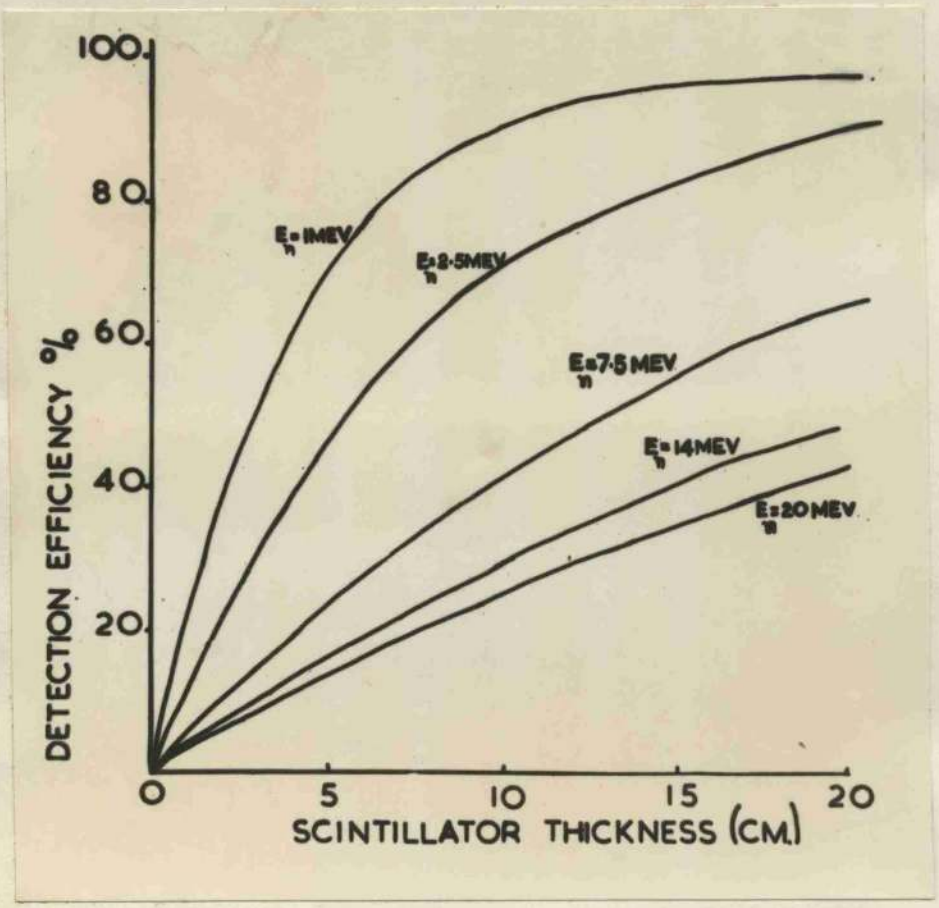

FIG.II.12.3. DETECTION EFFICIENCY OF TERPHENYL IN XYLENE FOR NEUTRONS.

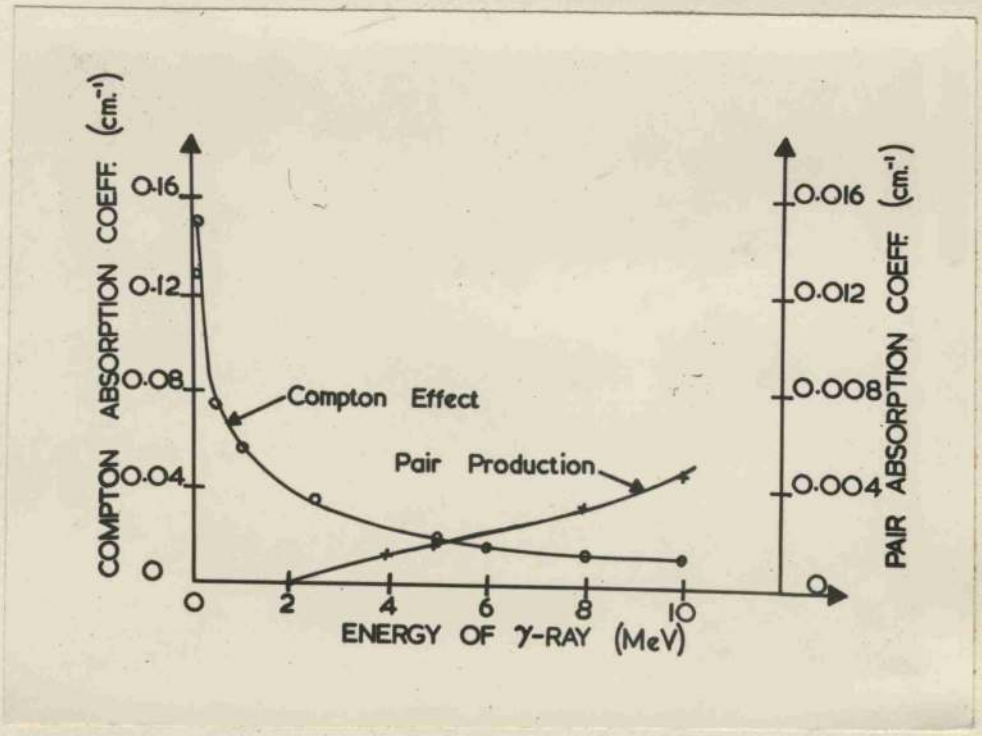

FIG.II.12.4. ABSORPTION COEFFICIENTS FOR XYLENE.

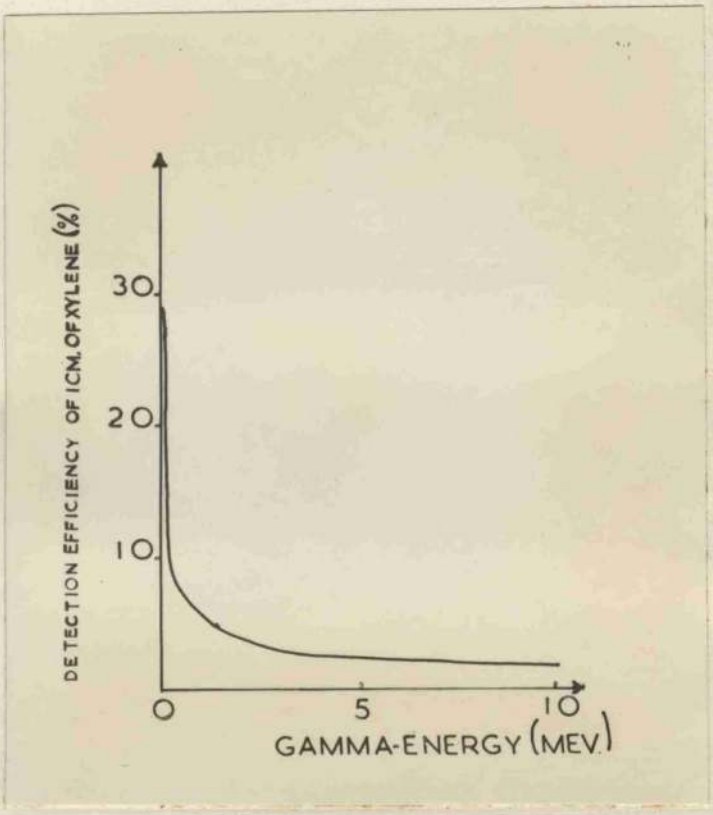

FIG.II.12.5. DETECTION EFFICIENCY OF XYLENE FOR γ-RAYS.

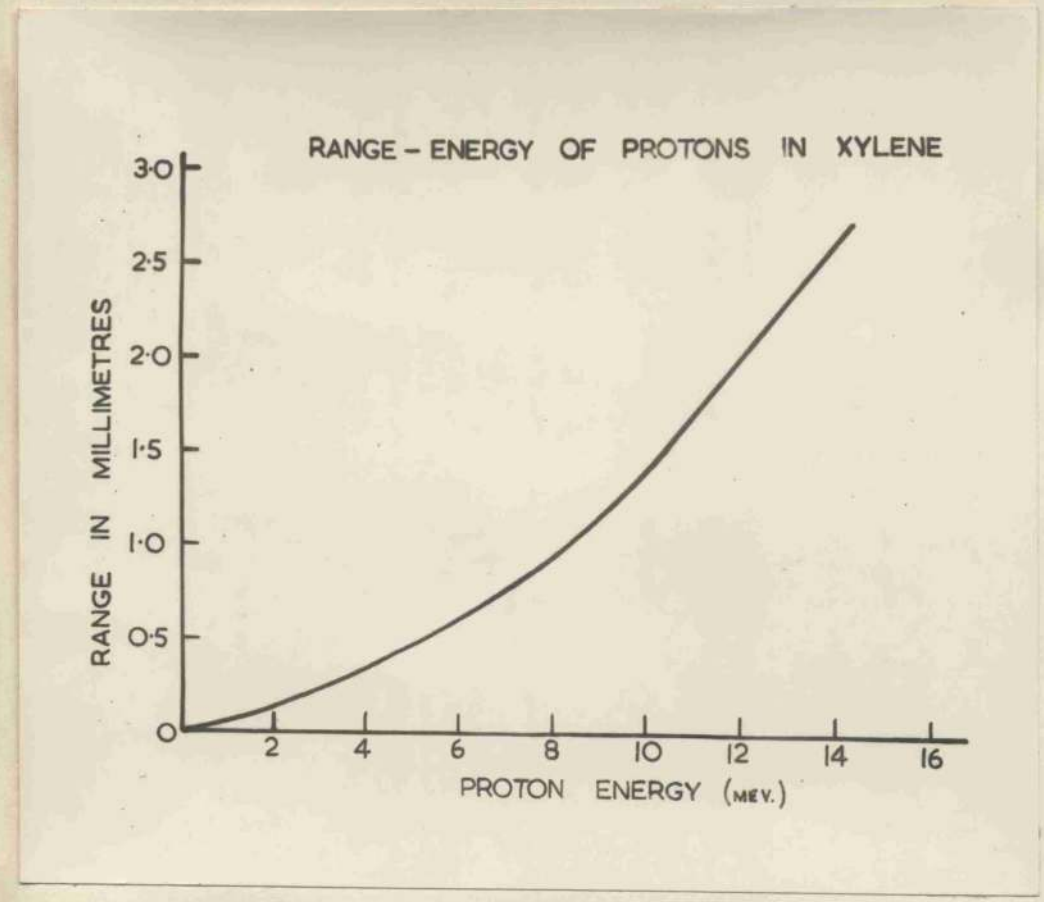

FIG.II.13.1.

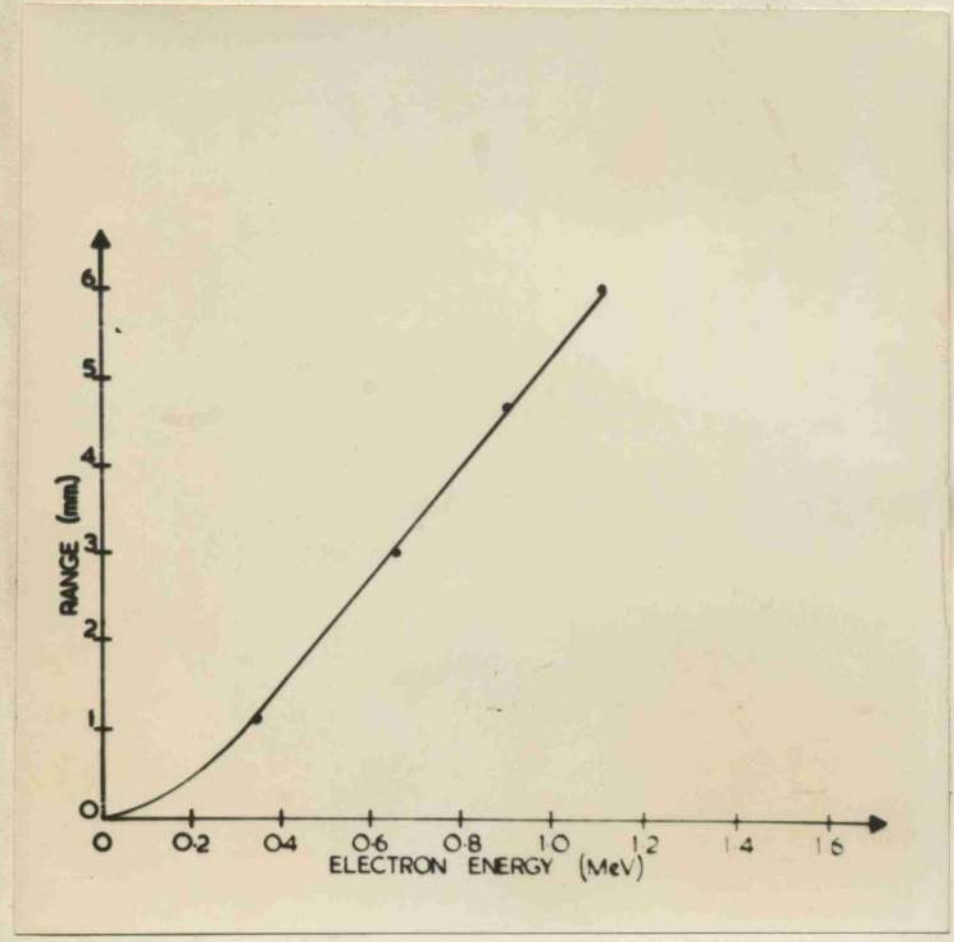

FIG.II.13.2.
RANGE ENERGY OF ELECTRONS IN XYLENE.

energy for ℓ = 1 cm in Fig.II.12.5. Comparison of Figs. II.12.3 and 5 shows that the scintillator detects γ-rays and neutrons with approximately the same efficiency.

13. RANGES OF PROTONS AND ELECTRONS IN THE SCINTILLATOR.

The finite ranges of recoil protons and electrons may have considerable effect on the performance of spectrometers exposed to neutrons and to γ-rays. The effects, as will be seen, may also be turned to advantage. Accordingly, the ranges of protons and electrons in xylene were calculated.

The range energy relationship for protons in xylene is shown in Fig.II.13.1. and for electrons in Fig.II.13.2. The curve for protons was calculated from the stopping powers for carbon and hydrogen given by LIVINGSTON and BETHE (1937) and the curve for electrons was derived from the range-energy relationship for electrons in aluminium given by the same authors.

III. SINGLE SCINTILLATOR SPECTROMETERS.

1. INTRODUCTION.

If a volume of scintillator is exposed to a source of neutrons then proton recoils will be formed in the scintillator. If the scintillator is viewed by a photomultiplier, whose output is fed into a pulse analyser, then a distribution of pulses will be obtained from the analyser.

An ideal scintillator would satisfy certain conditions: recoil protons of a given energy in the scintillator would produce pulses of a unique size at the multiplier output; the pulses would be independent of the point of origin in the scintillator of the recoils and the recoils would have zero path length. If such an ideal scintillator were exposed to a neutron source then the pulse height distribution obtained would depend on the neutron energy spectrum and the size, shape and orientation with respect to the neutron source of the scintillator. It should then be possible to choose geometries for the scintillator in such a way that particularly simple distributions would be obtained from which the energies and intensities of the neutrons emitted by the source could be deduced either at once or after very little calculation.

Practical scintillators fail to satisfy the ideal conditions specified: the failure is caused by a variety of factors which have been discussed in Part II. When practical scintillators are arranged in geometries that would, ideally, lead to simple distributions, these factors cause distortions to appear in the observed distribution. In some arrangements the distortions are so great as to make the distributions useless for the analysis of neutron spectra. In certain arrangements, however, the effect of the distorting factors may be minimised and the distributions may be analysed, usually after considerable calculation.

Such simple arrangements are, of course, sensitive to γ-rays. This limits their utility although, by careful choice of the scintillator dimensions, the pulses corresponding to γ-rays can, in certain experiments, be sufficiently attenuated whilst the distribution corresponding to neutrons is relatively unaffected.

No simple scintillator arrangement has yet been produced which satisfies all the requirements for a fast neutron spectrometer. However, the simplicity of the experimental arrangement required has much to recommend it and, in certain experiments, useful information can be acquired fairly quickly and easily using a single scintillator. Accordingly in this part of the thesis some possible choices of single scintillator geometry are discussed and experiments which were performed with them are described; similar experiments by other workers are also analysed briefly. Some of the discussion is rather more detailed than the utility of this type of arrangement would appear to warrant. It has been included, however, because of its relevance to the more refined techniques described later.

Another approach to the use of a single scintillator as a spectrometer is described in Section 4. In that case it was attempted, not to minimise the effects of the deviations from an ideal scintillator of a practical scintillator, but to emphasise and to turn to advantage the fact that the proton recoils have finite ranges.

This part of the thesis concludes with a very brief description of a single scintillator spectrometer which was constructed by Shields after an idea by Muelhause. In this arrangement a slow neutron detector is introduced into the scintillator. This leads, in principle, to several advantages including good γ-ray discrimination. It involves, however, more complicated electronic auxiliaries and was, in practice, not very successful. The description is included here in order to complete the survey of

single scintillator devices and because, with the changes in design suggested here, it might be sufficiently improved to be useful at higher neutron energies. That is the region where the performance of the time-of-flight spectrometer described in Part IV begins to decline.

2. A TOTAL ABSORPTION SPECTROMETER.

(a) The Principle.

The first logical choice for the geometry of a single counter is to choose the counter to be so large that most of the neutrons incident upon it are totally absorbed. It follows from the high detection efficiencies available that this is practicable. In this case, the distribution obtained will approximate to the distribution obtained from an infinite volume.

If an infinite volume of ideal scintillator were irradiated with monoenergetic neutroms then the pulse height distribution obtained would be an infinitely narrow line whose position and height would lead to the energy and intensity of the neutrons. For a finite but large volume of scintillator the line would be spread into a narrow peak.

(b) Effect of Distorting Factors; Conclusions.

In practice, such a large volume of scintillator would lead to a very broad peak whose resolution would be well outside the limits of usefulness.

Each pulse in the distribution is the sum of the pulses corresponding to all the recoils formed by one particular neutron in being reduced to thermal velocities. Since the response of the scintillator is non-linear a group of monoenergetic neutrons would therefore lead to a distribution of pulses varying from zero up to the maximum possible pulse. An approximate calculation based on a non-linear response, $L \propto E^{1.3}$, shows that the distribution would be a broad peak with mean pulse height slightly less than two-

thirds of the pulse corresponding to a head-on recoil. The resolution of the peak would be approximately 50%.

The effect of non-uniform light collection would further spread this peak and the arrangement would be extremely sensitive to γ-rays.

3. A SINGLE SCATTERING SPECTROMETER.

(1) The Principle and Theoretical Distribution.

The spectrometer which is described now follows logically as being the next in simplicity. The same difficulties that are encountered in a total absorption spectrometer are inherently present in this method but, under certain circumstances, may be sufficiently mitigated to make it a practical and useful technique.

The arrangement again consists of a simple scintillation counter connected directly to a pulse analyser. In this case, however, the dimensions of the scintillator are chosen so that, ideally, neutrons which are scattered in the scintillator are scattered once only and the energy of every recoil proton is dissipated entirely within the scintillator. Also, ideally, the response of the scintillator to protons would be linear and protons of a given energy would yield pulses of a unique size.

If neutrons of energy E and source intensity I fall upon this (idealised) counter and cause N_o (single-scatter) recoils then it follows from the consideration of I.5 (ii) that the resulting pulse height distribution will be given by

$$\frac{dN}{dL} = N_o/L_o, \quad L \leq L_o; \quad \frac{dN}{dL} = 0, L > L_o, \qquad \text{III.3.1.}$$

where L_o is the pulse resulting from a head-on recoil. The energy of the neutrons is proportional to L_o and the source intensity is given by

$$I = \omega/\sigma \int_o^{L_o} \frac{dN}{dL}\, dL$$

$$= \omega N_o/\sigma \qquad \text{III.3.2.}$$

where ω is the solid angle subtended at the source by the counter and σ is the n-p scattering cross-section corresponding to E. In practice, only pulses above a minimum value B are analysed. In that case, if the number of pulses counted is N_B, then

$$I = \frac{\omega}{\sigma} \frac{N_B L_0}{L_0 - B} \qquad \text{III.3.2}$$

If the source contains several homogeneous groups of neutrons of different energies then the pulse height distribution is the sum of the individual distributions. That is, a series of steps. The energies may be deduced from the edges of the steps and the intensities from the extrapolated individual contributions.

(ii) Choice of Dimensions in Practice.

In practice it is not possible to choose the dimensions of the scintillator to satisfy exactly the first two ideal conditions specified above. This follows from consideration of the mean free path of neutrons and of the ranges of protons in xylene given in Sections II.12 and 13. However, choices can be made which give an approximation to these conditions. It is not profitable at this point to discuss at length the possible choices but an example is given to illustrate the significant points which must be observed.

A suitable choice would be a scintillator which was symmetrical about the line of flight of the neutrons from the source; for example, a cylinder with axis pointing at the source. To determine the diameter and length of this cylinder an average neutron-proton collision may be considered; that is, a collision at the centre of the cylinder in which both the neutron and the proton are scattered at 45° to the incident beam.

If the diameter of the cylinder is D, the range of the scattered proton R_{45} and the mean free path of the scattered neutron λ_{45}, then it follows from the values given in Sections II.12 and 13 that it is possible to choose D such that, for neutrons over most of the range 1 to 20 Mev,

$$\lambda_{45}/10 < D\sqrt{2} < 10R_{45} \qquad \text{III.3.4.}$$

Similarly, the length, L, of the cylinder may be chosen so that

$$\lambda_o/10 < L < 10R_o \qquad \text{III.3.5.}$$

where λ_o is the mean free path of an incident neutron and R_o the range of a head-on recoil.

With L and D chosen within these limits it would be expected that the observed distribution would correspond predominantly to the single-scattering desired. In practice, however, both edge-effects and multiple-scattering still markedly affect the observed distribution: these effects are considered below.

(iii) Energy Resolution and Intensity Measurement.

In practice, departures from all the ideal conditions specified are inevitable and cause the observed distributions to exhibit considerable deviations from the ideal distribution. These deviations affect both the energy resolution and the accuracy of the intensity measurements obtainable with this spectrometer.

The resolution obtainable is determined by the sharpness with which the leading edges of the steps are reproduced in practice. The resolution of each step may be related to the peak obtained by differentiating each step with respect to L. In this discussion the resolution will be taken as the ratio of the full width at half maximum height of this peak to the pulse size at the centre of the peak. For the distribution given by equation II.3.1. it is, of course, zero.

The accuracy of the intensity measurement depends on the extent to which the shape of each individual distribution can be calculated so that it may be extrapolated from the total distribution. This demands that the effects of the departures from the ideal conditions be calculable: these are considered now.

(iv) Distorting Effects.

(a) Statistical Fluctuations; Non-uniform light collection; electronic fluctuations.

Statistical fluctuations have been considered in Section II.5. Their effect in the present case is to make the observed distribution the sum of all the gaussian distributions corresponding to all the proton recoils. An integral expression for the resultant pulse height distribution may readily formulated; it may be expressed by

$$\frac{dN_l}{dL} = \int_0^\infty \frac{\alpha e^{-\left(\frac{L-l}{\Gamma_l}\right)^2}}{\Gamma_l} \frac{dN}{dL} dl \qquad \text{III.3.6.}$$

where α is a constant, Γ_l the full width at half height of a pulse l, and $\frac{dN}{dl}$ is given by the equation II.3.1. That is

$$\frac{dN_l}{dL} = \alpha \frac{N_0}{L_0} \int_0^{L_0} \frac{e^{-\left(\frac{L-l}{\Gamma_l}\right)^2}}{\Gamma_l} dl \qquad \text{III.3.7.}$$

Evaluating the integral, the distribution is given, to a good approximation by the ideal distribution of II.1.3.with the front edge spread over L values from $L = L_0 - \Gamma_{L_0}$ to $L = L_0 + \Gamma_{L_0}$.

The effect of the statistical fluctuations on the resolution may be obtained by differentiating equation III.3.7. with respect to L. To a good approximation it is given by

$$R = \Gamma_{L_0}/L_0 \qquad \text{III.3.8.}$$

That is, the resolution of the gaussian distribution resulting from the head-on recoils. In principle, therefore, no resolving power is lost by using this method in which a homogeneous group of neutrons gives rise to a continuous distribution of recoil energies. Limits for the resolution obtainable in practice have already been calculated in Section II.5.

Calculation of the intensities of the groups of a complex neutron spectrum is unaffected by the statistical fluctuations

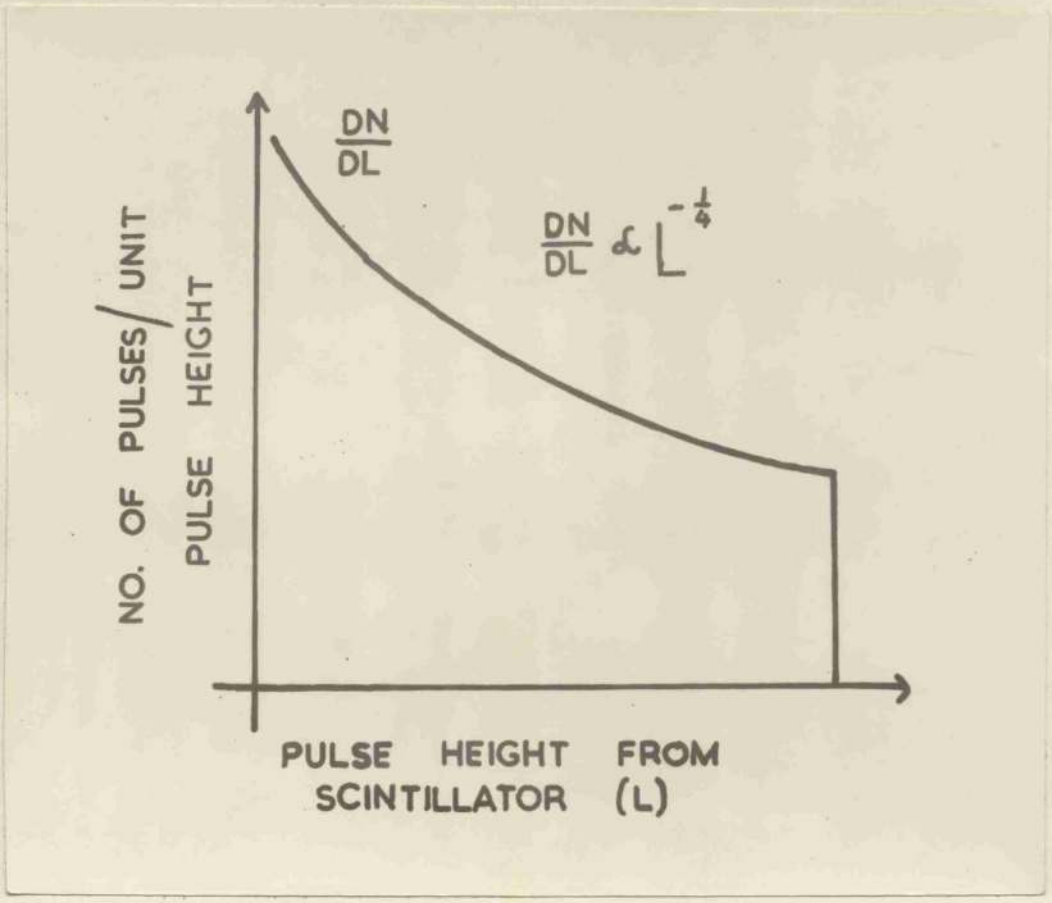

FIG.III.3.1. EFFECT OF NON-LINEAR RESPONSE ON SINGLE SCATTERING DISTRIBUTION.

provided that they can still be resolved: if N_1 pulses greater than B are observed, then

$$N_1 = \int_B^\infty \frac{dN}{dL} dL \qquad \text{III.3.9.}$$

Then, provided $B < L_0 - \Gamma_{L_0}$, to a good approximation,

$$N_1 = \frac{L_0 - B}{L_0} N_0 \qquad \text{III.3.10.}$$

Non-uniform light collection was also considered in Section II.5. With the scintillators employed in the experiments described below the effect on the resolution was negligible.

Drifts in the supply voltages for the electronic analyzing equipment introduce a further decrease in the resolution. The effect, with the well-stabilized equipment used, was again negligible. The effect of the finite channel width of the analyzer was also small compared with the other factors affecting the resolution.

(b) Non-linear response of the scintillator.

If the response of the scintillator is given by

$$E = g(L) \qquad \text{III.3.11.}$$

then the pulse height distribution due to this effect is given by

$$\frac{dN}{dL} = \beta \frac{dg}{dL}, \text{ for } L \leq L_0; \frac{dN}{dL} = 0, \text{ for } L > L_0 \qquad \text{III.3.12.}$$

where β is a constant, since the distribution of recoil energies is uniform in the centre-of-mass system. It was seen in Section II.12 that for the scintillator used

$$L \propto E^{1.3} \qquad \text{III.3.13.}$$

which leads to a distribution given, to a good approximation, by

$$\frac{dN}{dL} \propto L^{-\frac{1}{4}} \qquad \text{III.3.14.}$$

This distribution is shown is Fig.III.3.1.

The effect of this distortion combined with the statistical

fluctuations is obtained by substituting the value of $\frac{dN}{dL}$ given by equation III.3.12. in equation III.3.6. The resultant distribution is approximately that of equation III.3.14. with the front edge spread over L values from $L_o - \Gamma_{L_o}$ to $L_o + \Gamma_{L_o}$, provided the g(L) is not a very rapidly varying function of L. This is, in fact, the case in the present instance so that the combination of these two distortions has little effect on the resolution obtained in equation II.3.8.

In calculating the intensity of each group of a complex spectrum, each group must be extrapolated using equation III.3.14. For any group, if N_2 pulses greater than B are observed, then

$$N_2 = \frac{g(L_o) - g(B)}{g(L_o)} \qquad \text{III.3.15.}$$

(c) Multiple-scattering.

Some multiple-scattering of the neutrons in the scintillator is inevitable however the dimensions are chosen. For any particular case it is always possible to calculate the expected distribution allowing for this effect. However, in all cases the calculation demands numerical integration. The integrations are complicated by the non-linearities of the response of the scintillator and the mean free path of the neutrons as a function of neutron energy.

Since detailed calculation of particular geometries would be of little utility, the discussion here is general and mainly qualitative and is illustrated below by reference to observed distributions.

In Section III.2.(ii) it was seen that a total absorption spectrometer with non-linear response, $L \propto E^{1.3}$, would give a broad peak with mean pulse height slightly less than two-thirds of the pulse corresponding to head-on recoils. The same peaking effect tends to occur in small scintillators where relatively

little multiple-scattering takes place. Pulses corresponding to neutrons which have scattered more than once are displaced towards the high energy end of the distribution. However, the width and position of the peak due to neutrons which have scattered more than once will vary with the geometry of the arrangement. For example, the geometry of the arrangement may be chosen so that only neutrons which have initially scattered through large angles have an appreciable probability of being scattered again. This would lead to a comparatively narrow peak with the maximum nearer to pulses corresponding to head-on recoils.

In general, if the linear dimensions of the scintillator are all of the same order of magnitude, then neutrons which have initially scattered at all angles have an appreciable probability of being scattered again. Of course, neutrons which have initially scattered through large angles are preferred for secondary scattering to some extent owing to their reduced mean free path.

Thus, in general some multiple scattering tends to cancel the distortion due to non-linear response. As the proportion of neutrons which are scattered more than once rises, a noticeable peak occurs near, but not at, the leading edge of the single-scattering distribution. In all cases, however, the net effect is to decrease the resolution of the leading edge, since the edge tends to rise towards the maximum of the broad peak (concealed or evident) which corresponds to those neutrons which have been scattered more than once. The decrease in resolution will depend on the proportion of neutrons which are scattered more than once and, of those neutrons, the proportion initially scattered through large angles.

(d) Edge effects.

Some of the recoil protons which acquire energy in collisions near a wall of the scintillator may dissipate part of their energy in the wall and give reduced pulses. The calculation of this effect involves the same sort of difficulties that are encountered

with multiple-scattering. A general picture of the effect of this distortion on the observed distribution may be gained as follows.

The effect is limited to small volumes at the surfaces of the scintillator. The expected distribution from these small volumes (allowing for the edge-effects) may be calculated and added to the distribution from the remainder of the scintillator in proportion to the relative volumes.

Some approximate calculations have been made of the pulse height distribution at two typical boundaries. The range of a proton, R_θ, is given approximately by $R_\theta = R_0 \cos^{2.6}\theta$, where θ is the angle through which the proton recoils relative to the direction of motion of the neutron which strikes it. It follows that, at faces parallel to the direction of incidence of the neutrons, protons which recoil at very large and very small angles are little affected. Very approximately, for all organic scintillators, the pulse height distribution at such a face is given by

$$\frac{dN}{dL} \propto \frac{1}{L^2} \qquad \text{III.3.16.}$$

for all L except in the region $L = L_0$, where the distribution rises slightly. At a face perpendicular to the direction of incidence of the neutrons, head-on recoils are most affected. Very approximately, the distribution is given by

$$\frac{dN}{dL} \propto \frac{1}{L} \qquad \text{III.3.17.}$$

If follows from the form of equations III.3.16 and 17 that edge-effects do not have a deleterious effect on the resolution of the leading edge of the single scattering distribution.

(v) Response to γ-rays.

(a) Theoretical Distribution.

If the scintillator is exposed to a source of γ-rays (whose energies are in the range 1 to 10 Mev) then the observed pulse

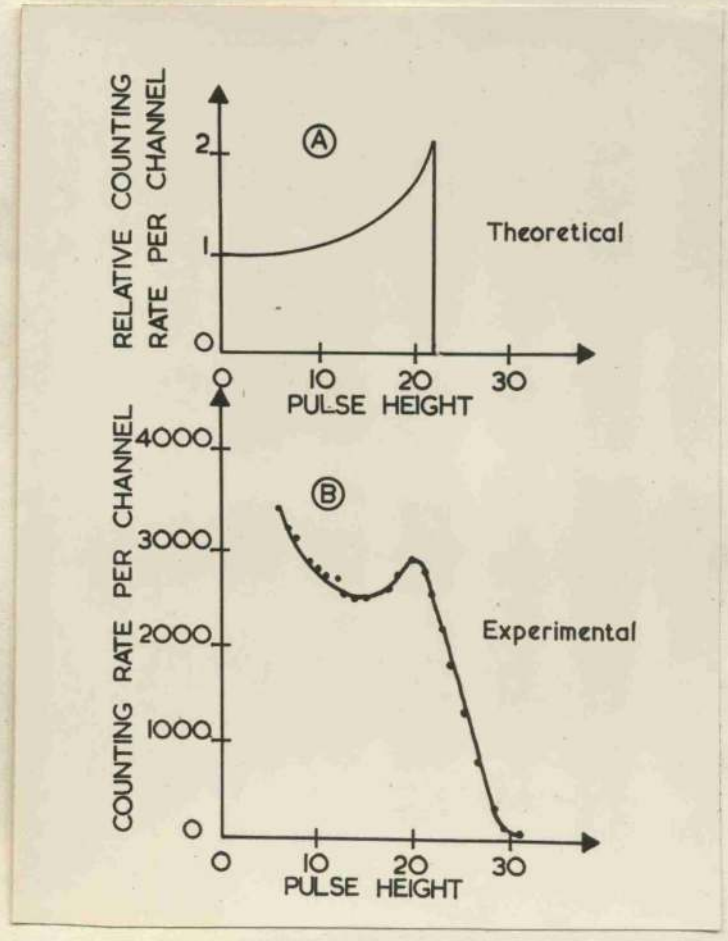

FIG.III.3.2.

FIG.III.3.5.

SINGLE SCATTERING DISTRIBUTION
FROM γ-RAYS.

height distribution will correspond to electrons which have acquired their energies as the result of Compton scatterings of the γ-rays. For single-scattering events only, the distribution in energies of the recoiling electrons is given by the Klein-Nishina formula (See HEITLER, 1936). Since the response of the scintillator is linear for electrons of more than 100 kev, the pulse distribution should also have the same form: this distribution is shown in Fig.III.3.2.

(b) Distorting effects: Resolution.

The same distorting factors affect the distribution obtained in practice with γ-rays as affect that obtained with neutrons. The major differences in these effects is that for electrons the response is linear as opposed to the non-linear response to protons; the dependence of the energies of scattered γ-rays (and their intensities) on angle of scattering is different from that for neutrons which leads to less double-scattering; the longer ranges of the recoil electrons leads to more edge-effects, though this effect is slightly compensated for by the fact that the tracks of the recoil electrons are not straight.

In practice the leading edge of the distribution (which corresponds to head-on recoils) observed is not vertical: the energy of the γ-rays may be found by differentiating the distribution observed and finding the pulse height at the centre of the peak obtained in this manner. The resolution is then again defined as the ratio of the full width at half maximum height of this peak to the mean pulse size.

(vi) Experimental Arrangement and Results.

Scintillators of various sizes and shapes were exposed to the neutrons from the D-D and D-T reactions, γ-rays from natural and artificially-produced γ-emitting isotopes, and to the products of the reaction $B^{11}(d,n)C^{12}$. The D-D and D-T reactions were induced with the 50 kev H.T. Set (See Appendix B) and the $B^{11}(d,n)C^{12}$

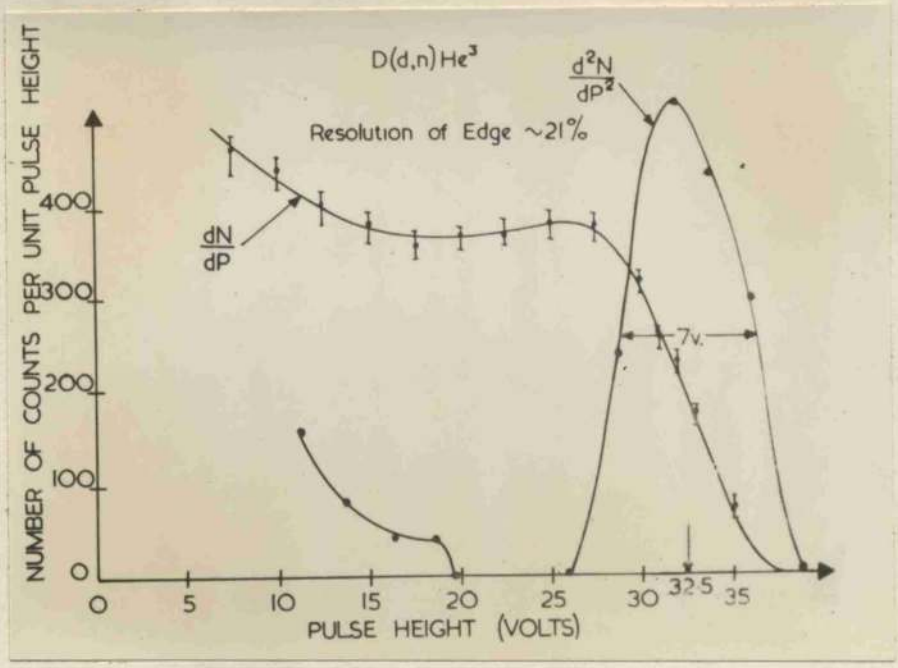

FIG.III.3.3. DISTRIBUTION FROM D-D NEUTRONS ON SINGLE COUNTER.

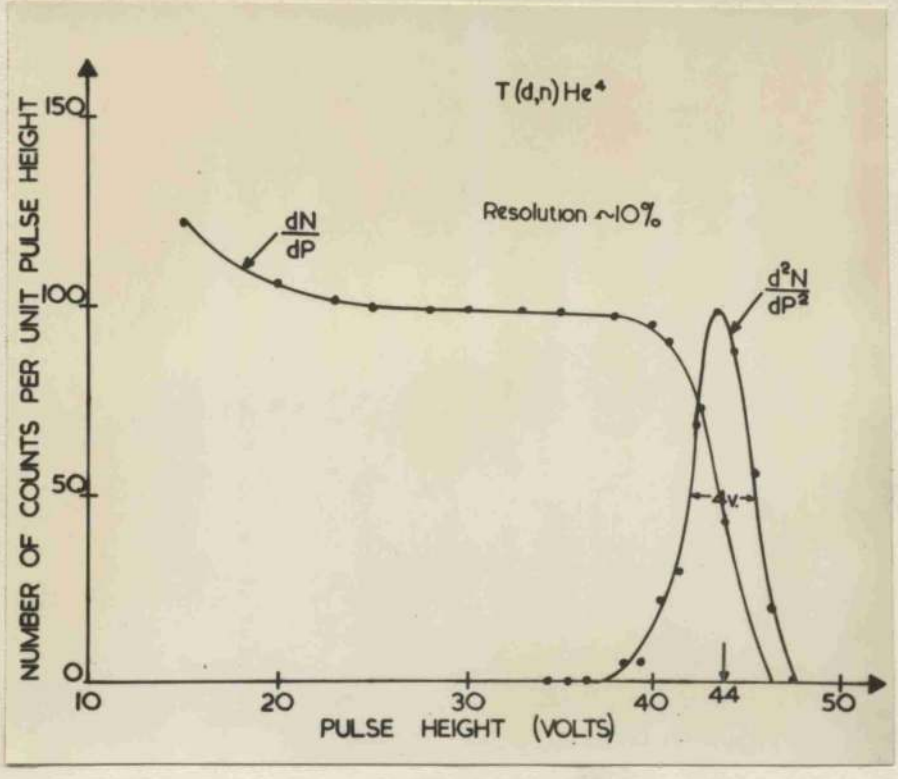

FIG.III.3.4. DISTRIBUTION FROM D-T NEUTRONS ON SINGLE COUNTER.

reaction was induced with the Departmental 1 Mev H.T. Set.

The experimental arrangement of the scintillation counter was in all cases that shown in Fig.II.2.1. Various methods of pulse analysis after amplification were used. Firstly, the pulses were lengthened and brightened (at maximum height) and displayed on a C.R.O. screen: they were photographed and counted after re-projection. (The lengthening and brightening units are described in Appendix C) Secondly, a single-channel pulse analyser was used. All the results given here were obtained using a 100 channel, HUTCHINSON and SCARROT (1951), pulse analyser of which the channel width was stable to the order of 1 in 1000. All electronic supplies were also stable to this order. The distributions shown here were obtained with a cylindrical counter 1" in diameter and 1" long: in each case the axis of the cylinder was arranged to point at the source.

(a) D-D neutrons.

The distribution obtained when the scintillator was exposed to 2.6 Mev neutrons from the D-D reaction is shown in Fig.III.3.3.

At this energy the scintillator had a detection efficiency of approximately 30%. Pulses corresponding to protons which entered the walls accounted for less than 3% of the total counts. An approximate calculation showed that about 40% of the counts corresponded to neutrons which had been scattered at least twice; one third of these had initially been scattered through at least 60°. These pulses account for the pronounced peak near the leading edge. They also account for the resolution obtained: 21% as compared with the calculated minimum value (allowing only for statistical fluctuations) of 9%.

(b) D-T neutrons.

The distribution obtained when the scintillator was exposed to 14 Mev neutrons from the D-T reaction is shown in Fig.III.3.4.

Before the response of the scintillator to protons was measured it was tempting to assume that the flat portion of the distribution obtained corresponded to the response becoming linear. (Allen et al, 1952, suggested that similar results which they obtained using a stilbene crystal under comparable geometrical conditions might indicate a linear response in stilbene.) However, calculation showed that the distribution may be explained by a combination of the other distorting factors with a non-linear response given approximately by $L \propto E^{1.3}$.

The scintillator had a detection efficiency of approximately 7% at 14 Mev. Of those neutrons detected approximately 10% were scattered again. 10% of the protons scattered suffered edge-effects at the wall parallel to the direction of incidence of the neutrons and another 10% at the wall perpendicular to the direction of the neutrons. The net result of these distortions was to give the flat portion of the distribution: neither a gradual fall, due to the non-linear response nor a peak, from multiple-scattering, is visible. However, the effect is shown in the observed resolution of the leading edge, about 9%, which is again poorer than the calculated minimum value by a factor of more than two.

(c) Co^{60} γ-rays.

The distribution obtained when the scintillator was exposed to the γ-rays from a Co^{60} source is shown in Fig.III.3.5. These γ-rays are known to have energies of 1.17 Mev and 1.34 Mev. The scintillator failed to resolve the two γ-rays. It is of interest to compare this result with that obtained using a double-scintillator counter arrangement (See Fig.IV.2.7.) where the two γ-rays are clearly resolved: this shows clearly that the scintillator has sufficient intrinsic resolving power. The lack or resolution is again due to the distorting effects in the single-scattering arrangement. The sharp rise at the low energy

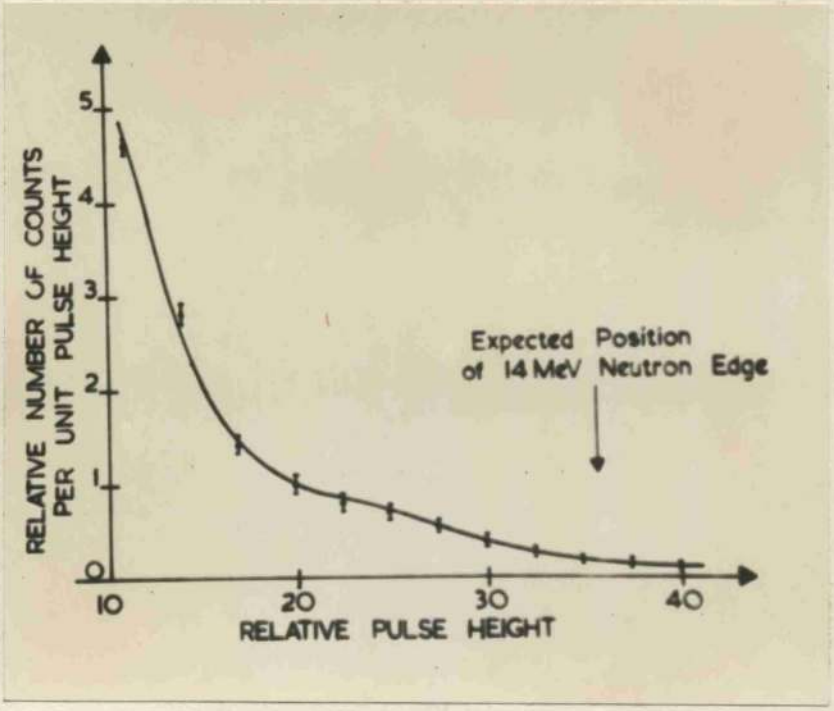

FIG.III.3.6. DISTRIBUTION FROM PRODUCTS OF $B^{11}(d,n)C^{12}$ ON SINGLE COUNTER.

end of the distribution, in contrast to the theoretically predicted fall, is accounted for by the edge-effects.

Distributions obtained from this and other γ-sources were used to establish an energy scale.

(d) Products of the reaction $B^{11}(d,n)C^{12}$.

The distribution obtained when the scintillator was exposed to the products of the reaction $B^{11}(d,n)C^{12}$ is shown in Fig.III.3.6. The energy of the deuterons was 500 kev. The highest energy neutron groups that were known to be emitted had energies of approximately 13.6, 9.3 and 4.7 Mev. γ-rays of 4.4 Mev were known to be emitted also.

The results do not show the steps that might have been expected. Consideration of the relative conversion efficiencies of the scintillator for protons and electrons leads to the expectation that pulses corresponding to the 4.4 Mev γ-rays would overlap those corresponding to 9.3 Mev neutrons and obscure them; they would also obscure pulses from all neutrons of lesser energies. The non-appearance of a step corresponding to the most energetic neutrons was disappointing. It was assumed that that was also obscured by the high-energy tail of the γ-distribution.

It was evident from this that a scintillator, chosen to give a high detection efficiency whilst recording predominantly single-scattering events, could not be used when γ-rays of the same order of energy as the neutrons, and emitted with comparable intensity, were present.

(vii) Discussion of similar work.

(a) Monoenergetic Neutrons.

Single scattering distributions obtained by other workers (POOLE, 1952, 1953; ALLEN et al, 1952; CROSS, 1951, 1952; SEGAL et al, 1954) using monoenergetic neutrons on single scintillators all show the effect of the distorting factors

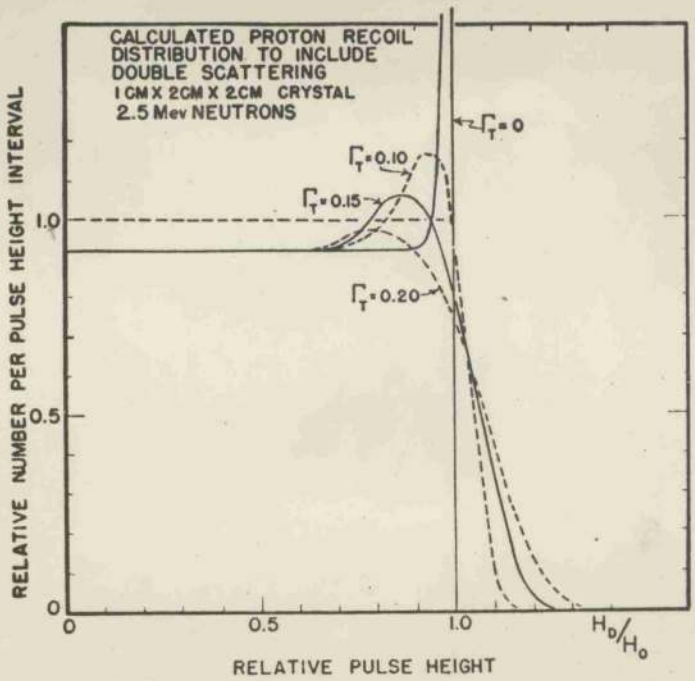

[redacted]. Calculated energy distribution of recoil protons due to 2.5-Mev neutrons, in a stilbene crystal 2 cm×2 cm×1 cm, including the effects of double scattering.

FIG.III.3.7. (After SEGEL et al)

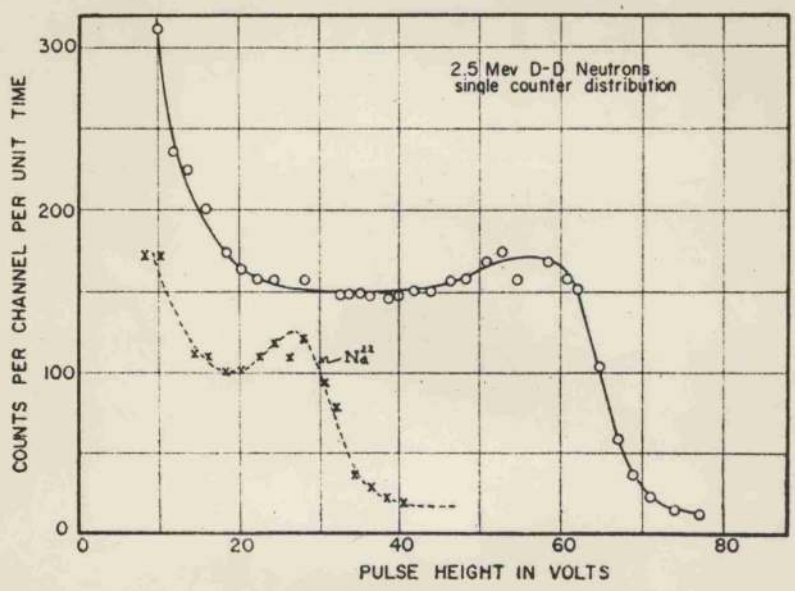

[redacted]. Pulse-height spectrum due to $D-D$ neutrons from a thin target, using the composite collimator of Fig. 3D. The spectrum due to annihilation radiation from Na^{22} is shown for comparison.

FIG.III.3.8. (After SEGEL et al)

discussed. Some approximate calculations have been performed on the results given by these authors. It was found that the resolution of the leading edges of the distributions obtained (which was in all cases poorer than the possible minimum values calculated earlier) could be explained by the effect of multiple-scattering combined with a non-linear response.

SEGAL et al have calculated the expected distribution from a stilbene crystal, 2cm x 2cm x 1cm, allowing for varying amounts of double-scattering in the crystal (Fig.III.3.7). They compare this with their results using D-D neutrons (Fig.III.3.8) in order to estimate the source intensity. Unfortunately, they do not allow for the non-linear response of the scintillator.

CROSS has reported that he has examined the single-scattering distribution in a stilbene crystal using 14 Mev neutrons from the D-T reaction. Different stilbene crystals were tried to overcome the distortions due to multiple-scattering and edge-effects. He verified that neutron-proton scattering was isotropic in the centre of mass system up to 14 Mev. Unfortunately, no values for the dimensions of the crystal used were given.

CROSS has also considered the problem of pulses corresponding to elastic and inelastic collisions between neutrons and carbon nuclei in the scintillator. In both cases the reduced conversion efficiency for heavy ionized particles lead to the conclusion that the effect is negligible except at the low energy end of the distribution and may be avoided by recording the distribution above a suitable bias level.

(b) Complex Spectra.

POOLE (1953) has used an anthracene crystal 1cm in diameter and 5mm thick to measure D-D neutrons scattered inelastically from Bi, Al, Fe, Ni, W and Au. He obtained two distributions of the scattered neutrons and their associated γ-rays using first a polythene and then a lead absorber between the scatterer and

the scintillation counter. (The absorbers had equivalent stopping powers for the γ-rays.) The pulses corresponding to γ-rays were then subtracted from the total distribution and clear steps corresponding to neutron groups were found. The resolution was sufficient to identify the positions of several low lying levels in the elements studied.

WARD and GRANT (1955) have used a cylindrical plastic scintillator, 4cm in diameter and 7mm thick, to measure the angular distributions of the neutron groups leading to the ground and first excited states of C^{12} in the reaction $B^{11}(d,n)C^{12}$. The cylinder was irradiated axially.

With this thin scintillator the tracks of the recoil electrons were attenuated and gave maximum pulse sizes corresponding to a proton energy of about 4 Mev. (Obscuring of the neutron spectrum by these γ-rays as in the results given earlier, Fig.III.3.6, was thus avoided.) Two steps were visible. Extrapolation of the individual distributions would have been extremely difficult if they had been calculated allowing for the distorting factors discussed earlier. However, at the low bombarding energy used (600 kev) the emitted neutrons did not have a large variation in energy with angle of emission: consequently it was reasonable to assume that the shapes of the distributions for each group were approximately independent of the angle of emission. The distribution for neutrons from the D-T reaction had been obtained previously with this scintillator. Since these neutrons had approximately the same energy as the neutrons leading to the ground state of C^{12} in the reaction $B^{11}(d,n)C^{12}$, it was possible to use this distribution to extrapolate the component corresponding to the first excited state from the complex spectra obtained. WARD and GRANT state that the results obtained are comparable in accuracy with those obtained in work on the angular distributions of γ-rays.

(viii) Conclusions.

From the foregoing discussion it follows that a single scintillator chosen to record predominantly single scattering events can provide rough measurements of neutron energies. Considerable calculation may be involved if accurate values of absolute or relative measures of the intensity of each neutron group in a complex spectrum are desired, unless the scintillator is calibrated with monoenergetic neutrons over the total range of energies for which it is to be used. Furthermore, for many experiments the use of this arrangement is precluded by the presence of γ-ray background. The work of POOLE and of WARD and GRANT, however, illustrates admirably both the advantages and limitations of this simple technique: by its use new information may be obtained, in certain experiments, fairly quickly and easily; these experiments are limited in number and many important experiments discussed in Part I cannot be coped with in this manner.

It appeared, therefore, that some arrangement whereby monoenergetic neutrons give rise, in principle at least, to pulses of a unique size and discrimination against γ-rays is, or may be, incorporated might lead to a better spectrometer. The first of the attempts to do this is described next: in principle this is also a single scintillation counter arrangement as is the arrangement used by SHIELDS (1954) which is then described. More refined double scintillation counter arrangements which achieve these objectives more effectively are described in Part IV.

4. AN EDGE EFFECT SPECTROMETER.

(1) THE PRINCIPLE.

The dimensions of the scintillator in a single scintillation counter arrangement may be chosen so that when the counter is

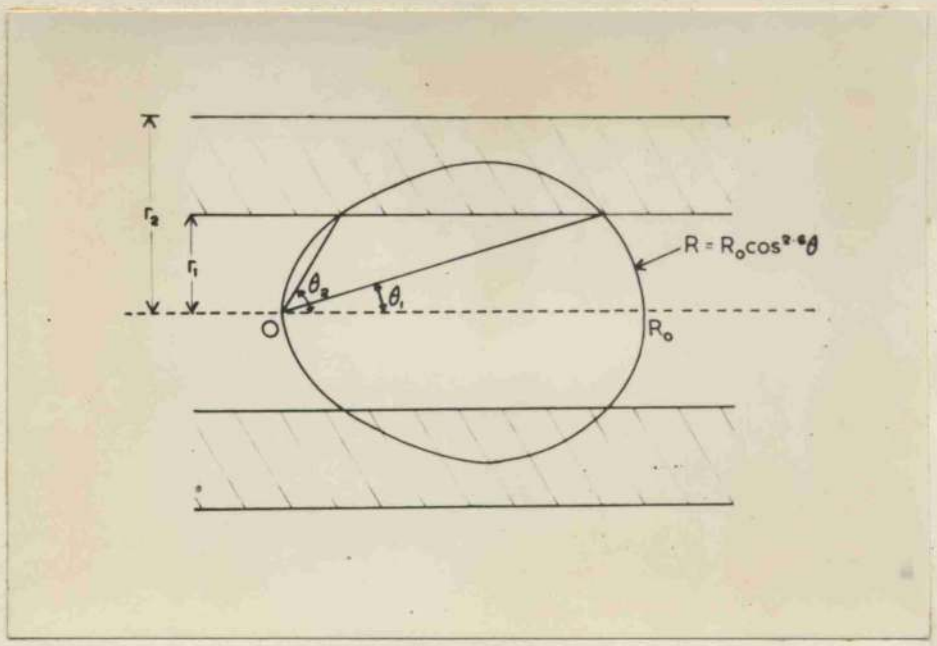

FIG.III.4.1. COLLIMATING TUBE.

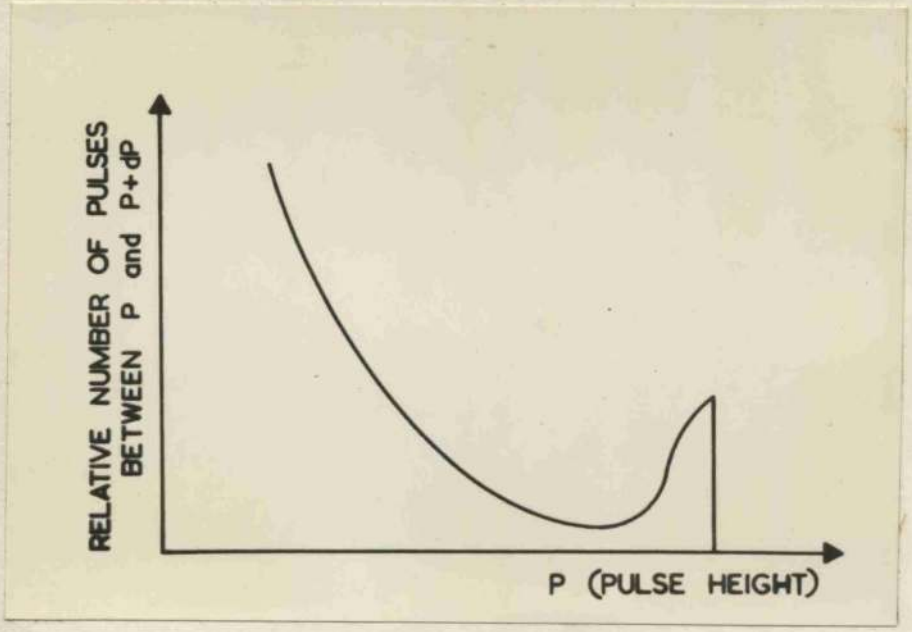

FIG.III.4.2. CALCULATED PULSE HEIGHT DISTRIBUTION.

irradiated with neutrons the resultant pulse height distribution depends mainly on the edge effects. Many sizes and shapes of scintillator will satisfy this condition but in the choice which is described here unattenuated head-on recoils are effectively isolated. In principle, this design could be made so that only head-on recoils would be recorded but this would lead to zero detection efficiency. It is an intrinsic property of this arrangement that γ-ray background is largely attenuated.

The scintillator is chosen to be in the form of a narrow cylinder: the axis of the cylinder is pointed at the source of neutrons. The tracks of approximately head-on recoils are contained entirely within the scintillator and give pulses corresponding to the total recoil energy. However, if the diameter of the cylinder is chosen sufficiently small, recoils which are not head-on expend part of their energy outside the scintillator (Fig.III.4.1.) and give reduced pulses. (Except recoils at very large angles) Fig.III.4.1. shows a cylinder, internal and external radii, r_1 and r_2, of non-scintillating material (shaded portion) containing the liquid scintillator.

A calculation of the expected pulse height distribution from such a cylinder irradiated with monoenergetic neutrons is outlined below for the condition

$$r_1 = \frac{1}{10} R_0 \qquad \text{III.4.1.}$$

where R_0 = range of a head-on recoil. (The choice of the ratio r_1/R_0 follows from the consideration below of resolution and detection efficiency.) This distribution is shown in Fig.III.4.2. Such a distribution is of greater utility than the rectangular distributions considered in Section III.3.

Consideration of the ranges of protons in the scintillator (Fig.II.13.1.) shows that it is a practical proposition to construct a spectrometer in this manner: cylinders of the order of 1mm in diameter and 25mm in length are required.

(ii) Expected distribution: Resolution and Efficiency; Choice of r_1/R_0 and the neutron energy range.

Comparison of the pulse height - energy relationship (Fig.II.11.3.) and the corresponding range - energy relationship (Fig.II.13.1.) for protons in the scintillator shows that the pulse height - range relationship is approximately linear. Thus the distribution of pulses from this spectrometer may be calculated by finding the distribution of effective ranges of the recoils in the scintillator. (The implicit assumption that the specific light output per unit path length of the recoils is constant is not strictly true; however, the general form of the distribution obtained in this manner is approximately correct.)

In the simple case where the recoils originate along the axis of the cylinder the distribution of ranges may be found analytically. To show how the general shape of the distribution arises this is done now. A complete calculation must include the effect on the distribution of protons which originate off the axis of the cylinder: this involves graphical integration and is omitted here for reasons of brevity and only the final result is shown in Fig.III.4.2.

If the scintillator is irradiated axially with monoenergetic neutrons, energy E_o, which cause N_o recoils, then the distribution in energies of recoils originating along the axis is given by

$$\frac{dN}{N_o} = \frac{dE}{E_o} \quad , \text{ for } E \leqslant E_o; \quad \frac{dN}{N_o} = 0, \text{ for } E > E_o; \qquad \text{III.4.2.}$$

Protons which recoil at an angle θ to the line of flight of the neutrons have energy E, where

$$E = E_o \cos^2\theta \qquad \text{III.4.3.}$$

$$\text{Hence } \frac{dN}{N_o} = \sin 2\theta \, d\theta \qquad \text{III.4.4.}$$

Equation III.4.4 gives the fraction of the protons which recoil between the angles θ and $\theta + d\theta$.

The range, R, of a proton of energy E in the scintillator, provided it does not strike the wall, is given to a good approximation, by

$$R = KE^{1.3} \qquad \text{III.4.5.}$$

where K is a constant (See Fig.II.13.1.).
Hence, from equation III.4.3.,

$$R = R_0 \cos^{2.6}\theta \qquad \text{III.4.6.}$$

where R_0 is the range of a head-on recoil ($\theta = 0$), and R is the range of a proton recoil at angle θ (See Fig.III.4.1.).

Protons scattered between the angles θ_1 and θ_2 shown in Fig.III.4.1., do, however, strike the wall. Thus a proton scattered at an angle θ ($\theta_1 < \theta < \theta_2$) will have a range R' in the liquid, where

$$R' = r_1 \operatorname{cosec}\theta \qquad \text{III.4.7.}$$

Protons scattered at angle θ, ($0 < \theta < \theta_1$, $\theta_2 < \theta < \pi/2$) will have range R in the liquid given by equation III.4.6. θ_1 and θ_2 are the values of θ which satisfy the equation

$$r_1 = R_0 \cos^{2.6}\theta \sin\theta. \qquad \text{III.4.8.}$$

The light output from a proton scattered in the liquid is proportional to its range in the liquid and therefore the final measured pulse is also proportional to this range. If L is a measure of the pulse resulting from a proton scattered at an angle θ and there is a total of N_0 recoils, then, for $0 < \theta < \theta_1$ and $\theta_2 < \theta < \pi/2$,

$$L = R_0 \cos^{2.6}\theta \qquad \text{III.4.9.}$$

Hence $$dL = 2.6\, R_0 \cos^{1.6}\theta \sin\theta\, d\theta \qquad \text{III.4.10.}$$

and by combining equations III.4.4 and 10

$$\frac{dN}{dL} = \frac{N_0}{1.3 R_0^{10/13}} \frac{1}{L^{3/13}} \qquad \text{III.4.11.}$$

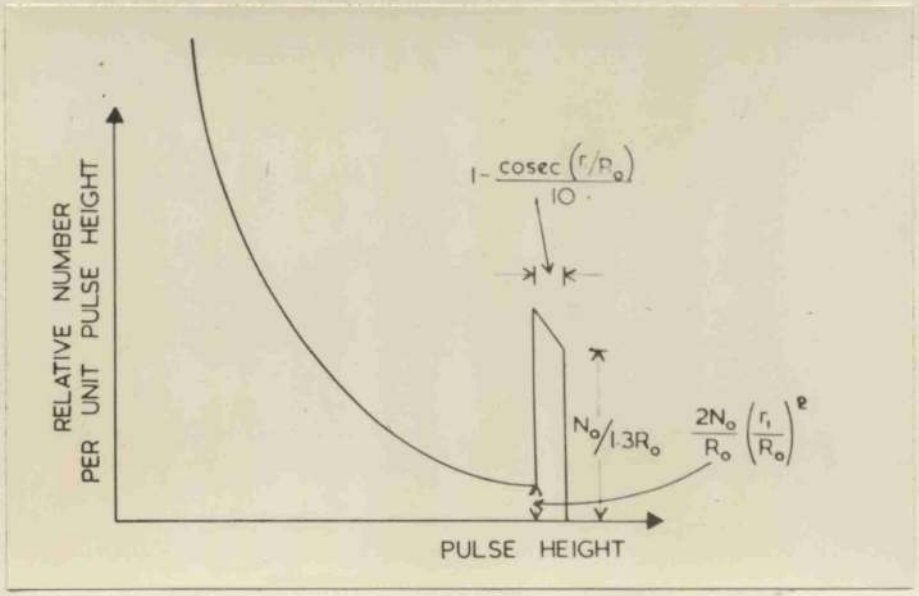

FIG.III.4.3. THEORETICAL DISTRIBUTION FROM RECOILS ORIGINATING ON THE AXIS OF THE TUBE.

For $\theta_1 < \theta < \theta_2$,

$$L = r_1 \operatorname{cosec} \theta \qquad \text{III.4.12.}$$

Hence $$dL = \frac{r_1 \cos\theta}{\sin^2\theta} d\theta \qquad \text{III.4.13.}$$

and by combining equations III.4.3 and 13

$$\frac{dN}{dL} = \frac{2 N_0 r_1^2}{L^3} \qquad \text{III.4.14.}$$

The expected pulse height distribution is given by equations III.4.11 and 13. For the spectrometer to work in the desired manner it is necessary that θ_1 be small. From equation III.4.8 this lead to

$$\theta_1 \simeq r_1/R_0 \qquad \text{III.4.15.}$$

This leads to the theoretical distribution shown in Fig.III.4.3. The expected resolution and efficiency may now be calculated.

Detection Efficiency.

The pulses in the 'peak' of Fig.III.4.3 are useful counts. If the ratio of useful counts to total counts is chosen to be 1 : 100 then the fraction of useful counts is given by

$$F = \int_0^{\theta_1} \frac{dN}{N_0} \qquad \text{III.4.16.}$$

$$\simeq \int_0^{r_1/R_0} \sin 2\theta \, d\theta, \text{ for } \theta \text{ small}$$

$$= (r_1/R_0)^2 \qquad \text{III.4.17.}$$

For F to be equal to $\frac{1}{100}$, $r_1/R_0 = \frac{1}{10}$

The overall detection efficiency (ratio of counts in peak to source strength) is limited by the distance between the scintillator and the source. This must be chosen large enough to preserve the geometrical conditions affecting the resolution. Typical values would be, length of cylinder $\sim$ 2.5cm, $r_1 \sim$ 0.025cm and distance from (point) source $\sim$ 1cm; this would give an overall detection efficiency $\sim 10^{-6}$ for 14 Mev neutrons.

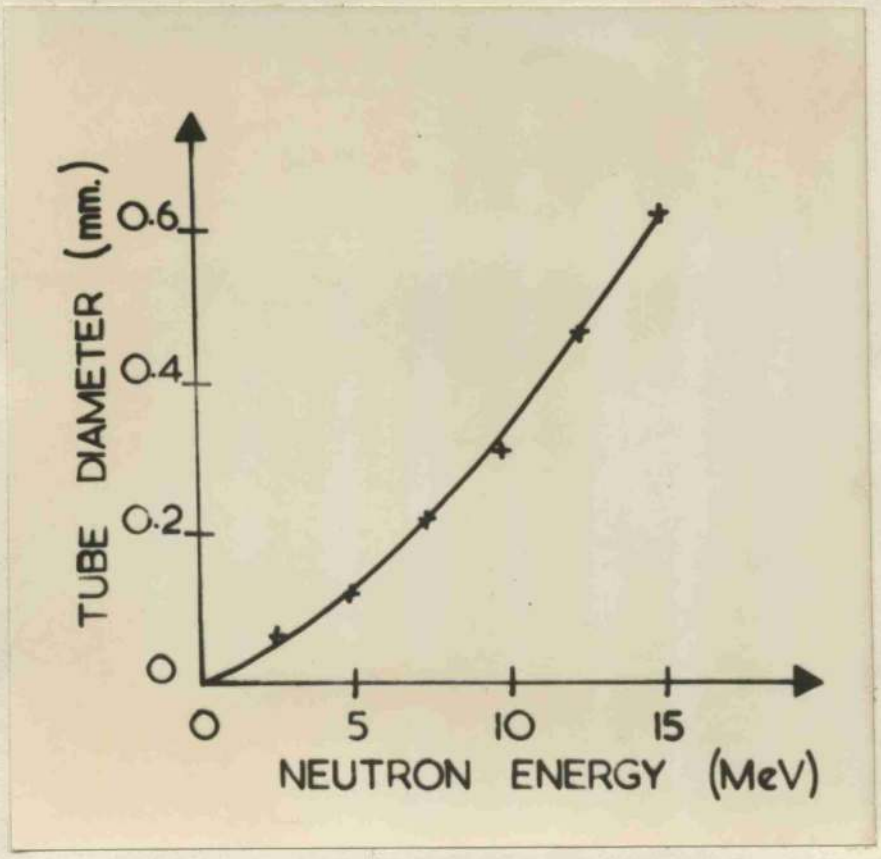

FIG.III.4.4. VARIATION OF TUBE DIAMETER WITH NEUTRON ENERGY.

However, the overall detection efficiency can, in principle at least, be increased by using several (~ 100) cylindrical scintillators viewed by one multiplier.

Resolution.

The resolution is given by the ratio of the peak width to the pulse height at the centre of the peak. To a good approximation this is given by

$$\rho = \frac{1}{R_0}(R_0 - r_1 \operatorname{cosec}\theta_1) \qquad \text{III.4.18.}$$
$$= 1 - 0.99$$
$$= 1\%.$$

when equation III.4.18 is solved for $r_1/R_0 = \frac{1}{10}$

When account is taken of recoils off the axis the calculated resolution is reduced to approximately 4%.

Choice of r_1/R_0 and the neutron energy range.

The choice of r_1/R_0 is limited. For $r_1/R_0 >> \frac{1}{10}$ the peaking effect disappears. For $r_1/R_0 << \frac{1}{10}$, the resolution imposed by the geometry improves. However, little is gained by choosing $r_1/R_0 << \frac{1}{10}$ since the observed resolution is limited by the statistical fluctuations in the scintillator-multiplier system (to $\sim$ 4% at 14 Mev). Moreover, as r_1/R_0 decreases the detection efficiency of the arrangement falls off rapidly.

These considerations also lead to the conclusion that a cylinder of given diameter is suitable only for the resolution of groups of neutrons whose energies differ by the order of 20%. Fig.III.4.4 shows the variation in tube diameter as a function of neutron energy to give a geometrical resolution of 4%.

(iii) Expected Response to γ-rays.

γ-rays are detected in the scintillator by collisions with electrons. The tracks of the recoil electrons are not

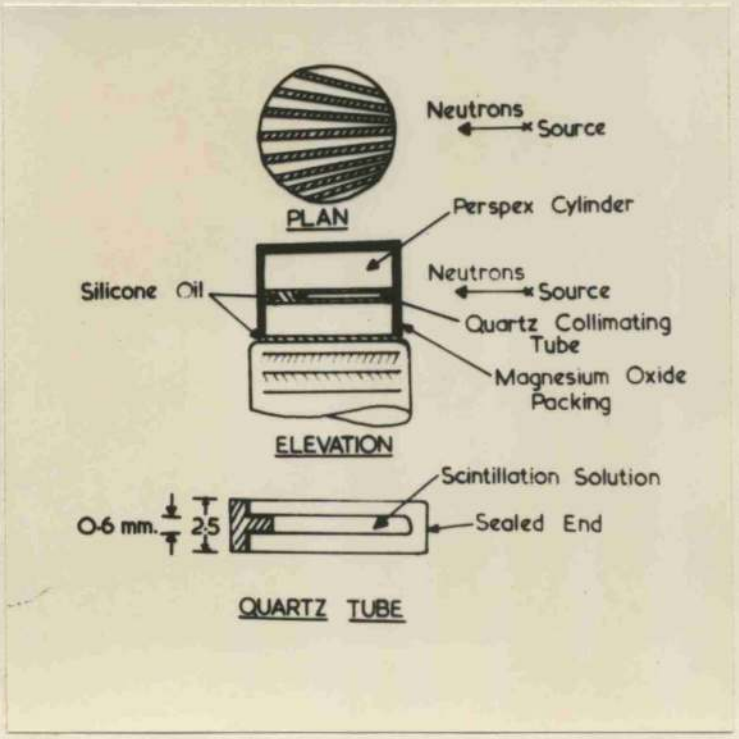

FIG.III.4.5. EXPERIMENTAL ARRANGEMENT OF COLLIMATING TUBES.

straight but suffer multiple atomic deflections. Since these tracks are of the order of a few centimetres in length for γ-rays of a few Mev, it follows that for most recoil electrons most of the energy will be dissipated outside the scintillator. For arrangements employing several cylindrical scintillators separated by non-scintillating material (the separation distance being approximately equal to the radius of the cylinders) at least half of the energy of each recoil would be dissipated outside the scintillator.

(iv) Experimental Arrangements.

(a) Construction of the scintillation counters.

Several approaches were made to the problem of making a narrow cylinder (and narrow cylinders) of scintillator surrounded by translucent non-scintillating material.

(A) Fine bore quartz tubes (r_1 = 0.3mm, r_2 = 0.5mm) were packed axially into a cylindrical quartz cell, 1" long by 1" in diameter. The cell was evacuated and then filled with scintillator. It was surrounded with magnesium oxide im the usual manner.

(B) It was attempted to drill holes of the appropriate diameter in a plastic block; these were to be filled with scintillator. Unfortunately, it was found impossible to drill accurately orientated holes of less than 1mm in diameter in plastic.

(C) It was attempted to mould holes by clamping sheets of xylonite about thin wires. This was also unsuccessful.

(D) A fine bore quartz tube was embedded in a plastic light-guide surrounded by magnesium oxide. This was extended by making a nest of quartz tubes in a plastic light-guide in the manner shown in Fig.II.4.5. (The axes of the tubes all intersected at a point outside the counter.) Nests with 8 and 60 tubes were made.

(b) Pulse analysis.

Analysis of the pulse distributions in the preliminary experiments was made by the photographic method mentioned earlier.

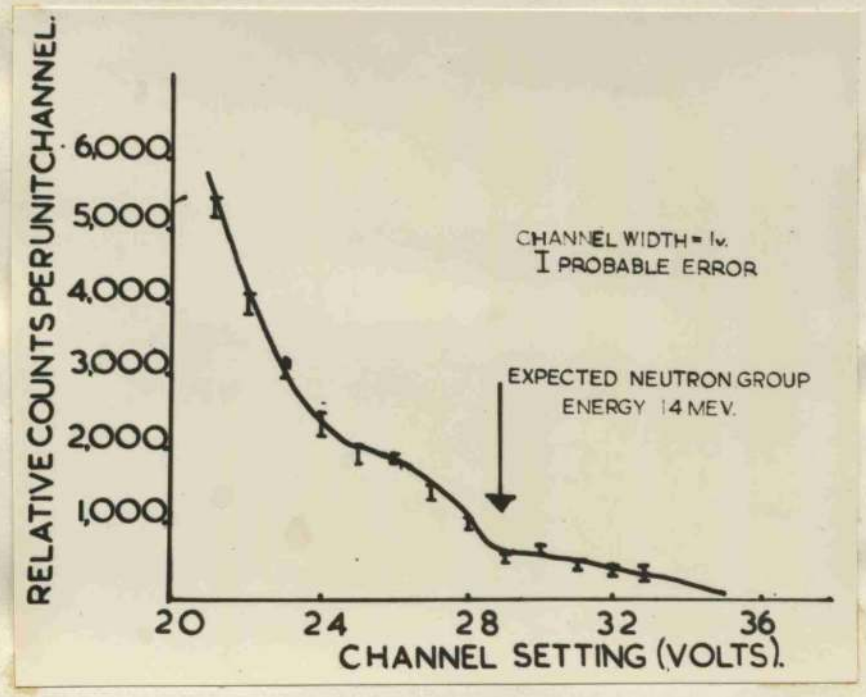

FIG.III.4.6. DISTRIBUTION FROM PRODUCTS OF $B^{11}(d,n)C^{12}$ ON COUNTER TYPE (A).

The 100 channel Hutchison-Scarrot pulse analyser was used for the later work.

(v) Experimental results and discussion.

(a) Preliminary experiments:

Preliminary experiments were made with a counter of the type (A) described in the preceding sub-section.

γ-rays.

The counter was irradiated with γ-rays from a Co^{60} source and from the reaction $Li^{7}(p,\gamma)Be^{8}$. The maximum pulses obtained were in each case less than half the size of those obtained when a similar (standard) counter without the quartz tubing was irradiated with the same γ-rays. (The results with the "standard" counter were used to establish an energy scale.)

The reaction $B^{11}(d,n)C^{12}$.

No tritium was available when these experiments were performed and it was impossible to test the spectrometer with monoenergetic 14 Mev neutrons. The results obtained when the spectrometer was exposed to the products of the reaction $B^{11}(d,n)C^{12}$ are shown in Fig.III.4.6.

Consideration of these suggests that the expected sharp peak corresponding to the most energetic neutrons ($\sim$ 14 Mev) emitted in this reaction has been spread over a large range of smaller pulses. This was attributed to two causes. First, the quartz tubes used in this preliminary work were selected to be approximately of the same bore. Accurate measurement showed that the bores varied by approximately $\pm$ 30% about a mean value of 0.7mm. Secondly, although both the quartz tubing and the scintillator were effectively completely transparent to the emission spectra of the scintillator, they did not have the same refractive index at this wavelength. The uniformity of light-collection may have been reduced by light being internally reflected at the tube-

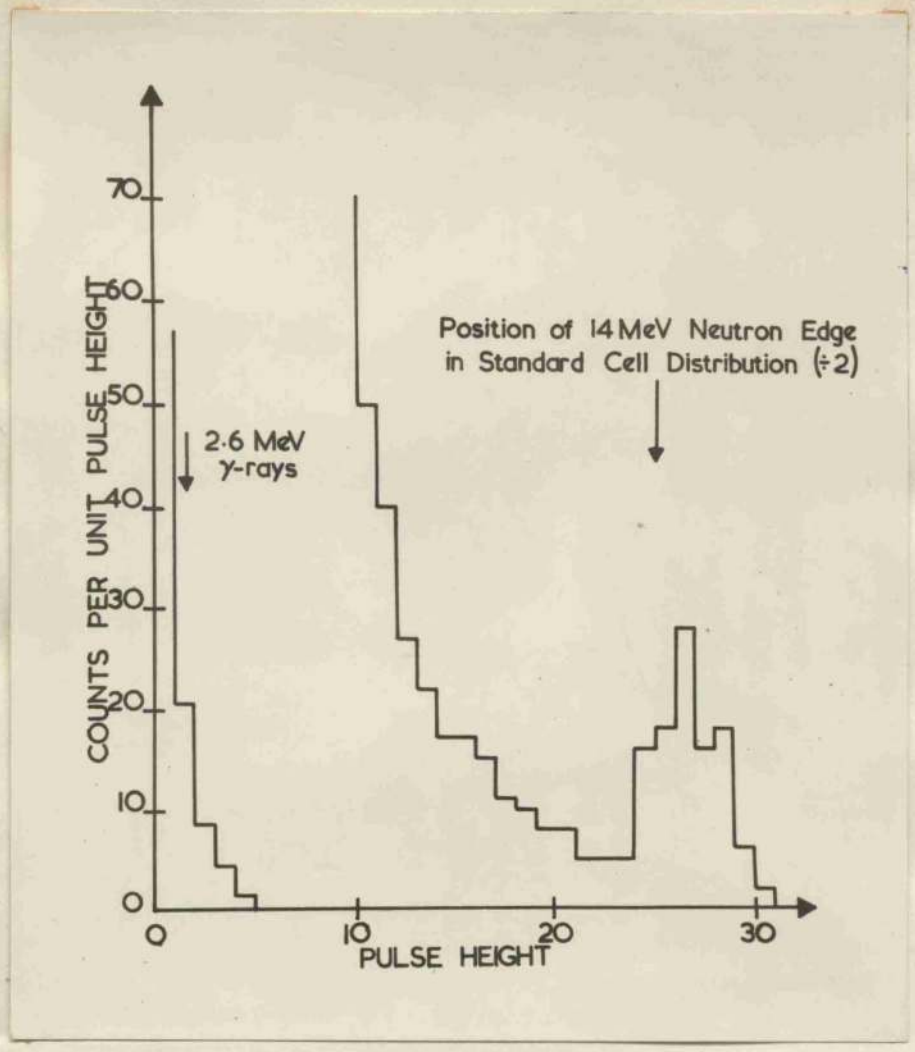

FIG.III.4.7. DISTRIBUTION FROM D-T NEUTRONS AND 2.64 Mev γ-RAYS FROM ThC'' ON 8-TUBE ARRANGEMENT.

scintillator boundaries. This would result in quanta from different points in the scintillator having varying lengths of optical path to the photocathode, with consequently varying light losses at the outside reflector.

These results, although poor, did suggest that it would be worthwhile to continue work on this spectrometer by counteracting both of the difficulties mentioned.

(b) Later Experiments.

These experiments were made with counters of the type (D) above.

Attempts to alter the refractive index of the scintillator (by mixing with additional solvents) to match that of quartz proved unsuccessful. It was decided, therefore, to set a quartz tube in a plastic light-guide and accept reduced, but more uniform, pulses. The results obtained with this arrangement were better than the earlier results and a counter with 8 tubes (Fig.II.4.5) was constructed. The tubes were chosen to be accurately 0.6mm in diameter.

D-T neutrons and γ-rays.

An energy scale was again established with a simple scintillation counter. The 8-tube arrangement was then irradiated with 14 Mev neutrons from the D-T reaction and 2.64 Mev γ-rays from a ThC'' source.

The results are shown in Fig.II.4.7. With the neutrons a clear peak (resolution $\sim$ 16%) is visible. The pulses obtained were reduced in size to about 60% of those obtained with a standard cell. When allowance was made for this reduction, the expected resolution, taking account of both statistical fluctuations and the geometry, was calculated to be about 10%. The difference between the observed and calculated resolution was attributed to non-uniform light collection.

The overall detection efficiency of the arrangement was

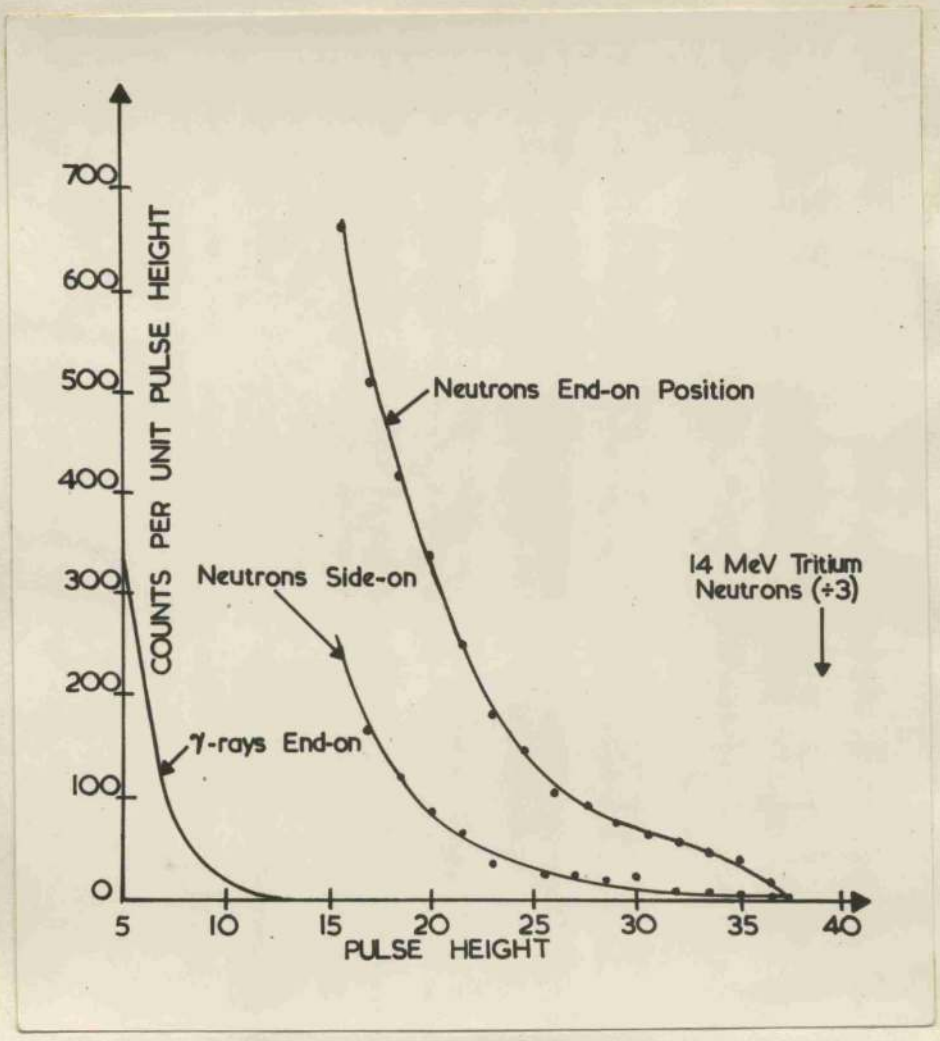

FIG.III.4.8. DISTRIBUTIONS FROM PRODUCTS OF $B^{11}(d,n)C^{12}$ AND $B^{11}(p,\gamma)C^{12}$ ON 60-TUBE ARRANGEMENT.

calculated to be $\sim 10^{-6}$ per neutron emitted by the source.

The results shown illustrate the high discrimination of the arrangement against γ-rays. Pulses from the γ-rays were reduced to about one fifth of those obtained with a standard cell; about one third of the reduction was due to the light guide.

The reaction $B^{11}(d,n)C^{12}$ and γ-rays from $B^{11}(p,\gamma)C^{12}$.

The reaction $B^{11}(d,n)C^{12}$ has a much smaller yield of neutrons than the D-T reaction. A 60 tube arrangement was used to investigate this reaction in order to increase the detection efficiency. The internal diameter of the tubes was chosen to be 0.5mm: this should have been capable of resolving the two groups of neutrons of highest energy, 13 Mev and 9 Mev. The results of this experiment are shown in Fig.III.4.8.

The curve marked 'neutrons end-on position' is the result obtained when the counter was used as designed with all tubes pointing radially at the source. The maximum pulses from the neutrons were further reduced and no peaks were visible. The loss of resolution was attributed to the increase in non-uniformity of light-collection when the number of tubes was increased.

The distribution obtained when the counter was rotated through 90° (side-on position) is also shown. The results when the counter was exposed to γ-rays from the reaction $B^{11}(p,\gamma)C^{12}$ show that the discrimination against γ-rays remained high.

(vi) Conclusions and Further Developments.

The results of Fig.III.4.7 show that this spectrometer works in principle. If it is to be used in a form with high detection efficiency the difficulties of non-uniform light collection will have to be overcome. This should be possible if further work leads to better matching of the refractive indices of the scintillator, quartz and light-guide.

In its present form the counter may be used as a detector of fast neutrons in the prescence of energetic γ-rays. It could also be used for investigating the angular distributions of individual neutron groups provided the variation of neutron energy with angle is not too great.

In theory it should be possible to make this arrangement almost exactly analogous to the proportional counter arrangement due to Giles which is described in Appendix A. The cylinder could be coated with a thin film ($\sim$ few wavelengths of the light emitted by the scintillator) of Aluminium. This could be surrounded by another scintillating medium, preferably liquid. Pulses from the inner cylinder which were in anti-coincidence with the outer cylinder would then be recorded. This would eliminate most of the unwanted pulses which appear below the peak. The range of energies for which a given cylinder would be useful would thus be increased and γ-ray background would be almost 100% eliminated. However, the very small radii of the cylinders necessary for neutrons in the energy range under consideration would make this procedure extremely difficult in practice. Some improvement might be effected by making the scintillator in the form of a disc of thickness of the order of one tenth of the maximum recoil range. The disc would be irradiated edgewise. With a similar anti-coincidence arrangement the distribution for monoenergetic neutrons would be approximately that of the ideal single-scattering distribution with the distortion due to a non-linear response plus a sharp peak superimposed on the leading edge. This arrangement would be relatively simple to make. γ-ray background would still be eliminated and the overall efficiency could be increased by making a multi-deck sandwich of alternate layers of recording and anti-coincidence discs.

5. A MULTIPLE SCATTERING SPECTROMETER.

(i) The Principle.

It has been noted earlier that there are two major difficulties in the use as a spectrometer of a single scintillator large enough to absorb completely most of the neutrons incident upon it. Firstly, non-linear response and imperfect light transmission, which leads to a pulse height distribution which consists of a broad peak with intolerable resolution. Secondly, the high sensitivity of a large volume of scintillator to γ-rays, which would obscure the neutron-induced pulses. However, by the addition of a suitable slow neutron detector to a relatively small scintillator it should be possible to utilise the multiple-scattering effect to give a peak of good resolution and, at the same time, largely eliminate the γ-ray background.

If the dimensions of the scintillator are chosen to be relatively small then only neutrons which suffer an initial collision which is approximately head-on are reduced to thermal velocities (by further collisions) in the scintillator; this ensures good resolution. The slow neutron detector announces the capture of the slowed down neutrons by emitting γ-rays or -particles. The slowing down process takes $\sim 10^{-8}$ secs and the lifetime for capture can be made considerably longer since it depends on the concentration of slow-neutron detector in the scintillator. Thus the neutron-induced pulses can be differentiated from γ-induced pulses by recording and analysing only pulses which are in delayed coincidence with a subsidiary γ- or α-pulse.

(ii) The slow-neutron detector.

Compounds of cadmium and boron, which have a high cross-section for slow neutron capture, would seem to be well suited for introduction into a scintillating medium for this purpose.

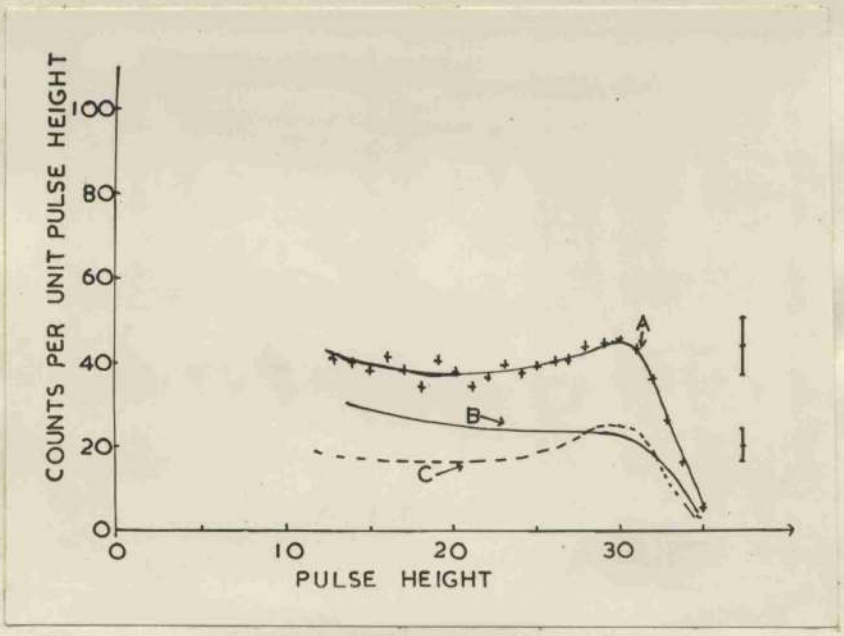

FIG.III.5.1. DISTRIBUTION FROM D-T NEUTRONS ON MULTIPLE-SCATTERING SPECTROMETER.

MUELHAUSE (1952, 1953) has described a very efficient slow-neutron detector made by adding methyl borate to terphenyl in xylene. Unfortunately, the addition of this solute has a considerable quenching effect on the conversion efficiency of the scintillator. SHIELDS (1954) has examined several Boron compounds and has found that least quenching occurred with tri-hexylene glycol biborate in a solution of 5 gm/l terphenyl + 0.1 gm/l phenyl alpha-naphthalamine in xylene from which the oxygen has been removed by bubbling. The ratio of biborate to xylene solution was 1:4.

(iii) Experimental Arrangement and Result.

This solution was used in a preliminary investigation into the possibilities of this type of spectrometer. From the concentration of biborate used it was estimated that the life-time for slow neutron capture was $\sim 1\mu$ sec. Pulses were recorded which were followed by delayed coincidences within $\frac{1}{2}\mu$ sec to $2\frac{1}{2}\mu$ sec. This ensured that $\sim 60\%$ of the neutrons which were captured were recorded.

Fig.III.5.1 (curve A) shows the results obtained when a cylinder 1" in diameter and 3" long was irradiated with 14 Mev neutrons from the D-T reaction. The contribution to the distribution from random coincidences (curve B) was found by inserting a delay of 3μ sec. Curve C is the difference of curves A and B and shows the noticeable peaking effect that was to be expected. The breadth of the peak is due to the large dimensions of the scintillator used which allowed neutrons which had initially been scattered through small angles to be recorded. The fact that the distribution does not fall away to zero may possibly be due to neutrons which were captured before being reduced to thermal velocities. This effect would be expected to increase with increasing concentration of biborate.

(iv) Conclusions.

The results, though rather disappointing, indicate that further development of this type of spectrometer would be worthwhile. Considerable improvement should be possible by making the scintillator in the form of a large flat disc of thickness of the order of 2% of the mean free path of the incident neutrons. The direction of incidence of the neutrons would be perpendicular to the plane of the disc. In this manner only neutrons which had initially scattered through $\sim 80^{\circ}$ at least would have an appreciable probability of being scattered again. This scintillator would record of the order of 1 in 10^4 of the neutrons incident upon it. However, it could subtend a large solid angle at the source since the geometry is not critical unless the neutrons emitted by the source exhibit a very large variation in energy as a function of direction of emission.

IV. DOUBLE SCINTILLATION COUNTER SPECTROMETERS.

1. INTRODUCTION.

The high detection efficiencies available with scintillation counters suggest the possibility of developing fast neutron spectrometers based on the successive detection of neutrons which have scattered in two separate scintillators. Considerable success has been achieved with similar arrangements in the analogous problem of the measurement of γ-ray energies (HOFSTADTER and McINTYRE, 1951) and it might be hoped to overcome in this way some of the difficulties encountered in the application of single-scintillator systems to the measurement of neutron energies. In particular, the elimination of γ-ray background is readily accomplished in double-scintillator arrangements by, for example, taking advantage of the difference in velocity of neutrons and γ-rays.

The use of two scintillators permits methods in which the time of flight of neutrons between the scintillators is measured as well as methods in which analysis of the pulse height distribution in either or both of the scintillators is employed. The resolution obtainable with any method employing pulse height analysis is limited by statistical fluctuations in the conversion efficiencies of the scintillator-multiplier system to, at best, the values calculated in II.5. At low neutron energies this is rather poor.

In time-of-flight methods the resolution depends effectively on the resolving time available with current coincidence units and the distance between the scintillators. Considerations of efficiency and the practical difficulties involved in separating the two scintillators by a large distance set a (much better) limit to the useful resolution that can be obtained in this way. However, these difficulties are evidently more apparent at high neutron energies where pulse height analysis would be expected to

yield the best results.

In this part of the thesis pulse height spectrometers are considered first and then time-of-flight spectrometers. A detailed discussion is given of a pulse height spectrometer in which analysis is made of pulses in one scintillator selected in the most straightforward manner by the second scintillator. Some of the results obtained with this spectrometer are quoted and results obtained by other workers with similar arrangements are also given. Conclusions are then drawn as to the limitations and usefulness of this instrument. (The application of this spectrometer to the establishment of the response of the scintillator is also explained.)

A brief discussion is then given of another pulse height spectrometer. In this spectrometer, due to BEGHIAN et al (1952), analysis is again made of pulses in one scintillator selected, in this case, in a more subtle manner by the second scintillator.

Finally, time-of-flight methods are considered. A detailed description is given of a novel time-of-flight spectrometer of high detection efficiency and capable of good energy resolution. The experiments performed with it are described and conclusions drawn as to the possibility of its application to most of the experiments outlined in Part I.

2. A DOUBLE SCATTERING PULSE HEIGHT SPECTROMETER (GEOMETRICAL SELECTION).

(i) The Principle.

The principle of this method may best be explained by considering the source and both the scintillators used as having zero dimensions. Neutrons from the source may scatter from one scintillator into the other. Pulses from recoils in the first scintillator are recorded only when the neutrons which cause these recoils scatter again in the second scintillator. For such

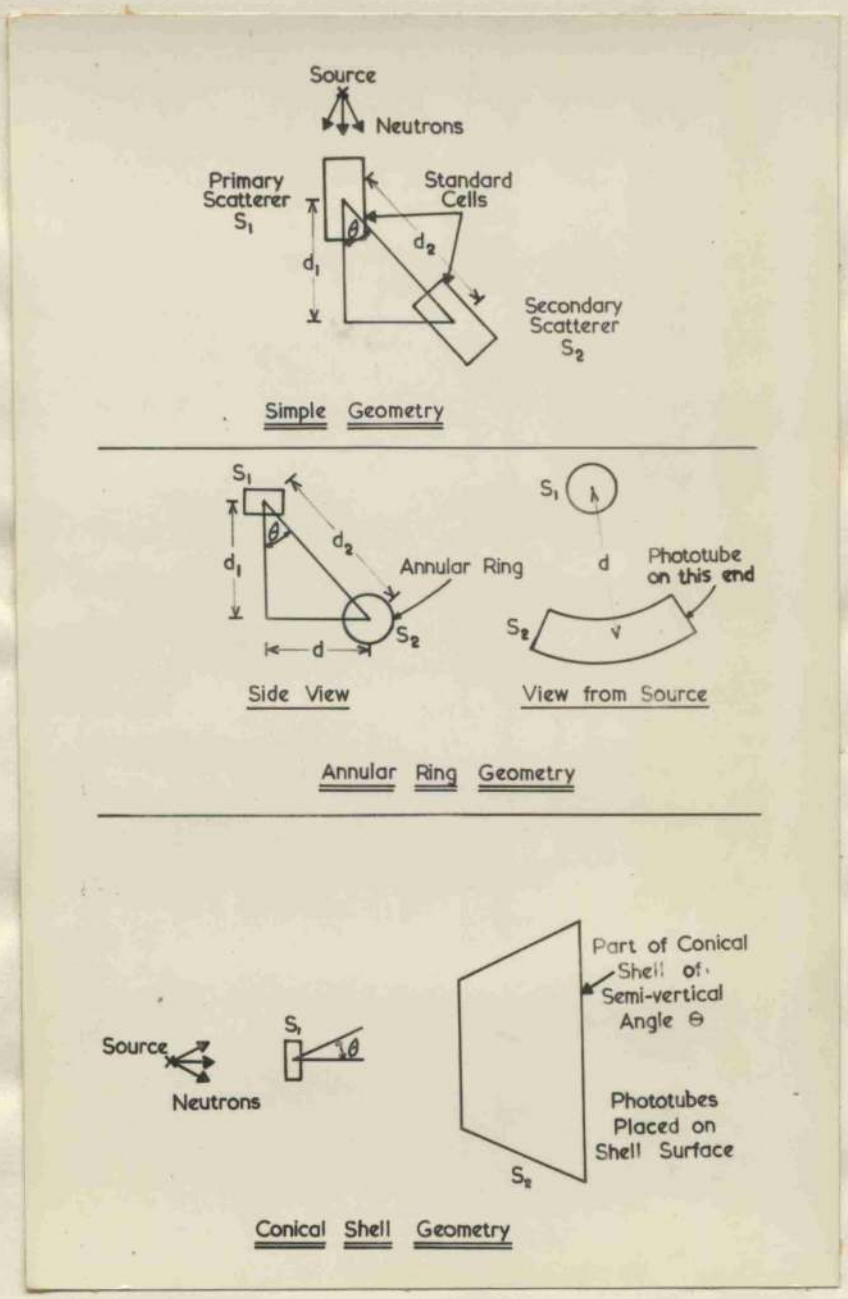

FIG.IV.2.1. GEOMETRIES FOR THE DOUBLE SCATTERING PULSE HEIGHT SPECTROMETER.

coincident events, the energy of the recoils in the first scintillator depends on the energy of the incident neutrons and, for a given neutron energy, has a unique value defined by the relative orientation of the source and the scintillators.

The situation is illustrated in the 'simple geometry' of Fig.IV.2.1. If the incident neutrons have energy, E_o, and the scattering angle is θ, then the energy of the proton recoil in the first scintillator (S_1) is given by

$$E_P = E_o \sin^2\theta. \qquad \text{IV.2.1.}$$

Measurement of the pulse height in S_1 and, hence, of E_P leads immediately to E_o.

(a) Resolution.

In principle, the geometry of this arrangement can be chosen to give perfect resolution. (This would lead to zero detection efficiency.)

In practice, the pulse height distribution from S_1 is observed (for coincident events) and the usual statistical fluctuations in the scintillator-multiplier system and in the associated electronic equipment will limit the resolution obtainable.

In addition, the finite dimensions of the scintillators and of the source in a practical arrangement will always introduce a spread in the definition of the scattering angle.

Also, neutrons which have scattered more than once in S_1 may scatter again in the second scintillator (S_2): pulses corresponding to such neutrons will be recorded and will further decrease the resolution.

(b) The Detection Efficiency.

The overall detection efficiency of this system is evidently less than that of a single scintillator arrangement. However, it may be increased by enlarging one of the scintillators in such a

manner that the geometrical condition for scattering in both scintillators still leads to the production of monoenergetic recoils in S_1.

This may be achieved by making S_2 in the form of an annular r ring or bi-conical shell whose axis lies along the line joining th the source to S_1. In the latter case it is theoretically possible to detect all neutrons which are scattered at the chosen angle in S_1. (See Fig.IV.2.1.)

Alternatively, S_1 could be chosen as part of the surface of revolution formed by rotating an arc of a circle which passes through the source and S_2. This arrangement is only of academic interest since poor resolution would result from difficulties of light collection and from the amount of multiple-scattering which would occur in this large volume.

(c) γ-rays.

If no discrimination against γ-rays is specifically built into the spectrometer then it will detect γ-rays in an exactly similar way to that in which neutrons are detected. With γ-rays of up to 10 Mev, Compton scattering will take place in both scintillators. The energy of a recoil electron in S_1 is given by

$$E_e = \frac{h\nu}{1 + m_0c^2/h\nu(1-\cos\theta)} \qquad \text{IV.2.1a.}$$

where $h\nu$ = energy of the incident quantum and θ is the scattering angle.

Since the variation of the energy of recoil electrons with the scattering angle is different from the variation of the energy of recoil protons with scattering angle, the resolution imposed by the geometry will be different for neutrons and γ-rays; with γ-rays the geometrical resolution depends strongly on the energy. Similarly, the detection efficiencies will differ in the two cases and the amounts of double-scattering in the first scintillator will be different.

(ii) Resolution and Detection Efficiency.

(a) Resolution.

The resolution of the spectrometer depends on several factors. These may be considered in two groups. Firstly, R_S, which arises from statistical fluctuations in the scintillator-multiplier system, drifts in the supply voltages, and the channel width of the analyser. Secondly, R_θ, which arises from the mean error, θ, introduced in the scattering angle, θ, by the finite dimensions of the source and the scintillators.

The overall resolution of the spectrometer is given by

$$R = \left[R_S^2 + R_\theta^2\right]^{\frac{1}{2}} \qquad \text{IV.2.2.}$$

The only factor of importance contributing to R_S is the statistical fluctuations in the scintillator-multiplier system. This determines the ultimate resolution obtainable since the other factors may always be made small compared with it. From the considerations of Section II.5 and equation IV.2.1 it follows that

$$R_S = A / \sin\theta \qquad \text{IV.2.3.}$$

where A is a constant for a given E_0.

R_θ is given, to a good approximation, by twice the mean fractional deviation, ΔL_p, in the pulse height, L_p, corresponding to a proton recoil of energy, E_p. For the scintillator used, $L = KE^{1.3}$, so that, from equation IV.2.1,

$$R_\theta = \frac{2\,\Delta L_p}{L_p} = \frac{2.6\,\Delta E_p}{E_p}$$

$$= 5.2 \cot\theta\, \Delta\theta \qquad \text{IV.2.4.}$$

$\Delta\theta$ depends on the sizes and orientation of the source and the scintillators and derivation of a general expression for it is complicated. When the experiments described here were performed

a very approximate method of calculating $\Delta\theta$ was used. Subsequently, a detailed analysis of the factors contributing to $\Delta\theta$ was given by OWEN, NEILER et al (1951) for the case where S_1 was a rectsngular block and S_2 was in the form of an annular ring. A shortened version of this calculation was made available by CHAGNON et al (1953). The expression they give has been adapted to allow for a cylindrical primary scintillator and has been used to obtain values given later. It was found that

$$\Delta\theta = \left[\tfrac{1}{4}(r_2/d_2)^2 + \tfrac{1}{8}(d_3/d_2)^2 + \tfrac{1}{3}(r_1/d_1)^2 + \tfrac{1}{2}(r_0/d_1)^2\right]^{1/2} \quad \text{IV.2.5.}$$

where r_0 = radius of source.
r_1 = radius of S_1.
r_2 = radius of S_2.
d_1 = mean distance from source to S_1.
d_2 = mean distance from S_1 to S_2.
d_3 = extension of S_1 in direction of neutron beam.

(b) Detection Efficiency.

The number of neutrons which are scattered in S_2 after being scattered in S_1 is readily found.

If N_0 = number of neutrons emitted by the source.
N_1 = number of neutrons scattered in S_1.
N_2 = number of neutrons scattered again in S_2, then

$$N_1 = \frac{1}{4\pi}\left[N_0 \Omega_1 K \sigma(E_0) d_3\right] \quad \text{IV.2.6.}$$

where,

Ω_1 = solid angle subtended at source by S_1.
K = number of protons per cm-barn of scintillator.
$\sigma(E_0)$ = n-p scattering cross-section in barns for neutrons of energy E_0.

Also,

$$N_2 = N_1 \sin 2\theta \, d\theta \, K \sigma(E_0 \cos^2\theta) 2r_2 \quad \text{IV.2.7.}$$

That is

$$N_2 = \frac{1}{\pi}\left[N_1 \Omega_2 \cos\theta K \sigma(E_0 \cos^2\theta) 2r_2\right] \quad \text{IV.2.8.}$$

where

Ω_2 = solid angle subtended by S_2 at S_1, since

$$\Omega_2 = 2\pi \sin\theta d\theta \qquad \text{IV.2.9.}$$

Hence

$$N_2 = \frac{1}{4\pi^2}\left[N_0 \Omega_1 \Omega_2 K^2 \cos\theta\, \sigma(E_0)\sigma(E_0\cos^2\theta)\, 2r_2 d_3\right] \qquad \text{IV.2.10.}$$

The overall detection efficiency is given by

$$\eta = N_2/N_0 \times F \qquad \text{IV.2.11.}$$

where F = the number of neutrons which are scattered in S_2 which operate the coincidence unit.

That is

$$\eta = \frac{1}{4\pi^2}\left[\Omega_1 \Omega_2 K^2 \cos\theta\, \sigma(E_0)\sigma(E_0\cos^2\theta)\, 2r_2 d_3 F\right] \qquad \text{IV.2.12.}$$

(In order to calculate good approximations to numerical values of η for given geometrical arrangements equation IV.2.12 may be rewritten in the form

$$\eta = \frac{1}{32\pi} \times r_1^2/d_1^2 \times r_2^2/d_2^2 \times x d_3 \times E^{1.5}/\cos^{1.5}\theta \times F \qquad \text{IV.2.12a.}$$

This expression for η was derived from equation IV.2.12 using the accurate relations $\frac{1}{\lambda_0} = K\sigma(E_0)$ and $\frac{1}{\lambda_\theta} = K\sigma(E_0\cos^2\theta)$, and the approximate relations $\lambda = 4E^{0.75}$ (See Fig.II.12.2.), $\Omega_1 = \pi r_1^2/d_1^2$ and $\Omega_2 = 2x r_2/d_2^2$, where x is the length of the annular segment.)

(iii) Choice of scattering angle and the dimensions.

(a) Limitation of $\Delta\theta$.

The choice of the scattering angle and of the dimensions of the scintillators affects both the resolution and the detection efficiency obtainable.

For a given scattering angle the resolution can never be better than R_S and from equation IV.2.3 it follows that the best value will be obtained when $\theta = \pi/2$. The detection efficiency depends on the geometrical resolution, R_θ, introduced which may be

chosen arbitrarily. In order to determine the optimum conditions for both resolution and efficiency it is necessary to impose some limitation on the allowable values of $\Delta\theta$. This may reasonably be done by choosing

$$R_\theta = A_0 R_S \qquad \text{IV.2.13.}$$

where A_0 is a constant. (In the following argument $A_{1,2,\ldots,6}$ are all constants.) Combining this with equations IV.2.3 and 4 it follows that the allowable variation in $\Delta\theta$ is given by

$$\theta = A_1 / \cos\theta \qquad \text{IV.2.14.}$$

The final resolution is now given by

$$R = A_2 R_S \qquad \text{IV.2.15.}$$

which has its best value when $\theta = \pi/2$.

The detection efficiency (equation IV.2.12) may be rewritten in the form

$$\eta = A_3 \Omega_1 \Omega_2 \cos\theta\, \sigma(E_0 \cos^2\theta)\, r_2 d_3 F \qquad \text{IV.2.16.}$$

For an ideal coincidence unit (F = 1) and scintillators of fixed size this becomes

$$\eta = A_4 \Omega_1 \Omega_2 \cos\theta\, \sigma(E_0 \cos^2\theta) \qquad \text{IV.2.17.}$$

So that, if the maximum linear angles subtended by S_1 at the source and by S_2 at S_1 are α and β, then

$$\eta = A_5 \alpha^2 \beta \sin 2\theta\, \sigma(E_0 \cos^2\theta) \qquad \text{IV.2.18.}$$

α and β are related to $\Delta\theta$ by the approximate relation

$$2\Delta\theta = \sqrt{\{\alpha^2 + \beta^2\}} \qquad \text{IV.2.19.}$$

However, $\Delta\theta$ is given by equation IV.2.14. Since α and β must both remain finite it follows that they both vary, very approximately, inversely as $\cos\theta$. That is, approximately,

$$\eta = A_6 \sin\theta\, \sigma(E_0 \cos^2\theta) / \cos^2\theta \qquad \text{IV.2.20.}$$

$\sigma(E_o\cos^2\theta)$ increases with θ, so that this calculation leads to η being infinite when $\theta = \pi/2$. This is obviously fallacious but the calculation is valid in showing that η tends to a maximum at $\theta = \pi/2$, for finite scintillators and for a finite range of θ.

It follows from the above argument that the optimum values for both resolution and efficiency are obtained when $\theta = \pi/2$. This choice must be modified in view of the limitations of practical coincidence units ($F \neq 1$) and the effects of multiple-scattering, both of which are considered now. The scale of the arrangement is also determined by the multiple-scattering.

(b) The coincidence unit.

The coincidence unit requires pulses of a minimum size to operate. Usually the pulse required corresponds to protons with energy of about 0.5 Mev. That is, if the scattered neutrons have energy for example of 1 Mev, approximately 50% of these neutrons will trigger the coincidence unit. The energy range for which the spectrometer is to be used thus determines the minimum scattering angle if the efficiency is to approach its theoretical maximum. For neutrons of 2.5 Mev, a suitable choice is $\theta \sim 45^o$; the resolution is then decreased by a factor of the order of 1.5. For higher energies, a larger angle may be used, with a corresponding improvement in the resolution.

(c) Multiple-scattering.

The effect of multiple-scattering in the first scintillator is primarily to decrease the resolution, although any attempt to minimise this effect results in a decrease in efficiency. The effect is difficult to calculate quantitatively. However, some qualitative considerations help to determine when it is significant and how it may be minimised.

A good indication is given by the fraction of the neutrons which are scattered in S_1 in the direction of S_2 which are scattered again before escaping from S_1. (Most of the neutrons

which suffer such a secondary collision will not enter S_2; from considerations of the incoherent motion of neutrons which are reduced to thermal velocities in a scintillator, it is reasonable to assume that, to an order of magnitude, the same number of neutrons enter S_2 after more than one collision in S_1.) This fraction is readily evaluated to an order of magnitude. It increases as the volume of S_1 is increased. Also, for a fixed size of scintillator the fraction increases with the scattering angle since the mean free path of the scattered neutrons decreases with increasing scattering angle.

The effect of multiple-scattering may be reduced by reducing the size of S_1. The scale of the arrangement may then be reduced proportionately; this leaves $\Delta\theta$ unaltered and the overall efficiency is then reduced by the square of the scale factor. Unless S_1 is reduced to zero dimensions (thus leading to zero efficiency) it is necessary to choose the scattering angle to be much less than $\pi/2$, to avoid multiple-scattering since the mean free path of the scattered neutrons falls rapidly to zero, as θ approaches $\pi/2$. Approximately, $\lambda_\theta \propto \cos^{1.5}\theta$.

Further insight into the lack of resolution produced by this effect may be gained from an examination of the results obtained using several scattering angles and scintillators of different sizes. It is further illustrated by the results of other workers which are discussed later.

(d) Conclusions.

From the above considerations it follows that the choice of the scattering angle, θ, is limited to values such that $45^\circ \lesssim \theta \lesssim 75^\circ$.

The dimensions of the first scintillator are determined mainly by the effect of multiple-scattering: the importance of this effect is most easily found by experiment but as a preliminary guide it would be reasonable to choose the dimension of the first scintillator in the direction of scattering, d_θ, to be much less than the mean free path, λ_θ, of the scattered neutrons.

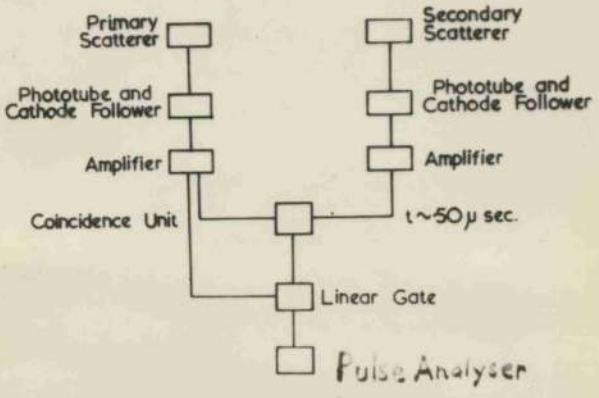

ELECTRONIC BLOCK DIAGRAM
FOR
DOUBLE SCATTERING EXPERIMENTS

FIG.IV.2.2.

Say, $l_\theta \gg \lambda_\theta/5$

That is,

either $d_3/\cos\theta$ or $r_1/\sin\theta \gg \lambda_\theta/5$

(iv) Electronic Arrangement.

A block diagram of the electronic arrangement used is shown in Fig.IV.2.2. Pulses from the photomultiplier outputs were fed into cathode followers, amplified and mixed in the coincidence unit. The pulses from the primary amplifier were also fed into a linear gate which was opened by the coincidence unit; these primary pulses were then analysed. The secondary amplifier was operated at high gain in order to achieve the maximum coincidence rate; most of the output pulses from this amplifier were saturated and the corresponding discriminator in the coincidence unit was set just above the amplified photomultiplier noise level.

The amplifiers were standard Harwell 1008 two ring-of-three units. The coincidence unit used in the preliminary experiments had a resolving time of 1 μsec; the coincidence unit used in the later experiments had a resolving time of 5×10^{-7} sec: it is described in Appendix C. All the results were obtained using direct coincidences and no attempt was made in this particular set of experiments to discriminate against γ-rays by taking delayed coincidences.

(v) Experimental Arrangements and Results: Discussion.

(a) Preliminary Experiments: Simple Geometry.

(A) Arrangement.

The counters and their arrangement for the preliminary experiments were chosen to be simple and to give a high detection efficiency at the expense of poor geometrical resolution. The arrangement is shown diagramatically in the 'simple geometry' of Fig.IV.2.1. Both founters were cylinders 5 cm in length and 1.2 cm in diameter. The axis of S_1 pointed at the source and the axis of

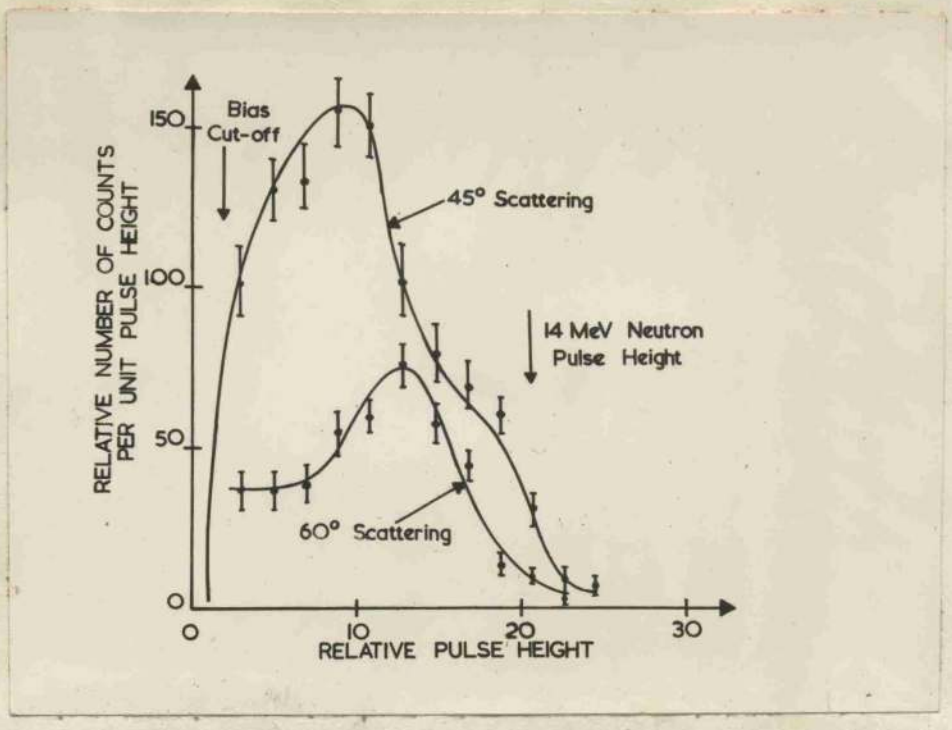

FIG.IV.2.3. D-T NEUTRONS SCATTERED AT 45° AND 60°.

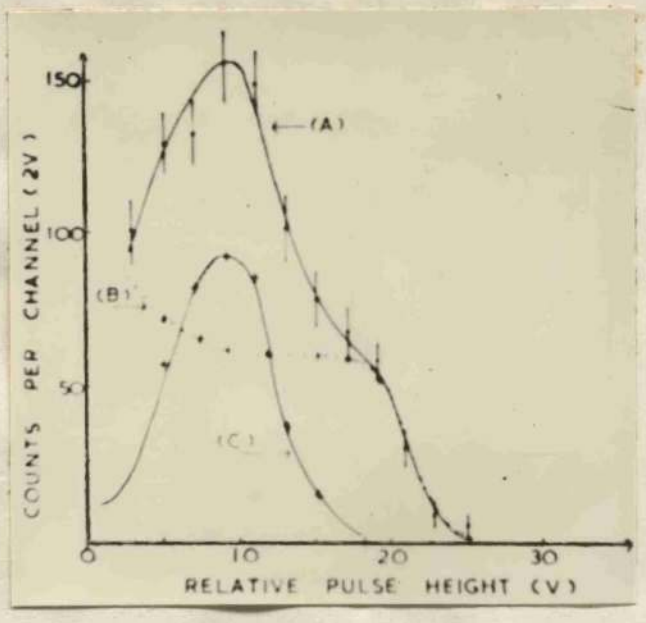

FIG.IV.2.4. (A) D-T NEUTRONS SCATTERED AT 45°.
(B) RANDOM COINCIDENCES.
(C) DEDUCED DISTRIBUTION OF REAL COINCIDENCES.

S_2 pointed at the centre of S_2. Using the nomenclature of IV.2.(ii)(a). the dimensions for 45^o scattering were:

r_o = 0.6 cm, r_1 = 1.0 cm, r_2 = 1.0 cm,

d_1 = 12 cm, d_2 = 12 cm, d_3 = 5 cm.

(B) Results for 14 Mev neutrons.

The results obtained when D-T neutrons from the 50 kv H.T. Set were scattered at 45^o and 60^o are shown in Fig.IV.2.3. Figs. IV.2.4 (A), (B) and (C) show respectively the distribution for 45^o scattering again, the distribution due to random coincidences and the deduced distribution of real coincidences.

For 45^o scattering the ratio of real to random coincidences was approximately 1 : 3 and the ratio of real coincidences to source strength was approximately $2 : 10^6$. The observed resolution was $\sim 85\%$.

(C) Discussion.

The calculated geometrical resolution, R_θ, in the case of 45^o scattering was 86%. The other factors influencing the resolution were small compared with this; thus, although good agreement was obtained between the calculated and observed values of resolution nothing further could be deduced about the effects of the other factors. (It was estimated that $\sim 8\%$ of the scattered neutrons suffered a second collision on their way towards the second counter.)

The detection efficiency calculated according to equation IV.2.12 was 1.7×10^{-6} which was in good agreement with the efficiency calculated from the source strength and the coincidence counting rate.

The ratios of the mean pulse height, L_{45}, L_{60} and L_{90}, corresponding to scattering at 45^o, 60^o and head-on collision (from the leading edge of the single scattering distribution) were found to be given by $L_{45} : L_{60} : L_{90} = (\sin^2 45^o : \sin^2 60^o : \sin^2 90^o)^{1.3}$. That is, pulse height as a function of proton energy is given by

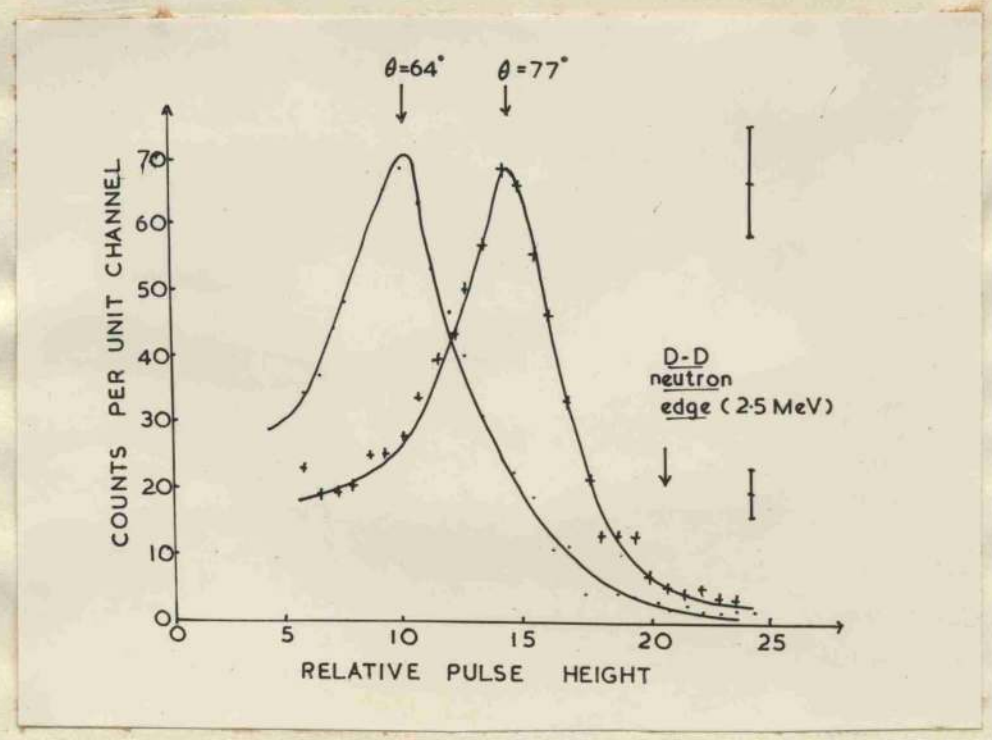

FIG.IV.2.5. D-D NEUTRONS SCATTERED AT 64° AND 77°: ANNULAR RING GEOMETRY.

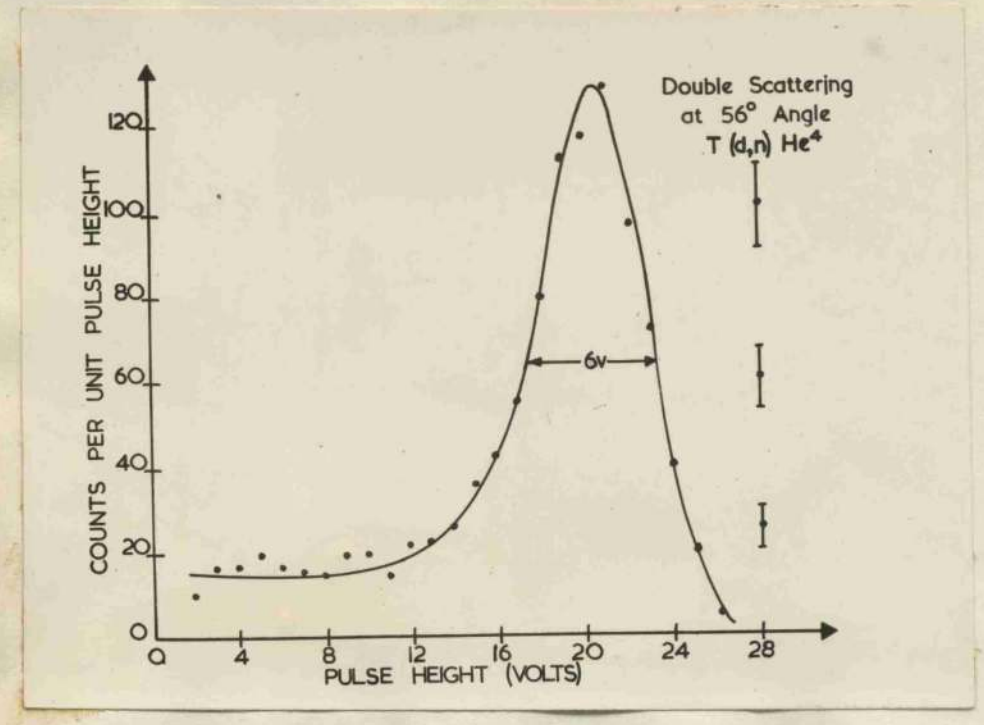

FIG.IV.2.6. D-T NEUTRONS SCATTERED AT 56°: ANNULAR RING GEOMETRY.

$L \propto E^{1.3}$.

The experiments showed that this type of arrangement would function in practice. Accordingly, more refined experiments were made with better resolution whilst maintaining the detection efficiency.

(b) Later experiments: annular ring geometry.

(A) Arrangement.

In these experiments it was attempted to obtain a much improved resolution. The efficiency was maintained by extending S_2 into a segment of an annular ring. That is, the annular ring geometry of Fig.IV.2.1.

In the experiments with D-D neutrons the dimensions were: r_o = 0.3 cm, r_1 = 1.0 cm, r_2 = 0.6 cm, d_1 = 10 cm, d_2 = 8.3 cm, d_3 = 2.5 cm and S_2 had a mean radius of curvature = 7.5 cm and length = 15 cm.

In the experiments with Co^{60} γ-rays and D-T neutrons the dimensions were:

r_o = 0.3 cm, r_1 = 1.0 cm, r_2 = 1.0 cm, d_1 = 12 cm, d_2 = 30 cm, d_3 = 1.25 cm and S_2 had mean radius of curvature = 25 cm and length = 25 cm.

(B) Results for 2.5 Mev and 14 Mev neutrons and for Co^{60} γ-rays.

The results obtained when D-D neutrons from the 50 Kv H.T. Set were scattered at 64° and 77° are shown in Fig.IV.2.5. For 64° scattering the observed resolution is 60% and for 77° scattering is 40%. In both cases the ratio of real coincidences to source strength was approximately $1:10^6$ and the random coincidence rate was negligible.

The results obtained when D-T neutrons from the 1 Mev H.T.Set were scattered at 56° are shown in Fig.IV.2.6. The observed resolution is approximately 29%. The ratio of real coincidences to source strength was again $1:10^6$ and the random coincidence rate was again negligible.

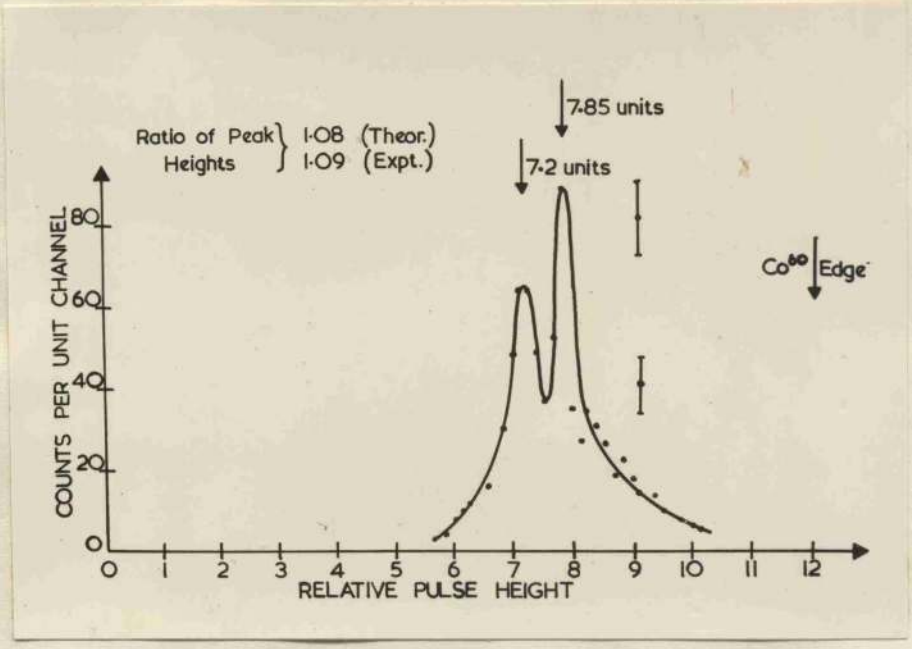

FIG.IV.2.7. Co^{60} γ-RAYS SCATTERED AT 60°: ANNULAR RING GEOMETRY.

The results obtained when Co^{60} γ-rays were scattered at 60° are shown in Fig.IV.2.7. The result of interest here is that both γ-rays are clearly resolved and the resolutions of the two peaks are approximately 12% and 15% respectively.

(C) Discussion.

For the scattering of the D-D neutrons at 64° and 77° the calculated geometrical resolutions of the apparatus were 34.6% and 16.8% and the resolutions introduced by statistical variations were 10% and 9.7% respectively. The calculated total resolutions were thus 36.3% and 19.0% respectively. These have to be compared with the experimental values of 60% and 40% respectively.

The explanation of the discrepancies appeared to lie in the multiple-scattering of neutrons in S_1. It was calculated that for 64° scattering, 41% of the scattered neutrons suffered a second collision on their way towards S_2; for 77° scattering the fraction of neutrons scattered again was 67%.

The assumption that the discrepancy between observed and calculated resolution might be attributed to multiple-scattering in the first scintillator was verified by further experiments with D-T neutrons and Co^{60} γ-rays. In the experiments with D-T neutrons the calculated geometrical resolution for 56° scattering was 19.45% and the calculated statistical resolution was 4.6%, leading to a calculated total resolution of 20%, which has to be compared with the observed 29%.

The fraction of neutrons scattered on their way from S_1 to S_2 was in this case calculated to be 9.0%. It may be seen that as the amount of double-scattering in the first scintillator decreases, the ratio of observed to calculated resolution decreases.

In the experiments with the Co^{60} γ-rays, 1.17 Mev and 1.34 Mev, the fractions of γ-rays scattered again on their way towards the second scintillator were smaller: 7.0% and 6.5% respectively. There was a corresponding improvement in the agreement between

observed resolutions, 10% and 8%, and calculated resolutions 9% and 7.9%.

The calculated detection efficiencies of the apparatus for the different experiments agreed well with the values calculated from source strengths and real coincidence rates.

(vi) Response of the scintillator to protons and to electrons.

The results given in the two preceding sub-sections, with similar unquoted results were used to establish the response of the scintillator as a function of both electron and proton energy.

The energies of the neutrons and the γ-rays used in the experiments were known. Consequently, for known scattering angles, the energies of recoil protons and electrons could be calculated from equations IV.2.1 and IV.2.1a. The corresponding measured pulse heights were plotted against the calculated energies: the resulting curves have already been given in Figs.II.11.3 and 4.

(vii) Discussion of similar work.

The performances of spectrometers similar to that which has just been described have been investigated by CHAGNON et al (1953) and by DRAPER (1954). The selection of scattered neutrons was made in exactly the same manner by the geometry of the scintillators. The only significant difference in their arrangement was that faster coincidence units were used so that discrimination against γ-rays might be effected.

Chagnon et al used a coincidence unit with resolving time, $\tau = 3 \times 10^{-8}$ secs; in Draper's experiments, $\tau = 2.7 \times 10^{-8}$ secs. The discrimination was accomplished by delaying the pulses from the first counter and measuring only those pulses which were in delayed coincidence with pulses in the second counter. The distance between the primary and secondary counter, the delay time and the resolving time of the coincidence unit were adjusted so that γ-rays, with effectively zero time of flight, failed to register as coincidences whilst scattered neutrons with flight-

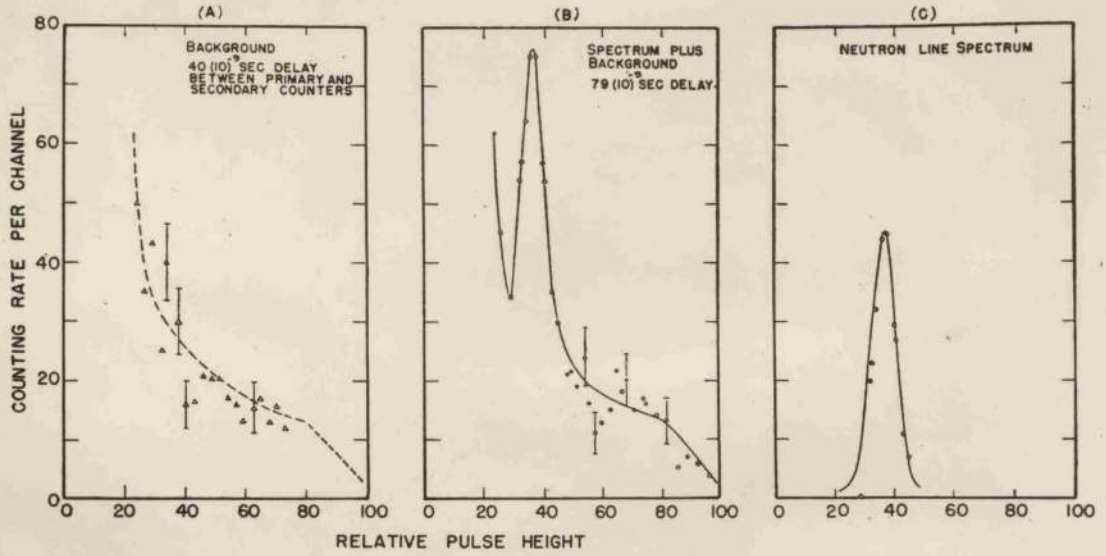

FIG. (A) Background distribution, with delay too short for true coincidences. (B) Over-all pulse-height distribution observed for the products of the D, D reaction. (The points of curve *B* are from two separate runs. (C) Subtracted points, fitted with theoretical curve.

FIG. IV.2.8. (After CHAGNON et al)

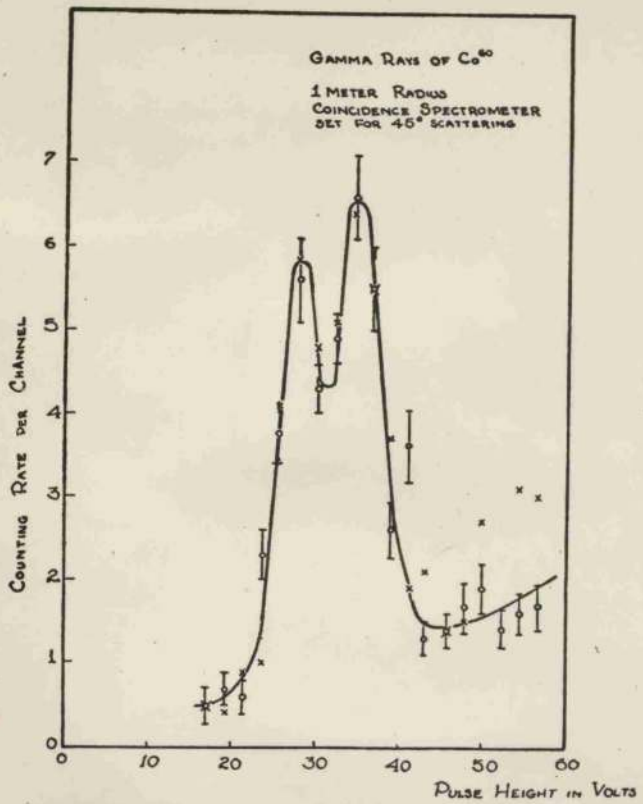

FIG. Gamma-ray spectrum of Co^{60}. (Two runs of 1 hour each.) The peaks correspond to gamma energies of 1.17 and 1.34 Mev. The delay between counters is 4×10^{-9} sec in this case.

FIG.IV.2.9.
(After CHAGNON
et al)

times in the approximate range $t - \tau/2$ to $t + \tau/2$, where t was the delay inserted, triggered the coincidence unit.

(a) Experimental Arrangements and Results: discussion.

Chagnon et al used a stilbene crystal 1 cm x 2 cm x 2 cm as the first scatterer and an annular ring, composed of 5 segments, of terphenyl in xylene. The scattering angle was 45° and the distance between the scatterers was 140 cm. The geometrical resolution (for neutrons) was given as 5.6%.

Their results when the spectrometer was exposed to the products of the D-D reaction are shown in Fig.IV.2.8. The observed resolution of the final curve, with the background subtracted, is 22%.

They calculated that this 22% was accounted for by 5.6% (geometrical) and 20% (statistical). The figure of 20% was derived from single-scattering work with the same crystal (SEGEL et al, 1954) which was discussed in Part III. In fact, this procedure ignores the multiple-scattering in the first scintillator. A figure of about 12% for the resolution due to statistical fluctuations might have been more realistic. It may again be seen that multiple-scattering in the first scintillator has a marked effect on the resolution.

Their results for Co^{60} γ-rays are shown in Fig.IV.2.9. These results are very similar to those shown in Fig.IV.2.7, the rising background in this case is due to the pulse height sensitivity of the coincidence unit.

Chagnon et al also measured the coincidence rate as a function of the delay inserted for Co^{60} γ-rays (hence establishing the resolving time of the unit) and for the products of the D-D reaction. The results of these experiments are shown in Fig.IV.2.10. Discussion of these results is given in the section describing the time-of-flight spectrometer.

Draper used two cylindrical stilbene crystals 1.9 cm long and 3.2 cm in diameter. The scattering angle was 45°; the

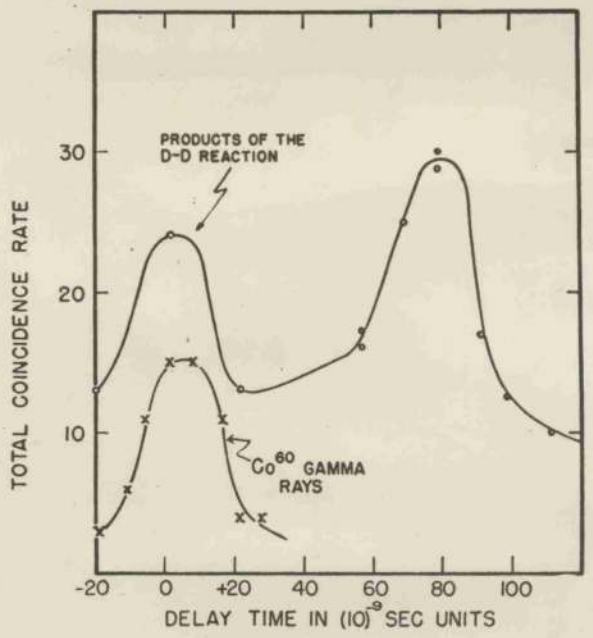

FIG. Delayed coincidence rate *versus* delay between pulses from the primary and secondary counters, for Co^{60} gamma-rays and for the products of the D, D reaction.

FIG.IV.2.10. (After CHAGNON et al)

distance from the source to the first counter was 28 cm and from the first to the second counter was 50 cm. The calculated geometrical resolution was 19%.

His results for neutrons from the D-D reaction gave an observed resolution of 28%. He noted that 70% of the neutrons scattered in the correct direction were scattered again in the first counter and he attributed the discrepancy between the observed and calculated values to this.

(viii) Conclusions.

The conclusions which can be drawn from the results of the work described in IV.2.(v) are confirmed by the results of Chagnon et al and of Draper.

The resolution obtainable with this type of spectrometer is severely limited by the inherently poor response of organic scintillators to protons. This is aggravated by scattering at an angle less than 90° since the maximum possible energy transfer to the protons is reduced. The spectrometer would not be of use for neutrons with energies less than about 7 Mev. Above this energy its usefulness would increase with increasing neutron energy.

The resolution is markedly affected by multiple-scattering in the first scintillator; (this effect is more pronounced at low neutron energies). This can be overcome by reducing the size of the first scintillator with a consequent reduction in detection efficiency. In order to achieve an overall detection efficiency of $1:10^5$ it would then be necessary to have the second scintillator in the form of a cone.

If the spectrometer is to be used when γ-rays are present then some form of discrimination must be included. If this is effected by delayed coincidences then fast scintillators must be used. An alternative method might be to use anthracene for the first scintillator (this would improve the resolution); if the scattering angle were, say, 60° then the maximum possible energy of any quantum scattered at 60° would be 1 Mev. The discriminator

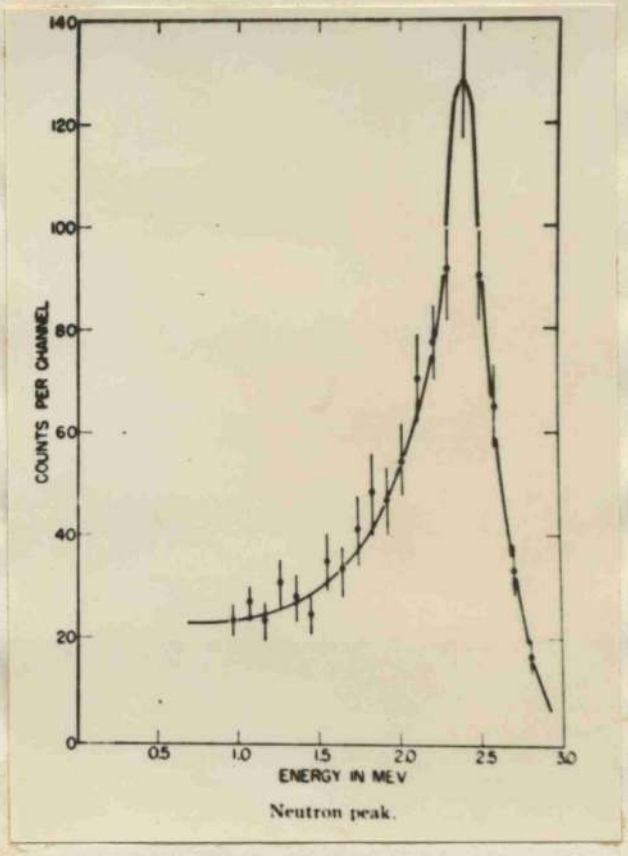

FIG.IV.3.1. (After BEGHIAN et al)

on the secondary line to the coincidence unit would then be set to accept only pulses greater than those corresponding to 1 Mev electrons. Such an arrangement would be useful only for neutrons of more than about 7 Mev and would have reduced efficiency.

If the spectrometer were improved by reducing the size of the first and increasing the size of the second scintillator and γ-ray discrimination were incorporated then it would prove extremely useful for performing many of the experiments outlined in Part I, provided the neutrons have energy greater than about 7 Mev.

3. A DOUBLE-SCATTERING PULSE HEIGHT SPECTROMETER (TIME-BAND SELECTION).

(i) Principle.

BEGHIAN, ALLEN, CALVERT and HALBAN (1952) have described a double-scattering pulse height spectrometer in which only approximately head-on recoils in the first scintillator are recorded. This is accomplished, not by arranging that S_2 subtends a small linear angle at S_1, but by having an extended second scintillator recording only those pulses in S_1 which are in delayed coincidence with S_2, where the distance between the scintillators, the time-delay inserted and the resolving time of the coincidence unit are chosen so that only slow neutrons corresponding to head-on collisions trigger the coincidence unit.

(ii) Experimental Arrangement and Results.

Beghian et al used a stilbene crystal (1.5 cm diameter x 0.5 cm) as the primary scatterer. The slow neutron detector was a NaI crystal surrounded by silver. The distance between the scintillators was 6 cm, the resolving time of the coincidence unit was 3×10^{-8} secs and the delay inserted was 3.5×10^{-8} secs. This favoured neutrons with times of flight between 2 and 5×10^{-8} secs. That is, 5 to 30 kev.

Their results when the spectrometer was exposed to the products of the D-D reaction are shown in Fig.IV.3.1. The

observed resolution is 20%.

(iii) Discussion and conclusions.

This arrangement should have resulted in good energy resolution and high detection efficiency. In practice, the time-selection employed was too severe; 5 to 30 kev in 2.5 Mev is equivalent to a resolution of 2%, whereas the limit imposed by statistical fluctuations is ~10%. Thus efficiency was sacrificed without a significant gain in resolution.

The method also suffers from the fact that the scattered neutrons have a very small mean free path and many of them are consequently completely absorbed in S_1 or scattered away from S_2. The corresponding effect of neutrons which reach S_2 after more than one collision in S_1 is shown well by the long tail at lower energies in Fig.IV.3.1. (This follows from the non-linear response of the scintillator.)

This spectrometer could be improved by reducing the dimensions of S_1 perpendicular to the incident neutrons, reducing the restrictions imposed by the time-selection and using a better slow neutron detector. Its performance would be comparable with a spectrometer of the type described in Section IV.2, and it would be useful for the same experiments particularly with neutrons of more than 10 Mev.

4. A TIME-OF-FLIGHT SPECTROMETER.

(i) General.

The fast response of scintillation counters to the passage of neutrons suggests the possibility of their application to measurements of the times-of-flight of neutrons between known points. From such measurements the energies of the neutrons may immediately be deduced.

Neutrons in the range of energies 1 to 20 Mev have velocities in the approximate range 1 to 5 x 10^9 cm/sec. At present the best

resolving time that can be obtained with coincidence units which receive signals from organic scintillators is about 3×10^{-10} secs (POST and SCHIFF, 1950, and POST, 1952). (If the scintillators used are so large that the transit times of the photons to the photocathode are comparable with the resolving time desired, or if the energy expended by the ionizing radiation in the scintillator is small, then such short resolving times can only be maintained at the expense of the efficiency of the coincidence unit.) If resolving times $\sim 3 \times 10^{-10}$ secs are used, it follows that if the times of flight of neutrons in the energy range 1 to 20 Mev are measured over distances of the order of a metre, then these times may be measured to a very high order of accuracy, $\sim 1\%$. Alternatively, if large scintillators are required and if the efficiency of the coincidence unit must be kept high then a resolving time $\sim 2 \times 10^{-9}$ secs must be accepted. In practice this is usually the case. Consequently, longer flight paths must be used, which in practice, although not in theory, leads to reduced neutron detection efficiencies; or poorer time resolution must be accepted.

The simplest paths over which neutrons may be timed are between a small source and a small scintillator and between two small scintillators. By increasing the distance between the detectors (whilst the overall detection efficiency is kept constant) the resolution of the time measurement may be reduced to negligible proportions. The resolution of the final energy measurement will then depend only on the detection efficiency required and may also be made negligible, with a corresponding loss in detection efficiency. This is in contradistinction to pulse height measurements where no arrangement, however inefficient, can obtain energy resolution better than that imposed by the statistical fluctuations in the scintillator-multiplier system.

The non-linear response of organic scintillators which is a difficulty in pulse height spectrometers has no effect in time-of-

flight methods since, provided pulses exceed a minimum size, it is their occurence and not their relative magnitude which is of interest.

The inhomogeneous distribution of recoil energies which results from a homogeneous group of neutrons is a difficulty common to all proton recoil methods. In methods employing pulse height analysis the problem appears to have only one satisfactory solution. The solution is to select a limited band of the recoil protons from the continuous distribution. The same solution may be adopted in time-of-flight methods. The most efficient arrangement would then be the annular ring geometry (Fig.IV.2.1.) used in the double-scattering pulse height spectrometer described earlier. (The neutrons selected have equal energies and equal flight paths.) The detection efficiency of this arrangement cannot be increased, as in the pulse height method, by extending the annular ring into a cone and would be insufficient for many experiments. An alternative solution, which does not involve the selection of a particular recoil energy has, however, been found. This arrangement leads to a detection efficiency which is an order of magnitude better than any of the methods which have been described earlier, whilst the resolution is essentially limited only by presently available resolving times and by the size of spectrometer which it is practicable to construct. The remainder of section IV.4 is devoted mainly to a discussion of this spectrometer and the results obtained by its use.

All time-of-flight methods automatically incorporate discrimination against γ-rays.

(ii) The principle of the method and immediate considerations.

In this method neutrons from an effective point source are scattered from one scintillator, S_1, into another, S_2. The time of flight of the neutrons from S_1 to S_2 is measured.

S_1 may be considered as having point dimensions. S_2 is

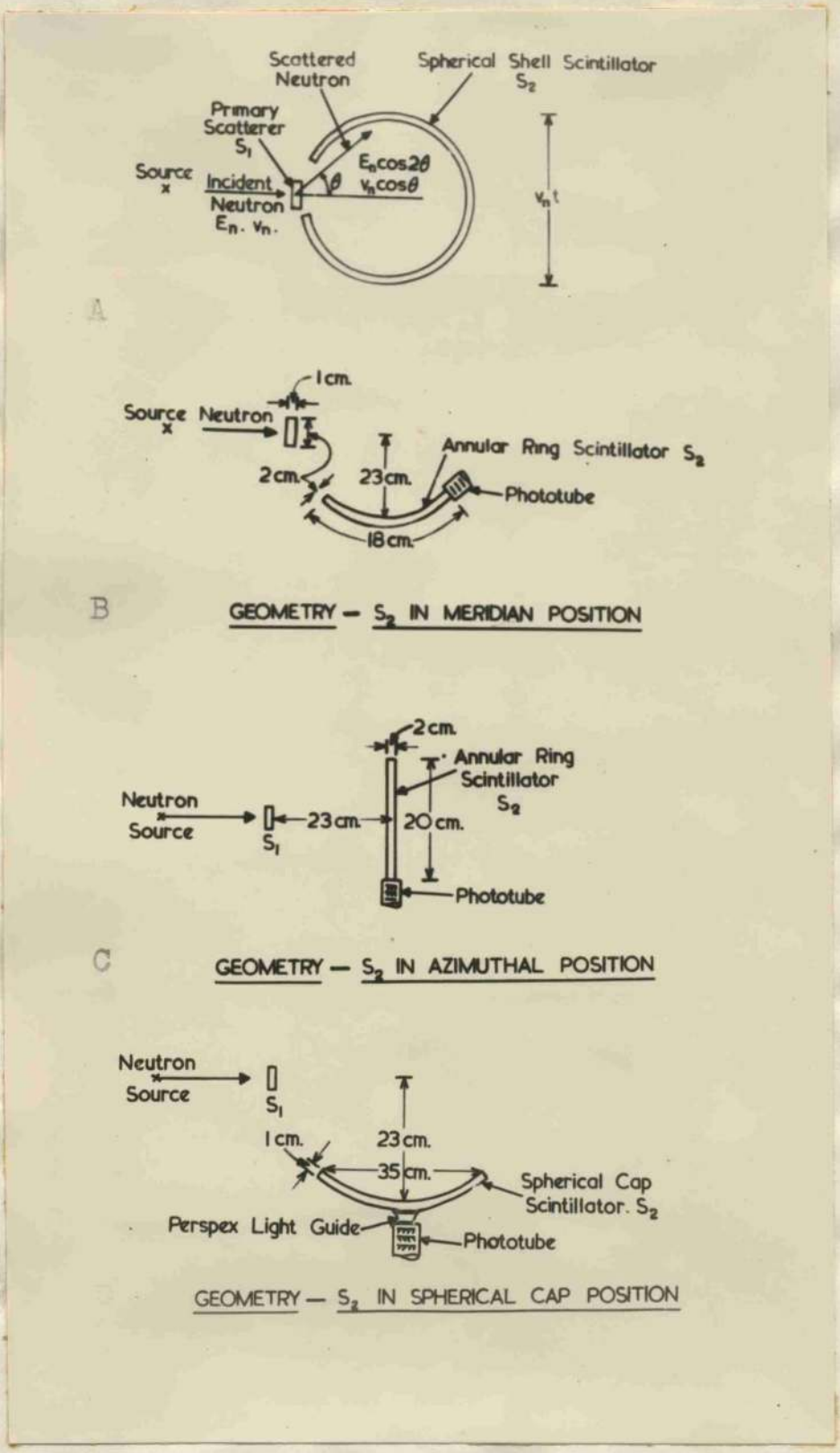

FIG.IV.4.1. GEOMETRIES FOR TIME-OF-FLIGHT SPECTROMETER.

chosen to be an extended surface such that the time of flight of all neutrons from S_1 to S_2 is the same and is independent of the angle at which the neutrons were scattered in S_1. The time of flight of the neutrons then depends only on the energy of the incident neutrons and the scale of the arrangement.

Surfaces which satisfy the conditions prescribed for S_2 are spherical shells which pass through S_1 and have a diameter which is a continuation of the line joining the source to S_1. (The situation is illustrated in Fig.IV.4.1.A.) The derivation of the form of S_2 is straightforward and is given now:

If a neutron of energy E_n, and corresponding velocity v_n, emitted by the source is scattered at an angle θ is S_1, then the energy of the scattered neutron is given by

$$E_\theta = E_n \cos^2\theta \qquad \text{IV.4.1.}$$

and its velocity is

$$v_\theta = v_n \cos\theta \qquad \text{IV.4.2.}$$

Now if the distance from S_1 to S_2 along the line of flight of the scattered neutron is S_θ, then the time taken by the neutron from S_1 to S_2 is

$$t = S_\theta / v_\theta = S_\theta / (v_n \cos\theta) \qquad \text{IV.4.3.}$$

But this has to be the same for all θ, hence

$$S_\theta = \text{constant} \times \cos\theta \qquad \text{IV.4.4.}$$

Equation IV.4.4 is the polar equation of S_2 referred to S_1 as origin, with θ measured from the axis through the source and S_1, and represents the system of spheres described above.

For a sphere, S_2, of given radius r cm, the time of flight of neutrons from S_1 to S_2 is given by

$$t = 2r/v_n \qquad \text{IV.4.5.}$$

or $$t = 1.44 \times 10^{-9} \times r \times E_n^{-\frac{1}{2}} \text{ secs.} \qquad \text{IV.4.6.}$$

The spectrometer is operated by observing the delayed coincidence rate between S_1 and S_2 as a function of an artificial time delay between S_1 and S_2. If neutrons of energy $E_{1, 2, 3, \ldots}$ are incident on S_1, then the delayed coincidence rate will have maxima at delay times $t_{1,2,3,\ldots}$ where $E_{1,2,3,}$ and $t_{1,2,3,}$ are related by equation IV.4.6.

(iii) Resolution.

In practice S_1 has finite dimensions and S_2 has finite thickness. Thus neutrons may be scattered from S_1 to S_2 in such a way that their time of flight is not given exactly by $t = 2r/v_n$. Thus, in practice, the resolution is not determined solely by r and τ (the resolving time of the coincidence unit) but also by the finite geometry of S_1 and S_2. The overall time resolution of the spectrometer is given by

$$R_t = \left[R_\tau^2 + R_G^2\right]^{\frac{1}{2}} \qquad \text{IV.4.7.}$$

where R_τ = resolution introduced by r and τ,

R_G = resolution introduced by finite geometry of S_1 and S_2.

Equation IV.2.6 relating the time of flight of scattered neutrons across the spectrometer to the energy of the incident neutrons may be written in the form

$$E_n = \text{constant} \times t^2 \qquad \text{IV.4.6a.}$$

It follows that the energy resolution of the spectrometer is given by

$$R_E = \frac{2\Delta E_n}{E_n} = 2R_t \qquad \text{IV.4.7a.}$$

(a) Resolution introduced by r and τ.

If a time t is measured with a coincidence unit of resolving time τ then, from the definition of resolving time, the accuracy of the measurement is τ/t. From equation IV.4.6 relating the flight times in the spectrometer with the radius of the sphere

and the energy of the incident neutrons, if follows that,

$$R_\tau = \tau/_t = \frac{\tau E_n^{\frac{1}{2}}}{1.44 \times 10^{-9} \times r} \qquad \text{IV.4.8.}$$

(b) Resolution introduced by finite geometry of S_1 and S_2.

If the finite geometry of S_1 and S_2 introduces a mean variation ΔT in the flight time t then

$$R_G = \Delta T/_t \qquad \text{IV.4.9.}$$

ΔT may be calculated for any given set of dimensions but the calculation is always complicated and demands numerical integration. In practice, the calculation is not worthwhile since, as will be seen later, it is only necessary to ensure that $R_G \lesssim \frac{1}{2} R_\tau$. It is reasonable to assume that, if S_1 and S_2 are extended in a regular manner, this last condition may be fulfilled by choosing the dimensions so that $\Delta t/_t \lesssim R_t$, where Δt is the maximum spread introduced by the finite geometry. $\Delta t/_t$ may readily be found in the manner shown below.

The relation between the time, t, the scattering angle θ, and the flight path, s, for a neutron with velocity, v_n, scattered from S_1 to S_2 is

$$t = s/(v_n \cos\theta) \qquad \text{IV.4.10.}$$

Provided the geometry introduces small variations in s and θ then, by partial differentiation,

$$\Delta t = \frac{\partial t}{\partial s} \Delta s + \frac{\partial t}{\partial \theta} \Delta \theta \qquad \text{IV.4.11.}$$

and hence

$$\Delta t/_t = \Delta s/_s + \Delta\theta \tan\theta \qquad \text{IV.4.12.}$$

Now, if S_1 be chosen as a cylinder of length $2d_1$, and radius, r_1, pointing axially at the source then

(A) The maximum fractional spread introduced by d_1 is

$$(\Delta t/t)_{d_1} = 2d_1 \cos\theta/s + (2d_1 \sin\theta/2r\cos\theta)\tan\theta$$

$$= d_1/r\,(1 + \tan^2\theta) \qquad \text{IV.4.13.}$$

(B) The maximum fractional spread introduced by r_1 is

$$(\Delta t/t)_{r_1} = 2r_1 \sin\theta/s + (2r_1\cos\theta/2r\cos\theta)\tan\theta$$
$$= 2(r_1/r)\tan\theta \qquad \text{IV.4.14.}$$

Similarly, the maximum fractional spread introduced by the radial thickness, r_2, of S_2 is

$$(\Delta t/t)_{r_2} = r_2/2r\cos^2\theta \qquad \text{IV.4.15.}$$

In the above approximate calculations the error introduced by the finite size of the source, radius r_o, and its distance from S_1, d_o, have been neglected. This is permissible provided $r_o \ll r_1$ and $d_o \sim r$.

(iv) Efficiency.

If N_o neutrons are emitted by the source, N_1 of these are scattered in S_1 and N_2 of those scattered in S_1 are scattered again in S_2, then the detection efficiency of the spectrometer is given by

$$\eta = N_2/N_o \qquad \text{IV.4.16.}$$

η may be evaluated in the manner shown below for the case where S_1 is a cylinder (r_1, 2d) and S_2 has radial thickness r_2, as before, and S_2 is further defined to be that portion of the spherical shell between the scattering angles θ_1 and θ_2. (For reasons which are given later, in practice, θ_1 20° and θ_2 70°.)

$$N_1 = N_o \frac{\Omega_1}{4\pi} \times \frac{2d}{\lambda_o} \qquad \text{IV.4.17.}$$

where Ω_1 = the solid angle subtended at the source by S_1
and λ_o = mean free path of the incident neutrons,
and provided $2d_1 \ll \lambda_o$.
The number of neutrons scattered out of S_1 between the angles θ and $\theta + d\theta$ and subsequently scattered in S_2 is given by

$$dN_2 = N_1 \sin 2\theta\, d\theta \times (r_2/\cos\theta)/\lambda_\theta \qquad \text{IV.4.18.}$$

where λ_θ = mean free path of scattered neutrons,
and provided θ is not $\sim 90^\circ$.

Hence $$N_2 = \int_{\theta_1}^{\theta_2} N_0 \frac{\Omega}{4\pi} \times \frac{2d}{\lambda_0} \times \sin 2\theta \times (r_2/\cos\theta)/\lambda_\theta \qquad \text{IV.4.19.}$$

In order to make a numerical estimate of η the following good approximations may be made

$$\frac{\Omega}{4\pi} = r_1^2/d_0^2$$, where d_0 = distance from source to S_1,

and $$\lambda_\theta = \lambda_0 \cos^{1.5}\theta$$

$$= 4E_0^{0.75}\cos^{1.5}\theta$$, provided θ is not $\sim 90^\circ$.

It follows that

$$\eta = \frac{r_1^2 d_1 r_2}{8E_0^{1.5} d_0^2}\left[\cos^{-1/2}\theta\right]_{\theta_1}^{\theta_2} \qquad \text{IV.4.20.}$$

(v) Choice of r, scintillator dimensions and θ_1 and θ_2: practical limitations.

The resolution and efficiency that can be attained with this spectrometer depend on τ, r, $r_{0,1,2}$, $d_{0,1,2}$, θ_1 and θ_2 in particularly simple ways.

The choice of r_0 and d_0 is not considered in detail here and it is assumed that they are chosen so as not materially to affect the resolution resulting from the choice of the other factors.

From equation IV.4.8 it follows that the best value of R_τ is attained by increasing r and decreasing τ. From equations IV.4.13, 14 and 15 it follows that the larger the value of r used, the larger are the values of $r_{1,2}$, and d_1 that may be employed whilst R_G remains less than R_τ. At the same time, as $r_{1,2}$ and d_1 are increased, η is increased. (For r, $r_{1,2}$ and d_1 fixed, it also follows if R_G is to remain less than R_τ that there is a limiting value for θ_2. However, the performance of the coincidence unit also determines θ_2, and θ_1, in another manner and this is discussed below.)

In principle, therefore, the choice is to have r, $r_{1,2}$ and d_1 large and τ small, while θ_2 is subject to certain restrictions. There are, however, practical limitations as to the extent to which the various dimensions may be increased and τ decreased. These limitations, and the practical limitations on θ_1 and θ_2 are discussed now.

(a) Multiple-scattering in S_1.

The size of S_1 is limited by the occurence of multiple-scattering. Neutrons which are scattered more than once in S_1 will not, of course, have the correct time-of-flight across the spectrometer.

(b) Manufacture of large spheres.

There are technical difficulties in the manufacture of large spheres, or portions of large spheres, of suitable reflecting or translucent materials. At the time when the experiments were performed the largest suitable surfaces that could be obtained were Pyrex faces from light floods: these were spherical caps with radius of curvature = 23 cm. This was the main limiting factor in the resolution obtained. Higher resolution could be obtained if spherical surfaces with larger radii of curvature were constructed. At the same time the detection efficiency could also be increased, if it were desired.

(c) Performance of the coincidence unit.

The resolving time of the coincidence unit also depends on the magnitude of S_2. If S_2 is sufficiently enlarged the transit time of photons in S_2 to the photocathode becomes comparable with the resolving time desired and it becomes impossible to obtain this resolving time. For r = 23 cm this effect is negligible.

Further, for a given resolving time, a minimum size of pulse is required in each counter to operate the coincidence unit. If S_2 is sufficiently large, pulses which originate far from the photocathode may be attenuated by self-absorption in the scint-

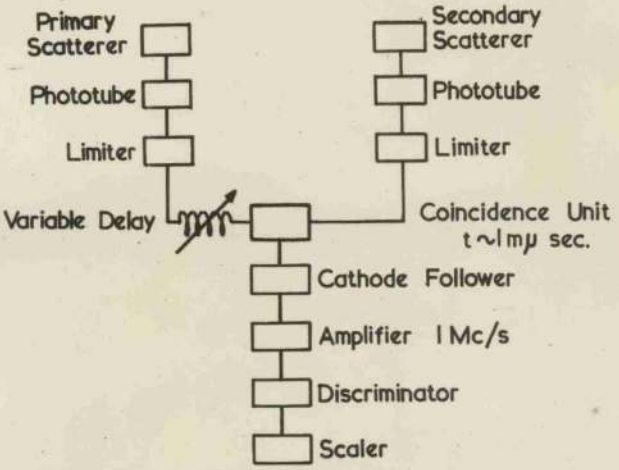

ELECTRONIC BLOCK DIAGRAM
FOR
SINGLE CHANNEL TIME ANALYSER

FIG.IV.4.2.

illator and fail to operate the coincidence unit. This effect was, in fact, appreciable with r = 23 cm but could be overcome with a more elaborate viewing system than that employed. (See Fig.IV.4.1D.)

The requirement of a minimum pulse size in each counter determines θ_1 and θ_2. For $\theta_1 \lesssim 20^\circ$ pulses in S_1 are too small to operate the unit. A similar effect occurs for $\theta_2 \gtrsim 70^\circ$ in S_2. If S_2 is constructed outside these limits no gain in efficiency is achieved. (Limitation of θ_2 in this way allows greater values of $r_{1,2}$ and d_1, for $R_G < R_\tau$, with a consequent gain in detection efficiency.)

The value of τ could be adjusted as desired. However, the efficiency of the unit fell off rapidly for $\tau \sim 2.5 \times 10^{-9}$ secs. The fall off was so rapid that, had a shorter resolving time been used, the gain in resolution would not have been worth the consequent loss in detection efficiency. This effect could be overcome with a better coincidence unit.

(d) Conclusions.

The above considerations led to the following choice of values: r = 23 cm., $\tau = 2.5 \times 10^{-9}$ secs, r_1 = 1 cm., $d_1 = \frac{1}{2}$ cm., $\theta_1 = 20^\circ$, $\theta_2 = 70^\circ$.

With these values $R_G \ll R_\tau$, except for $\theta \sim 70^\circ$ when $R_G \sim R_\tau$. To a good approximation, then, $R_t = R_\tau$. Thus as E_η increases from 1 Mev to 14 Mev, R_t increases from ~7% to ~25%, or R_E increases from ~14% to ~50%, whilst η (for the whole spherical surface between θ_1 and θ_2) falls from $\sim 6 \times 10^{-4}$ to 6×10^{-5}.

The above choice of values also leads to negligible multiple-scattering in S_1.

(vi) The electronic arrangement.

A block diagram of the electronic arrangement is shown in Fig.IV.4.2. The circuit is a modification of the one described by BELL et al (1952). The major modifications are comprised in

the cathode follower-mixing unit and in the discriminator and these are described in detail in Appendix C. The general principle of the operation of the circuit and some of the important operational details are summarised here.

Pulses from the photomultipliers are fed into the limiting valves which, in principle, produce pulses of zero rise time, constant height and slow decay. These pulses are passed along (variable) lengths of 100Ω cable to the mixing point where a shorted line converts them into square pulses whose width is determined by the length of the shorted line. The square pulses pass through a point contact diode which is a non-linear element: this favours the amplification of overlapping (coincident) pulses. The diode also lengthens the square pulses which pass through the cathode follower and can then be amplified by a 1Mc/s amplifier. Coincident pulses are then selected from single pulses by the discriminator and recorded by the scaling unit. In principle, the resolving time is determined by the length of shorted line used.

The photomultipliers were EMI Type 6262 and were operated at 2000 v in order to cut off the limiting valves as quickly as possible. The limiting valves were built into the multiplier assembly in order to improve the high frequency response. The rise times of the pulses from the limiting valves were, in practice, not zero and depended on the energy expended in the scintillator. This affected the efficiency of the coincidence unit at small resolving times. This may be seen as follows.

The shorted line cannot produce pulses shorter than the rise time of the pulse which it receives. Its effect on such a pulse is to produce an approximately triangular pulse of reduced magnitude. Thus, if the discriminator is set to allow (approximately) square coincident pulses through, slower pulses are rejected, with a consequent loss in efficiency. (Alternatively, if the discriminator level is lowered the resolving time is

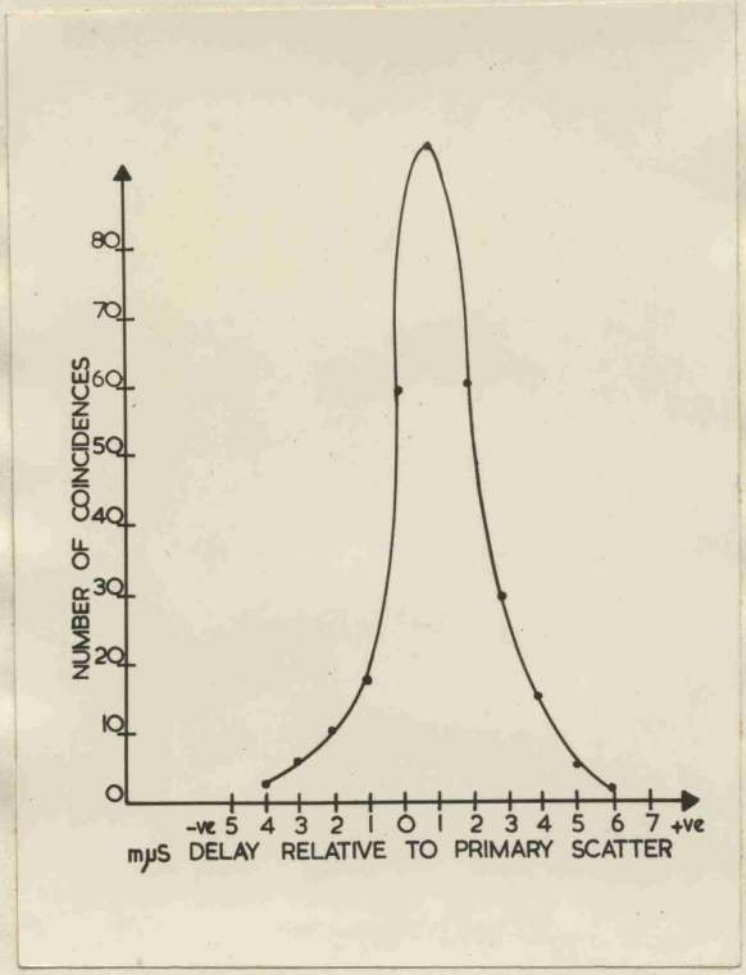

FIG.IV.4.3. RESOLUTION CURVE OBTAINED WITH Co^{60} γ-RAYS.

increased.) In practice the effect became marked only for resolving times less than 2.5×10^{-9} secs when the energy expended in each scintillator was that of an electron of about 0.5 Mev.

Coincidence resolution curves were measured by inducing prompt coincidences in both counters and observing the coincidence rate as a function of the delay time (variable length of cable) inserted in each input to the coincidence unit. Fig.IV.4.3 shows a typical resolution curve obtained in this way: the coincidences were the result of scattering Co^{60} γ-rays at 60° between two cylindrical counters (2.5 cm diameter, 5 cm long) which were 30 cm apart. It was estimated that under these conditions the unit detected 50% of the coincidences.

A multi-channel time analyser was also designed which was to enable the coincidence rates at ten different delays to be observed simultaneously. It is shown in detail in Appendix C. This arrangement not only allows results to be obtained ten times more quickly but reduces the difficulties, which are always present in millimicrosecond pulse technique, due to the fluctuations of the bias voltages at different delay settings. A fast amplifier is incorporated in this design which would enable shorter resolving times to be obtained without a loss in efficiency. That is, the resolving time would be less dependent on the energy dissipated in the counters. This analyser was successfully operated over three channels but, unfortunately, was not completed in time to be used in the neutron experiments.

(vii) Experimental Arrangements.

Experiments were performed using the three geometrical arrangements for S_2 shown in Fig.IV.1B,C and D. In the presentation of the results the situations are referred to as Arrangements B, C and D. The dimensions for each arrangement are shown on the figure.

Both the reactions investigated were induced on the

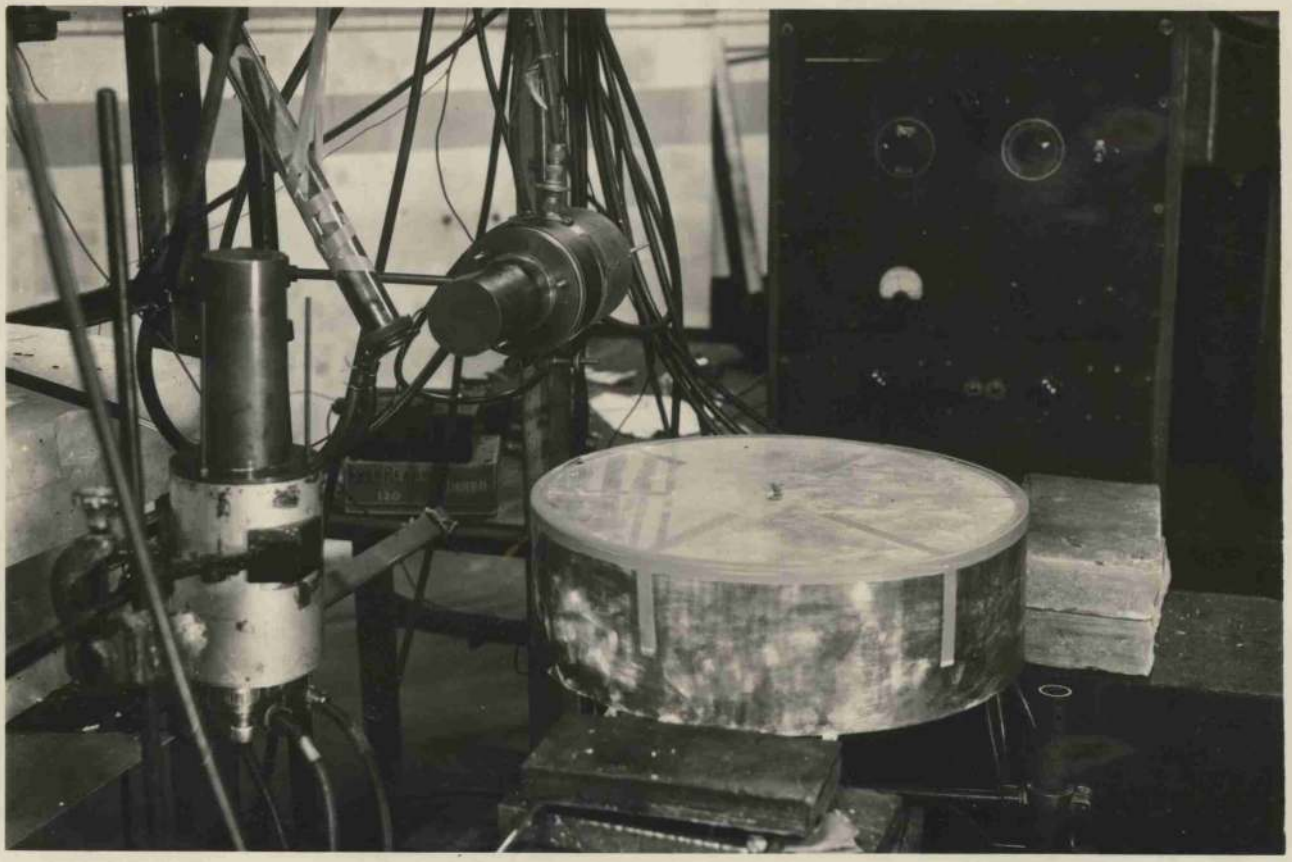

FIG.IV.4.4. TIME-OF-FLIGHT SPECTROMETER: ARRANGEMENT D.
LARGE CYLINDER CONTAINS SPHERICAL CAP.
(MONITOR COUNTER IN LEFT FOREGROUND.)

Departmental 1 Mev H.T. Set. For the reaction $T(d,n)He^4$ the deuterons had energy 350 kev and for the reaction $B^{11}(d,n)C^{12}$ the deuterons had energy 550 kev. In all the experiments the spectrometer was set to observe the neutrons emitted at 45^o to the incident neutron beam.

The neutron flux was monitored by a small liquid scintillation counter placed 100 cm from the source. The number of coincidences at a given delay was measured for a fixed number of counts on the monitor.

In Arrangements B and C, S_2 was viewed by a photomultiplier placed in contact with one end. In Arrangement D, S_2 was constructed by spacing two pyrex floodlight glasses with a strip of polished aluminium 1 cm wide. The joint was sealed with Araldite cement. A perspex light-guide was machined to fit the spherical surface (See Fig.IV.4.1D) and was placed at the centre on the convex side of S_2. A photograph of the actual situation is shown in Fig.IV.4.4: the spherical cap was enclosed in a cylindrical metal container and the space between the metal container and the cap was packed with magnesium oxide.

(viii) Experimental Results and Discussion.

(a) The reaction $T(d,n)He^4$.

The results obtained when Arrangement B was exposed to D-T neutrons are shown in Fig.IV.4.5.

The results were entirely satisfactory and showed that the spectrometer was functioning exactly as anticipated. The mean time of flight was 9.3 mμsec which was in good agreement with the time calculated from the known energy of the neutrons. The time resolution was 25% as estimated. The detection efficiency was not measured absolutely but a rough comparison of the source strength and the coincidence rates indicated that nearly all the coincidences were registered. The time taken to obtain each point on the curve was approximately four minutes.

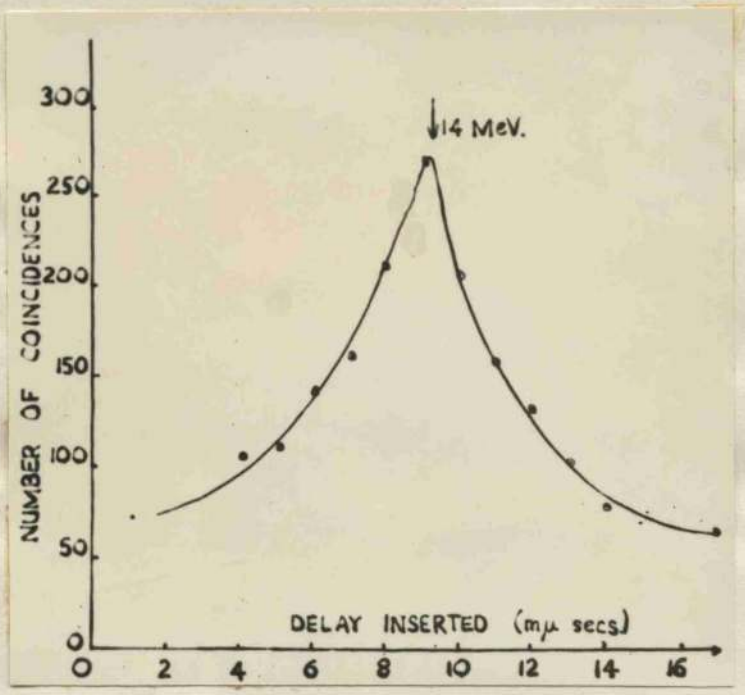

FIG.IV.4.5. NUMBER OF COINCIDENCES v DELAY INSERTED FOR D-T NEUTRONS ON ARRANGEMENT B.

Exactly similar results to Fig.IV.4.5 were obtained with Arrangement C. It was also attempted to use Arrangement C as a pulse height spectrometer by taking a linear output from S_1 and using a longer resolving time. This was unsuccessful due to (an unexplained) failure to obtain a linear output from an intermediate dynode in the primary photomultiplier. The cause of failure was probably feedback from the saturated final dynode to the intermediate dynode.

The results obtained when Arrangement D was exposed to D-T neutrons are shown in Fig.IV.4.6 (curve A). Curve C shows the distribution of random coincidences inferred from the coincidence rates at very large positive and negative delays. Curve B is the difference of curves A and C. The time of flight was again in good agreement with the calculated value and the resolution was not impaired by the increase in the size of S_2. The ratio of the detection efficiency of this arrangement to that of Arrangement B was 4, which was a factor of 3 less than anticipated. This was attributed to the poor light collection in S_2 in Arrangement D. This could be improved by using a better container for the scintillator or by viewing with either a more elaborate light-guide or more photomultipliers.

(b). <u>The reaction $B^{11}(d,n)C^{12}$</u>.

The neutrons from the reaction $B^{11}(d,n)C^{12}$ were measured with both Arrangements B and D. The results were extremely similar but better statistics were obtained using Arrangement D. The results for that case are shown in Fig.IV.4.7. Each point was observed in 4 minutes.

The results show the ability of this spectrometer to resolve the components of a complex neutron spectrum in the presence of γ-rays and with a high detection efficiency.

From the times of flight the energies of the neutrons were calculated to be 13.5, 9.3, 4.7 (not clearly resolved), 3.2 and

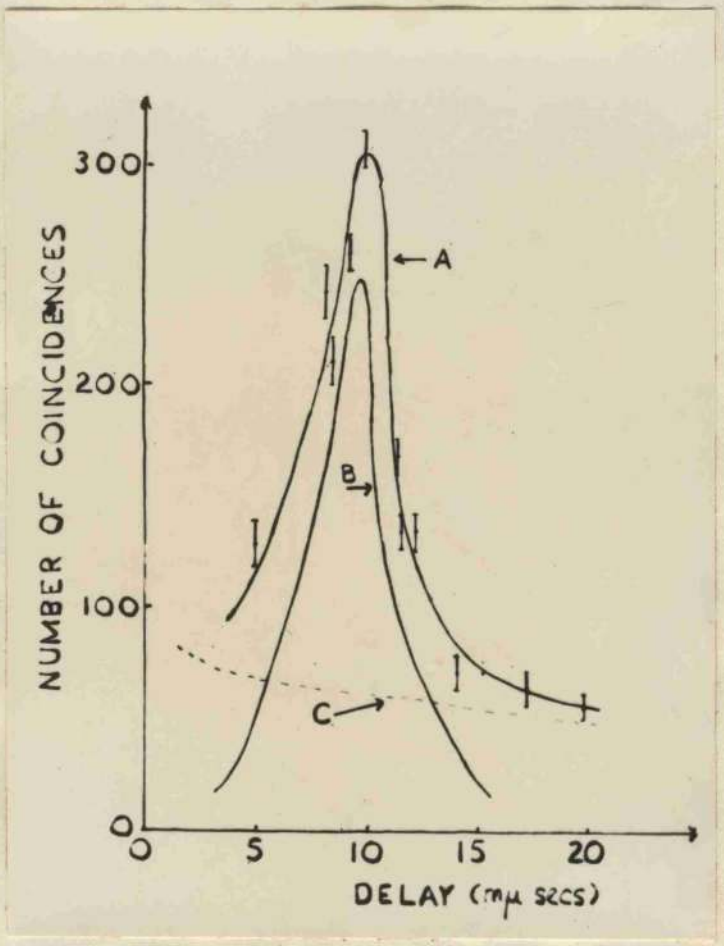

FIG.IV.4.6. NUMBER OF COINCIDENCES v DELAY INSERTED FOR D-T NEUTRONS ON ARRANGEMENT D.

A - OBSERVED DISTRIBUTION

B - DEDUCED DISTRIBUTION

C - RANDOM COINCIDENCES

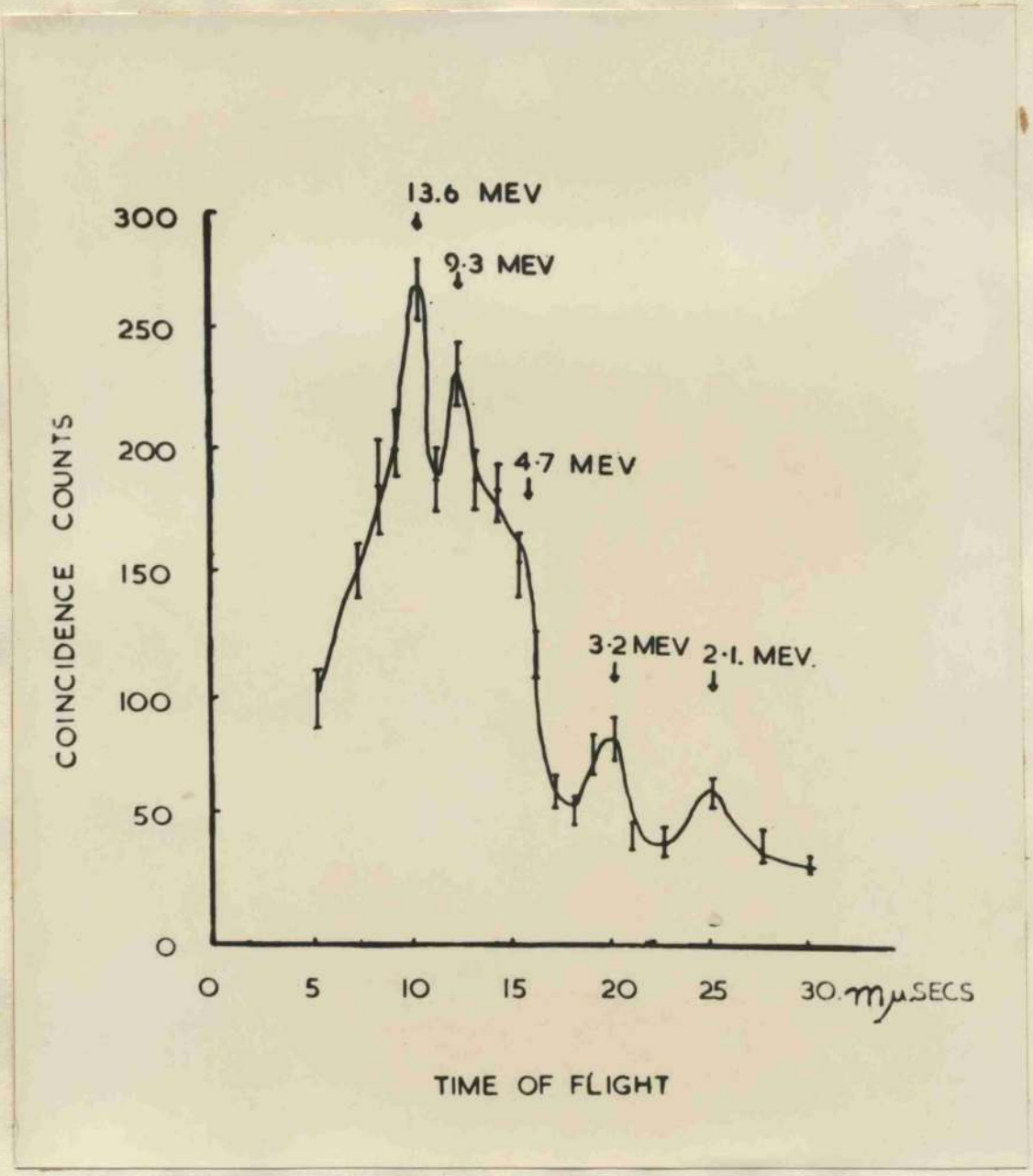

FIG.IV.4.7. NUMBER OF COINCIDENCES v TIME OF FLIGHT FOR THE PRODUCTS OF THE REACTION $B^{11}(d,n)C^{12}$ ON ARRANGEMENT D.

2.1 Mev. These correspond to the reaction proceeding to levels in C^{12} at 0, 4.4, 9.3, 10.7 and 11.9 Mev. Alternatively the group with energy 3.2 Mev could be the result of the reaction $D(d,n)He^3$ which arises from contamination of the target by deuterium. The relative intensities of the groups could not be deduced from these results due to the energy sensitivity of the coincidence unit used. This is discussed further below. The time resolution of each group is in excellent agreement with the calculated values, decreasing from 25% at 14 Mev to 10% at 2 Mev.

The energies and intensities of the neutrons emitted in the reaction $B^{11}(d,n)C^{12}$ had previously been measured, using photographic plates, by GIBSON et al (1948) and by JOHNSON (1952). The Q values, and corresponding energy levels of C^{12}, found by Johnson are shown in Fig.IV.4.8. A level of low intensity at 7.67 Mev which had been tenta tively suggested by Gibson was not found by Johnson. (An energy level diagram of C^{12} is shown in Fig.4.9.)

Comparison of the values found for the energy levels of C^{12} in the present experiments with those found by Johnson shows good agreement. It was expected that the energy sensitivity of the coincidence unit would distort the observed intensities of the neutron groups and emphasise the high energy groups. This is borne out by comparison of the relative intensities deduced from Fig.IV.4.7 with the results of Gibson. In the present experiments the 13.5 Mev group is more intense than the group at 9.3 Mev; correction for the n-p scattering cross-section would increase the ratio of these intensities whereas Gibson found that the group at 9.3 Mev was more intense than the group at 13.5 Mev. This deficiency in the present experimental arrangement is due to the coincidence unit and can be overcome by improvements in the circuitry which are known to be possible with existing techniques. Possible methods of achieving this are suggested in Appendix C.

Neutron groups from $B^{11}(d\,n)C^{12}$ (Jo 52a).

Q	C^{12}*
(13.740±0.014)[a]	0
(9.30 ±0.02)[a]	4.44
4.1 ±0.1	9.6
2.9 ±0.1	10.8
2.6 ±0.1	11.1
2.00 ±0.08	11.74
0.98 ±0.08	12.76
0.53 ±0.05[b]	13.21[b]
0.38 ±0.05[b]	13.36[b]
−0.42 ±0.05(?)	14.16(?)
−1.35 ±0.03	15.09
−1.78 ±0.03(?)	15.52(?)
−2.33 ±0.03	16.07

[a] Q values from other disintegration data.
[b] May be one level at 13.3 Mev.

FIG.IV.4.8.
(After HORNYAK et al)

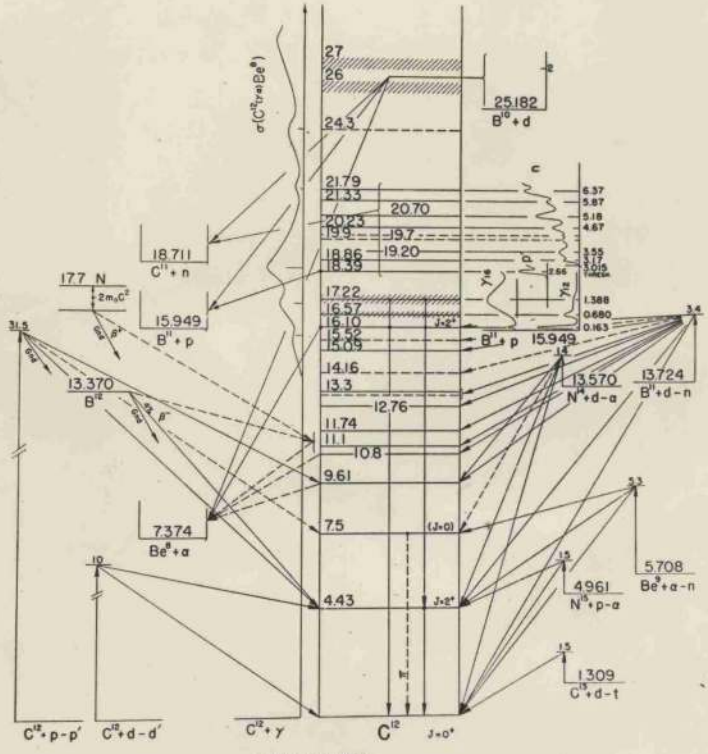

Energy levels of C^{12}:

FIG.IV.4.9.
(After HORNYAK et al)

In doing this the resolving time of the coincidence unit might also be improved, thus leading to better energy resolution.

(ix) Discussion of similar work.

No work has been published on the measurement of the time of flight of fast neutrons using the spherical geometry which was developed in the course of the present work. Only one time-measurement of neutrons scattered between two scintillators has been published: this was the work of CHAGNON et al (1953) whose results for D-D neutrons were shown earlier in Fig.IV.2.10. They used the straightforward annular-ring geometry (azimuthal position): the resolving time of their coincidence unit was a factor of ten greater than that of the unit described above; the flight path was approximately five times greater and there was a corresponding decrease in resolution. The detection efficiency of their arrangement was also correspondingly small.

JAMES and TREACY (1951) and WARD (1954) have measured the time of flight of neutrons from neutron sources to a single scintillation counter. The time origin was established by the detection near the source of γ - or α -particles known to be emitted in prompt coincidence with the neutrons. This method is evidently of limited applicability and the above authors found, as would be expected, that the detection efficiency of such an arrangement is very poor when the geometrical situation leads to good resolution.

(x) Conclusions.

The spherical spectrometer described here has been the most successful of the techniques developed during the present work on the measurement of neutron energies. Even in its present form it is capable of performing many of the experiments discussed in Part I: it has a sufficiently high detection efficiency and adequate resolution, for neutron energies up to about 7 Mev, to examine neutron spectra, angular distributions and some of the angular correlations required.

Improvement in it performance could be effected by the application of presently existing technical knowledge. The most immediate improvement necessary is to have an improved coincidence unit: reduction of τ to $\sim 10^{-9}$ secs would improve the energy resolution by a factor of about 2.5, thus extending the range of neutron energies to which it may usefully be applied. At the same time, not only would the dependence of the detection efficiency on the neutron energy (due to the coincidence unit) be removed but the absolute value of the detection efficiency would be increased. Also, both the resolution and detection efficiency would be improved by making a spherical shell of radius 50 cm. Such an increase is feasible with presently existing techniques and by using a more elaborate method of light-collection a shell of this radius could be used without appreciable losses due to self-absorption. Increases in the size of the primary scatterer, whilst they would increase the detection efficiency and not affect the time resolution introduced by the geometry, would be prohibited by the onset of multiple scattering.

If the two suggested improvements were carried out successfully then, for neutrons with energies 1 Mev and 14 Mev respectively, the resolution of the spectrometer would be $\sim 3\%$ and $\sim 10\%$ respectively, whilst the detection efficiency would be $\sim 10^{-3}$ and $\sim 10^{-4}$ respectively. These values would be more than adequate for the performance of all the experiments outlined in Part I except possibly for the examination of photoneutrons from synchrotons: in such experiments the high intensity of γ-ray background combined with the large volume of the spherical shell might lead to an unacceptable random coincidence rate.

It is of interest to note that the spherical shell geometry holds equally well for the proton recoils in the first scintillator. That is, if S_1 were made sufficiently thin for the proton recoils to be emitted from it with negligible energy loss, and if the space between S_1 and S_2 were evacuated, then the time of

flight from S_1 to S_2 of all recoils from neutrons of a given energy would be constant. This arrangement would lead to the same energy resolution and, while the detection efficiency of S_1 would be greatly reduced, the detection efficiency of S_2 could be made 100% if it were chosen a few millimetres thick. Such an arrangement would be largely insensitive to background and would be suitable for photodisintegration experiments.

Another possibility exists if it is decided to use a very thin scintillator as the primary scatterer and measure the time of flight of the recoil protons across an evacuated space. The simple relations between the energies and velocities of the protons and the angles at which they are emitted suggest that it may be possible to impose magnetic and electric fields on the protons in such a way that they have long flight paths in a small volume of space and are brought to a focus at a point or on a line. Such an arrangement would have long (easily measured) flight times and would not have the difficulties associated with a large secondary scatterer. A suitable arrangement of magnetic and electric fields has not yet been found and this problem remains an intriguing possibility for the future.

V. GENERAL CONCLUSIONS.

Some of the possibilities of applying scintillation counters to the rapid measurement of neutrons in the range of energies 1 to 20 Mev, which followed from the discovery of neutron-induced scintillations, have been realised in the work described in this thesis. It should now be possible to perform many experiments which had previously been precluded by either the low detection efficiencies or long resolving times of the available spectrometers, while other experiments, which would require extremely long times to complete if performed with earlier techniques, may now be completed in a few hours.

It has been seen that no single-counter arrangement is suitable for general application. The analysis of the distorting factors and the results for the Single Scattering Spectrometer given in Part III show that this technique can provide rough measurements of neutron energies extremely quickly and easily. In general, though, accurate determinations of intensities are precluded by the difficulties of calculation, and, if high energy γ-rays are present, this arrangement cannot be used. The work of WARD and GRANT (1955) showed that some angular distributions may be examined in this way provided the scintillator can be calibrated beforehand with neutrons of the same energy. The results obtained using this simple device are not, however, of high accuracy and their interpretation is complicated by the various distorting factors.

The Edge Effect Spectrometer described in Part III might be worth further development in the manner suggested earlier especially as it is compact and has very low γ-sensitivity. It would then be useful for work with photoneutron sources where the γ-background is very intense. (The application of the more accurate techniques would be difficult under such circumstances.) In its present form it is admirably suited to experiments where

the rapid detection, but not the energy measurement, of neutrons in an intense γ-ray background is required.

The Multiple Scattering Spectrometer constructed by SHIELDS (1954) is also best suited for detection measurements. Its inability to measure neutron energies is due primarily to the non-linear response of organic scintillators. Should any of the new (plastic) scintillators be found to have a more nearly linear response then this technique could be used satisfactorily if the changes in dimensions suggested earlier were adopted. Should a scintillator which has a completely linear response be found then this technique would be the best of the pulse height methods and would only be replaced by the Time-of-Flight Spectrometer for work on neutrons below a certain energy. That energy would be where the timing technique could achieve better resolution than that imposed by the statistical fluctuations in the scintillator-multiplier system.

With presently existing scintillators, any spectrometer which is to be capable of general application must be a double-counter device.

The Double-scattering Pulse Height Spectrometer which was described in detail in Part IV has a greater detection efficiency than the spectrometer designed by BEGHIAN et al (1952) and is to be preferred for that reason. All pulse height methods are, however, limited by the statistical fluctuations in the scintillator-multiplier system and, for accurate work, are not useful with neutrons of less than about 7 Mev.

If the changes in design suggested (smaller primary and cone-shaped secondary scintillator) were adopted, the Double-scattering Spectrometer should have adequate resolution and detection efficiency ($\sim 10^{-5}$) to measure spectra, angular distributions and angular correlations of neutrons of more than 7 Mev (γ-ray discrimination, of the type used by CHAGNON et al (1953), would be required). Its most useful field of application, however, would

be in the energy range 14 Mev to 20 Mev. Above 14 Mev the Time-of-Flight Spectrometer is unlikely, even with the improvements suggested, to have adequate resolution for many experiments. The disadvantages of the pulse height methods, on the other hand, become less serious above that energy. There are four main reasons for this.

First, although the response of liquid organic scintillators to protons of more than 14 Mev is not known, it is extremely probable from theoretical considerations and from the experimental results for anthracene, that the response tends to become linear above this energy. Secondly, the limit on resolution becomes progressively less as the neutron energy rises. Thirdly, the size of the primary scatterer may be maintained, thus retaining useful detection efficiency, with less multiple-scattering in the primary scatterer since this effect decreases with increasing neutron energy. Lastly, for neutrons in the range 14 Mev to 20 Mev, discrimination against γ-rays could be accomplished by the simple method of biassing the secondary output against the most energetic γ-rays, as suggested earlier, without great loss in detection efficiency.

In its present form, the Spherical Time-of Flight Spectrometer has proved the most successful technique for the rapid measurement of neutron energies up to 7 Mev. The energy levels found in C^{12}, whilst not new, are in good agreement with other published work and they were obtained in a very short space of time. Although other complex neutron spectra have been measured in the presence of γ-rays using scintillation counters, this is the only experiment in which the whole spectrum has been examined whilst the γ-rays have been completely eliminated. Without further improvement this spectrometer has adequate resolution and detection efficiency to measure spectra, angular distributions and correlations of neutrons up to 7 Mev.

With an improved coincidence unit and larger secondary scatterer these experiments could be performed on neutrons up to about 14 Mev. While an improved version of the Double-scattering Pulse Height Spectrometer would also be adequate for these experiments over the range 7 to 14 Mev the Time-of-Flight Spectrometer would be preferable by virtue of its much greater detection efficiency (10^{-3} to 10^{-4} over the range 1 Mev to 14 Mev).

In conclusion, it appears that by the use of the techniques developed here, or by improvements in these techniques which are known to be possible, much new data may be acquired. In particular, measurements of angular correlations, which have previously been completely outwith the scope of the available techniques, should yield much needed information about the angular momenta and parities of levels which can only be investigated by measurements on fast neutrons.

APPENDIX A. TECHNIQUES FOR THE DETECTION AND ENERGY MEASUREMENT OF FAST NEUTRONS.

1. GENERAL.

In this appendix some details of the techniques which have been used to obtain the results reviewed in Part I are discussed. Little work has been performed using scintillation counters and discussion of their use by other workers is contained in the main body of the thesis where it is compared with the present work.

The techniques considered first are best suited for flux measurements although, in principle, they can be adapted for energy measurements. They are not considered in detail as they are of much less interest than the techniques which are described next and which are designed to measure the energies as well as the intensities of neutron fluxes.

2. TECHNIQUES FOR FLUX MEASUREMENTS.

(a) Detection after moderation.

B and BF_3 counters.

The cross-sections for the interactions of slow neutrons with matter are, in general, much larger than those for fast neutrons. Advantage may be taken of this in the measurement of fast neutron fluxes by first slowing down the fast neutrons and then detecting the slowed-down neutrons by observing charged particle products of nuclear reactions which they initiate in an ionization chamber.

The most commonly used moderators are paraffin and graphite. The slow neutrons are usually allowed to interact with boron giving rise to the reaction $B^{10}(n,\alpha)Li^{7}$. The boron may be present as a gas, in the form boron trifluoride, or as a solid lining in the ionization chamber. One difficulty of the technique is obtaining a response which is independent of the original neutron energy. HANSON and McKIBBEN (1947) have described a "long counter" which has a response which is flat to within 5% for neutrons with energies up to 2 Mev. Detection efficiencies of up to about 80%

may be obtained in this way. Such arrangements are not as sensitive to γ-rays as to neutrons: however, they are not very suitable for measurements in intense γ-ray backgrounds as the pulses due to γ-rays may then overlap and give large pulses, which are indistinguishable from, and obscure the neutron-induced pulses.

Fission Chambers.

Similar chambers, surrounded by a moderator which employ U^{235} instead of boron may be used: with uranium instead of boron the detection efficiency is reduced but better discrimination against γ-rays may be obtained.

Extension to energy measurements.

The above counters, used without moderators, may be used to measure neutron energies. The reaction $B^{10}(n,\alpha)Li^{7}$ reaction has an appreciable cross-section for fast neutrons and, with knowledge of the Q value, the neutron energies may be calculated in the manner described in I.5. If a fission chamber is used then U^{238} must be used instead of U^{235}. The major difficulty arises from the facts that the cross-sections for the reactions are not smoothly varying functions of neutron energy and are inadequately known.

Conclusions.

These arrangements are suitable for the measurement of total neutron yields. They are not suitable for measuring variations in the intensity of a given neutron group, nor for use in intense γ-ray backgrounds.

Their usefulness in measuring neutron energies is limited for the reasons given above.

Full descriptions of the precautions that must be taken and the corrections that must be applied in the use of these counters have been given by ROSSI and STAUB (1949) and WILKINSON (1949).

(b) Induced-radioactivity techniques.

Certain elements, such as Ag, In and Rh, become radioactive under fast neutron bombardment. The cross-sections for the process are large, the radioactive half-lives are of the order of a few minutes and the decay leads to the emission of β^+ and β^-.

Such elements can be exposed to a fast neutron flux and the resultant activity measured using well-established techniques for counting charged particles. The method has been widely applied and has the great advantage of complete insensitivity to γ-ray background.

Extension to energy measurement: threshold detectors.

All the reactions which may be used have negative, and different, Q values. A series of elements may thus be used to establish a rough neutron energy scale in the manner described in I.5.

Conclusions.

This technique is excellent, although laborious, for measuring fluxes. There are many disadvantages in its use for energy measurements: for all the possible reactions the increase in yield above threshold is gradual so that the threshold is ill-defined; the cross-sections for the reactions are not well-known and are often sharply varying; there are not enough suitable reactions to cover the range of neutron energies 1 to 20 Mev. Suitable reactions for this technique and their application have been discussed by COHEN (1951) and by BARSCHALL, ROSEN, TASCHEK and WILLIAMS (1952).

3. TECHNIQUES FOR THE MEASUREMENT OF NEUTRON ENERGIES.

(a) Photographic Plates.

At the present time the photographic plate technique is still the most accurate method for the measurement of the energies of neutrons from effective point sources. The plates have been most

widely used as detectors of recoil protons; to a limited extent they have been used to measure the energies of the products of neutron-induced nuclear reactions. Proton detectors are discussed first.

Plates as Radiator and Detector.

Plates may be used as detectors of recoil protons from a thin hydrogeneous radiator or, since they contain hydrogen, both as a source and detector of recoil protons. The latter method is more direct but has less resolving power. In this case the plate is exposed edge-on to the neutron beam: measurement of the range - and hence the energy - and orientation with respect to the neutron beam of an individual proton track is sufficient to determine the energy of the neutron from which the proton recoiled. In practice it is usually simpler to measure only tracks at small angles ($\pm 10^{\circ}$) to the neutron beam and ignore the correction for the angle of scattering. With very weak sources it may be necessary to measure tracks at all angles in order to obtain good statistics but it is difficult to measure the orientation of very small tracks from scattering at large angles. Also, since the neutron energy is given by

$$E_n = E_p \sec^2\theta$$

where E_p is the proton energy and θ is the scattering angle, the error in the calculated neutron energy increases with θ for a given error in θ.

Plate as Detector.

By using the plate solely as a detector increased resolution may be obtained at the expense of detection efficiency. In this method the plate, which must be shielded from the neutron source, is placed in a vacuum at a distance from a small, thin radiator.

With neutron sources of high intensity a good geometry may be used in which the dimensions of the radiator are small compared

with its distance from the plate. The direction of the recoil protons is well-defined and it is only necessary to measure the lengths of the projections of the tracks on the surface of the plate. (Spurious tracks of protons which do not originate in the radiator may easily be avoided since they do not proceed in the geometrically allowed direction.) This is a great saving in time and labour which more than compensates for the increased exposure time necessary. With low intensity sources a poor geometry (large radiator) has to be used, but it is then necessary to measure the orientation in space of the recoil tracks.

Energy Resolution and Intensity Measurement.

ROSEN (1953) has reviewed very thoroughly the applications of photographic plates to the measurement of neutron spectra. A summary is given of the technical details peculiar to the processing of plates in such experiments and an evaluation is made of the optical equipment necessary. A complete bibliography of all experiments up till 1953 on neutron spectra using plates is included. Values are given for the resolution $\Delta E_n/E_n$ obtained using a plate with and without an external radiator. (ΔE_n equals the full width a half maximum height of a neutron peak of energy E_n.) For E_n = 14 Mev, $\Delta E_n/E_n$ = 2%, using an external radiator and $\Delta E_n/E_n$ = 3% using the plate alone. For neutrons with energy less than 2 Mev, intensity considerations preclude the use of an external radiator (the useful thickness of the radiator decreases with decreasing neutron energy); using the plate alone $\Delta E_n/E_n$ = 20%, for E_n = 1.5 Mev and $\Delta E_n/E_n$ = 40% for E_n = 0.4 Mev. The relative efficiencies of detection of the two methods for 14 Mev neutrons may be judged by the following figures given by Rosen. A flux of 2×10^8 neutrons per cm^2 gives 25 usable proton tracks per mm^2 in an emulsion layer 200 μ thick, if the plate is irradiated directly. If an external radiator is used in such a manner as to give comparable resolution then the flux must be increased by a factor of about 15 to give the same track density per mm^2.

Rosen also shows how to calculate the absolute intensities of the components of a neutron spectrum making allowance for the variation with energy of the neutron-proton scattering cross-section, plate shrinkage, losses by wall effects, etc. For the range of neutron energies, 2 to 14 Mev, the absolute intensities may be measured to $\pm 7\%$ using an external radiator and to $\pm 15\%$ using a plate alone. The corresponding values for the measurement of relative intensities are $\pm 5\%$ and $\pm 10\%$.

Loaded Plates.

Plates loaded with Li^6 have been used by KEEPIN and ROBERTS (1950) to measure neutron energies up to 5 Mev. Measurement of the ranges in the plate (and hence the energies) of the residual particles in each disintegration $Li^6(n,\alpha)He^3$ allows the energy of the neutron which caused the disintegration to be deduced. Keepin and Roberts have obtained ΔE_n values of the order of 0.1 Mev for E_n values up to 5 Mev. The method suffers from the disadvantage that the variation with energy of the disintegration cross-section for the reaction $Li^6(n,\alpha)He^3$ is not known very accurately. This renders measurements of the intensities of the components of neutron spectra obtained in this way unreliable. Measurements of the energies of neutrons from extended sources may also be made using this technique.

Conclusions.

Provided the time is available and source strengths are not prohibitively low photographic plates offer the most accurate method of determining neutron spectra and angular distributions. It is of interest to note that an order of magnitude calculation shows that a plate 1 cm^2 and with an emulsion layer 200 μ thick, exposed edge-on at 14 cm from a 14 Mev neutron source for 1000 hours requires a total strength of 2×10^5 neutrons per second to give 25 tracks per mm^2 in a cone of half angle 10° whose axis lies along the neutron beam. (The scanning of such a plate would

constitute several months work for one person.) Coincidence experiments are, of course, impossible using the plate technique.

(b) Cloud Chambers.

Most of the considerations of photographic plates apply equally to cloud chambers. The order of resolution obtainable is the same and the difference in the stopping power of a gas as compared with a solid is compensated for by the greater volume that may be employed.

It is usual for the cloud chamber to be used as both source and detector of recoil protons by filling it with hydrogen or methane. The chamber may also be used in this way when filled with helium: there are certain advantages to this in the measurement of very energetic neutrons. Alternatively, a thin solid radiator may be employed inside the chamber.

The technique suffers from the same disadvantages as photographic plates in that it is laborious and time-consuming and that its long resolving time (of the order of 10^{-1} second) precludes its use in coincidence work. It is no longer much used for the measurement of the energies of fast neutrons and it is frequently forgotten that most of the now classic measurements of neutrons were made in this way. Extensive references to these may be found in the well-known review article by LIVINGSTON and BETHE (1937).

One great advantage of the technique is that the reactions being studied can often be initiated in the chamber itself thus allowing a complete picture of all the products. Experiments of this type range from measurements of the recoiling He^3 nuclei in the reaction $D(d,n)He^3$ (DEE and GILBERT, 1935) to measurements of the recoiling oxygen nuclei in the inelastic scattering of 14 Mev neutrons by oxygen (CONNELL, 1953).

(c) Ionization Chambers and Proportional Counters.

Before the advent of scintillation counters, proportional chambers offered the only possibility of rapid, electronic measure -

ment of neutron energies. Such devices which depend upon the direct collection of ionized particles are intrinsically capable of better energy resolution than existing scintillator-photomultiplier combinations (BREITENBERGER, 1955; and Part II). In practice, existing proportional chamber arrangements do give better energy resolution than existing scintillation counter arrangements. Also, they do not suffer from the disadvantage of non-linearity of energy response which is characteristic of organic scintillators irradiated by heavily ionizing particles. These two advantages of the proportional chamber over the scintillation counter are, of course, not apparent when scintillators are used solely as detecting devices for timing the flight of neutrons between two successive elastic collisions. Also, satisfactory proportional chamber spectrometers for neutrons have a lower detection efficiency than existing scintillation techniques or logical developments of these techniques.

Single Scattering.

Ionization chambers (with or without gas multiplication) to be used in the measurement of neutron energies may either be filled with a hydrogeneous gas or have a solid hydrogeneous lining on one of the walls. Recoil protons are then formed either in the gaseous or the solid radiator. With either radiator, in principle, if the chamber is chosen so that neutrons which scatter in it are scattered once and once only, and if it is irradiated with monoenergetic neutrons then the pulse height distribution obtained from the recoil protons should have the shape of the ideal distribution of Fig.I.5.2. In practice the distribution obtained is dependent on several distorting factors: wall and edge effects, positive ion collection etc. By suitable design these factors may be minimised. ROSSI and STAUB (1949) have given an analysis of these distortions and have shown how the energy spectrum of the protons (and hence of the neutrons) may be deduced from the

observed pulse height distribution for several arrangements in which the counter geometry is simple enough to enable calculation to be made. Fair resolution may be obtained by such methods but the chamber pressures required in the measurement of neutron energies of a few Mev make γ-ray background a serious problem.

Collimation.

To avoid the complications of wall effects it is usually simpler to incorporate some additional device into the chamber to select recoils which are approximately head-on in direction. This reduces the apparent detection efficiency of the chamber. However, in addition to removing those recoils protons which enter or emerge from the chamber wall, such a method also avoids the inhomogeneity of the energy distribution of the recoils arising from homogeneous neutrons. Such arrangements have been described by ROSSI and STAUB (1949) and by WILKINSON (1949).

Thin Gaseous Radiator.

WORTH (1951) has used such a scheme to measure the energy spectrum of the neutrons for the reaction $Al^{27}(d,n)Si^{28}$. In his arrangement the recoils originated in the hydrogen gas filling of a proprtional counter. Those recoils which were approximately head-on passed through an aluminium absorber and were detected again in another proportional counter. The coincidence rate between the two proportional counters as a function of the aluminium absorber thickness was measured. Hence the range in aluminium of the recoils was obtained. Small corrections were made for the finite thickness of the radiator: the counter was 8 cm long and the pressure of the hydrogen filling was 30 cms Hg. The major drawback to this arrangement is the low efficiency of detection of neutrons in the first counter compatible with small loss of energy of the recoils in that counter. This reduces the number of neutrons detected to the order of 1 in 10^5 at E_n = 1 Mev and 1 in 10^6 at E_n = 10 Mev of those incident upon the radiator.

Thin Solid Radiator.

The last-mentioned drawback is common also to the more subtle, and probably more reliable, arrangement adopted by HOLT and LITHERLAND (1953) to measure the ranges of the recoil protons. They used a thin solid radiator. Approximately head-on recoils passed through two ionization chambers and stopped in a third chamber. Coincidences between the first two chambers actuated the time base of an oscilloscope. Pulses from the positive electrode of the third chamber were applied to the deflector plates of the oscilloscope. The time delay between the commencement of a sweep and the start of a pulse from the third chamber enabled the depth of penetration of a proton into the final chamber (and hence its range) to be deduced, since the start of a pulse from the third chamber corresponded to the arrival of electrons from the end of the track of the proton which triggered the time-base. The pulses were photographed and useful pulses were easily distinguished visually from spurious background pulses by their characteristic shape. From considerations of the time taken to obtain their results Holt and Litherland state that the detection efficiency of their spectrometer was such as to make it suitable for measurements of angular distributions. (The detection efficiency was of the same order of magnitude as the arrangement of Worth.) With 15.5 Mev neutrons from $Al^{27}(d,n)Si^{28}$, Holt and Litherland obtained a resolution $\Delta E_n/E_n \simeq 5\%$. The spectrometer was suitable for the measurement of neutron energies in the range 5 Mev to 25 Mev.

Thick Gaseous Radiator.

GILES (1953) has used a proprtional counter arrangement which utilises a thick gaseous radiator. A corresponding increase in detection efficiency over the last two methods described (a thick as compared with a thin radiator) was achieved. Unfortunately, for a given counter filling the range of neutron energies which could be measured was limited.

Essentially the arrangement consisted of one proportional counter, 1" in diameter and 2' long, inside another counter, 3" in diameter and 2' long. The counters were filled with hydrogen and separated by a transparent screen: this was achieved by making the 'wall' of the inner counter in the form of a cylindrical grid. The neutrons were incident along the axis of the counters. Pulses from recoils in the inner counter which were in anti-coincidence with the outer counter were recorded. For monoenergetic neutrons the pulse height distribution then observed corresponded to approximately head-on recoils and recoils through large angles, provided the range of the head-on recoils was about three times the diameter of the inner counter. With the same counter-filling neutrons of higher energy gave better resolution but the detection efficiency fell very rapidly. The useful range of neutron energies that could be measured simultaneously with a given counter filling was E_n to $2E_n$, where E_n was the minimum energy for which the counter selected head-on recoils.

With 2.6 Mev neutrons from the D-D reaction the counter was filled with 1 atmosphere of methane and Giles obtained a $\Delta E_n/E_n$ value of about 8%. The detection efficiency, defined as the ratio of the number of recoils observed in the peak to the total number of neutrons traversing the central counter, was about 4×10^{-4}. The counter was filled with Helium (shorter range recoils) to measure neutrons of higher energy (13.1 Mev and 9.1 Mev) from the reaction $B^{11}(d,n)C^{12}$. Poorer resolution was obtained.n The resolution with this arrangement at any energy could be increased indefinitely, with a corresponding loss in detection efficiency, by a suitable choice of the filling pressure. The counter was 99% insensitive to γ-ray background.

Measurement of Reaction Products.

The most successful attempt to estimate neutron energies from the measurement of the products of neutron-induced reactions in a

proportional counter has been made by BATCHELOR (1952). He has used the reaction $He^3(n,p)H^3$. The reaction is exothermic by 750 kev and is limited in its application to neutrons with energy not greater than 1 Mev; with neutrons of more than this energy confusion arises with pulses due to elastic collisions between neutrons and He^3 nuclei. The resolution obtained was 3%.

Conclusions.

The methods described in this sub-section are useful for the fairly rapid determination of neutron spectra (with $\Delta E_n/E_n \sim 5\%$) and for angular distributions. However, they all have resolving times of the order of 1 μsec. This fact, combined with their low detection efficiencies, would make the performance of coincidence experiments, if possible, extremely long if the random background rates were not to become intolerable.

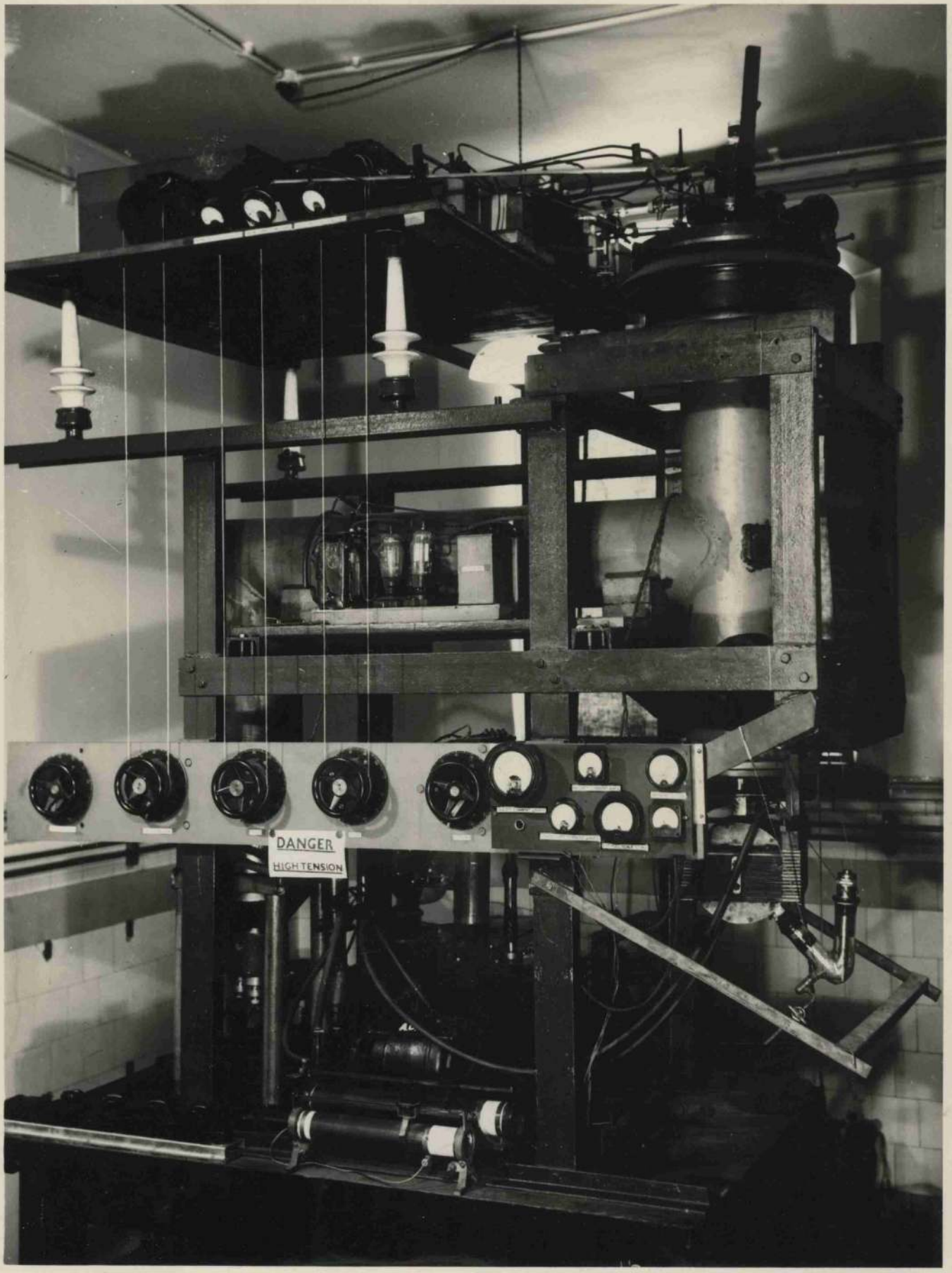

FIG.B.1. THE 50KV H.T. SET.

APPENDIX B: THE 50 KV H.T. SET.

1. GENERAL.

The bombardment of deuterium and of tritium by deuterons give high yields of monoenergetic neutrons at bombarding energies as low as 50 kev. At this bombarding energy the neutrons emitted in the forward direction in the D-D reaction have energy approximately 2.5 Mev and those from the D-T reaction have energy approximately 14 Mev. No γ-rays have been reported to occur in either reaction.

Sources of neutrons of these energies and free from γ-rays are particularly suited for testing the performance of the spectrometers described in this thesis. Also since these reactions have high yields at 50 kev, valuable running could be saved on the Departmental 1 Mev H.T. Set if they were induced on a separate small installation.

From these considerations it was decided that a rather makeshift apparatus, which had been constructed in connection with the development of a new type of radio-frequency ion-source by Dr.J.G. Rutherglen of this department, should be dismantled and re-erected in a form which was suitable and safe for inducing the above two reactions.

Accordingly, the apparatus was dismantled and the H.T. Set erected in its present form which is shown in the photograph of Fig.B.1.

The Set operates as follows:
Deuterium gas is fed into the ion-source (through a palladium-leak) where it is ionised. The ions are drawn out of the source and are then focused by anelectrostatic lens, which operates at a voltage of the order of 3 KV, into a fine beam which is led into the main high-vacuum tube where the ions are accelerated by 50 KV. Monatomic deuterium ions are then selected by passing the beam between the poles of an electromagnetic and this resolved beam strikes a target of deuterium or tritium.

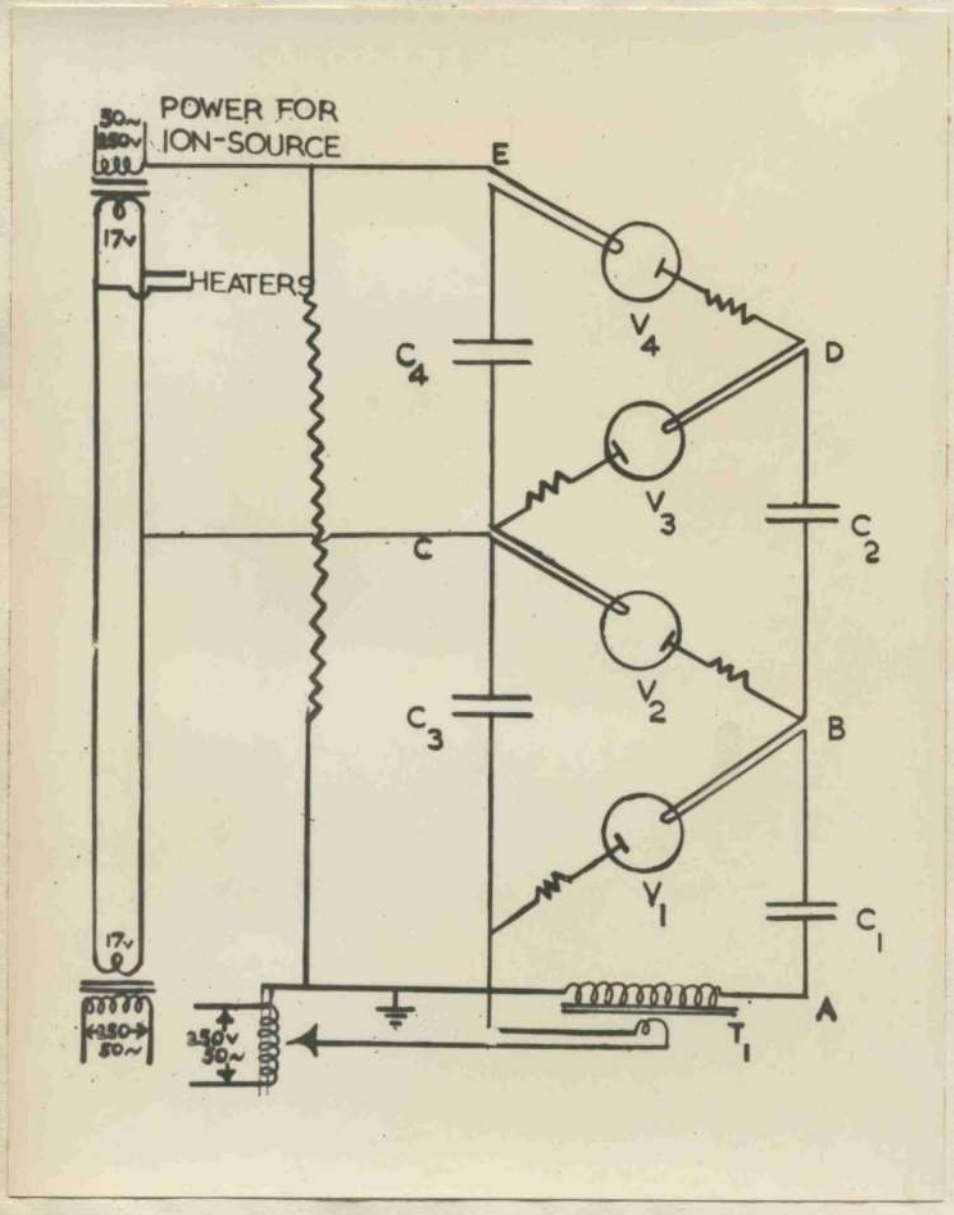

FIG. B.2 (a).
THE COCKROFT-
WALTON GENERATOR

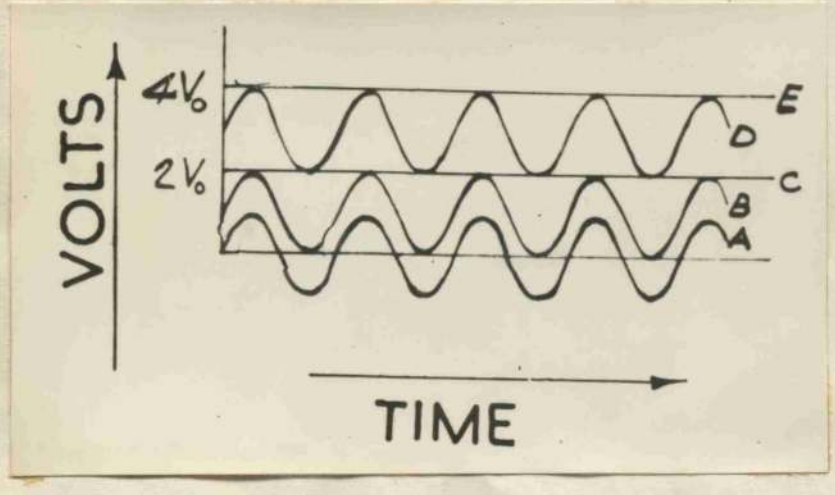

FIG. B.2 (b).
VOLTAGE WAVEFORMS.

2. THE 50 KV ELECTROSTATIC VOLTAGE GENERATOR.

The voltage generator is not visible in Fig.B.1. It is of conventional Cockcroft-Walton design consisting of a two-stage voltage-doubling circuit and was constructed mainly from ex-Admiralty equipment. The essential details of the operation of the generator may be seen from the schematic circuit diagram of Fig.B.2(a) and the voltage waveforms which are shown at various points in the circuit in Fig.B.2(b). The transformer T_1 is supplied with a controlled variable A.C. voltage from the 250 v, 50 cycles/sec. mains. This voltage may be varied by means of a variac. The secondary of T_1 develops a voltage with a peak amplitude of up to 12.5 KV. The condenser G and the rectifying valve V_1 act as a simple half-wave rectifier circuit so that C_1 becomes charged to the peak voltage of the transformer. The condenser C_3 is then charged to the peak voltage $2V_o$ reached by the point B, through the rectifier V_2. By an exactly similar process the condenser C_4 is also charged to a voltage $2V_o$, and since C_3 and C_4 are connected in series the high-potential terminal E reaches a voltage $4V_o$ with respect to ground. Thus, a voltage of 50KV is obtained with a peak voltage of 12.5 KV, from the secondary of the transformer T_1.

The voltage is measured by drawing a small leakage current through a large, known resistance-chain and an ammeter.

The filaments of the rectifier valves are heated by current from transformers whose secondaries are tied at appropriate voltages. (These are not all shown in the diagram.) Two back-to-back transformers capable of withstanding 25 KV between their windings are used to supply power for the equipment associated with the ion-source, all of which must be tied to H.T.

As stated above, the components used in the construction of this high-voltage generator were not new and considerable difficulty was experienced from time to time in eliminating sparking from the high voltage.

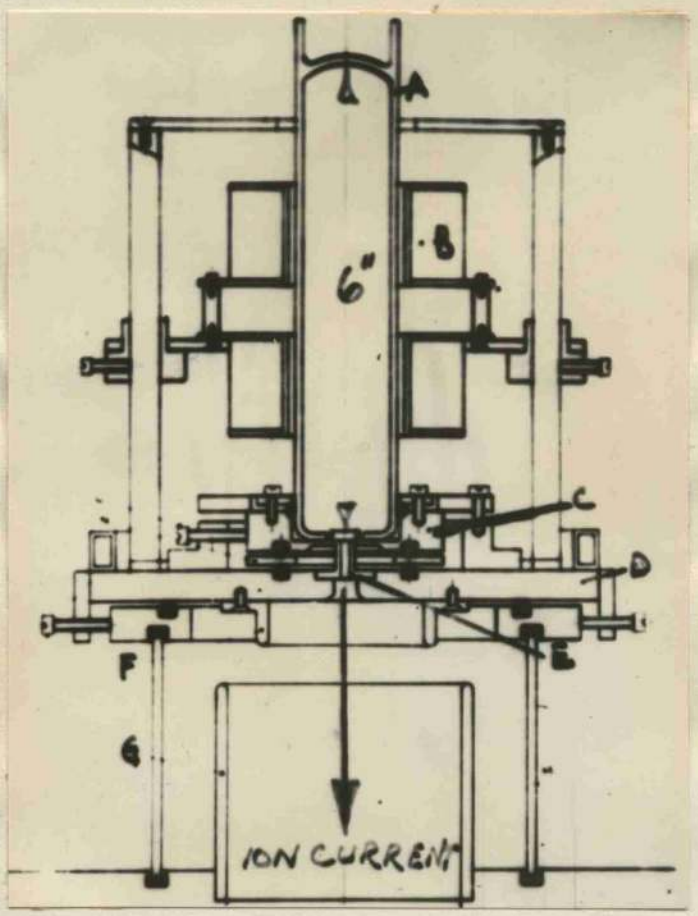

FIG.B.3. THE ION-SOURCE.

3. THE RADIO-FREQUENCY ION-SOURCE.

A schematic diagram of the ion-source is shown in Fig.B.3. No attempt will be made to follow the considerations which led to the development of the ion-source to its present (and best) form by RUTHERGLEN (1951). A brief description, however, of the ion-source and of its operation will be given.

The discharge takes place in the 6" long pyrex cylinder A. Deuterium enters through a small tube, let in through the plate D, which leads into the space between D and C. For simplicity, this tube is not shown in Fig.B.3. The system is continuously pumped through the canal E into the main vacuum system and the best operating conditions are obtained when the pressure in the ion-source is about 10 microns. A constant magnetic field of about 3000 gauss parallel to the axis of the discharge tube is provided by the Helmholtz coils B. The formers of these coils are insulated from each other and from ground and act as electrodes for the R.F. voltage which maintains the discharge. The R.F. voltage is supplied at 2000 mcs/sec. by an ex-Admiralty R.F. generator designed for pulse operation as a radar transmitter and modified to give a continuous output of about 30 watts. D.C. extraction voltages of up to 2 KV are applied between the plate C and the canal E which are insulated from each other by a rubber O-ring.

Because of the high mobility of the electrons as compared with the positive ions, when the extraction voltage is applied, the main plasma of the discharge takes up the same potential as the positive electrode and leaves a sharp 'dark space' above the negative electrode across which almost all the D.C. potential is developed. The boundary of this 'dark space' is sharply defined by the projecting lip on the plate C and is approximately hemispherical in shape. Thus, positive ions which diffuse across it from the main plasma are accelerated by the potential gradient and focused into a narrow beam which passes through the canal E.

It may be shown that almost all the ionisation produced in the discharge will be due to electrons which have gained energy from the R.F. field since the large mass of the positive ions only allows them to acquire a small amount of energy. Furthermore, the factors conducive to a high proportion of monatomic deuterons in the ion current which issues from the canal E are:

(a) A high rate of ionisation

(b) A low rate of recombination on the walls.

The purpose of the axial magnetic field is to help to maintain conditions (a) and (b). An electron which is oscillating in an R.F. field has, in general, a small drift velocity superimposed on its motion which will cause it to collide with the walls if it does not collide with a gas molecule first. If there is an axial magnetic field the component of the drift velocity perpendicular to the field will cause the electron to move in a circular path about the field. The component of velocity parallel to the field is unaffected and the electron spirals along the lines of force. This means that the electron will spend a longer time in the gas before it is lost by collision with the walls and hence a larger fraction of the R.F. power will be expended in ionising the gas relative to that expended in collisions with the wall.

4. THE HIGH VACUUM SYSTEM.

The high vacuum which must be maintained in the accelerating tube is achieved by two oil diffusion pumps (8" and 2" Metro-Vick) in series backed by a mechanical rotary pump. The absolute pressure in the main system is measured with an ionisation gauge and the backing pressure with a thermocouple gauge. Much difficulty was encountered in getting this system ($\sim$ 600 litres) vacuum-tight. However, normal pressure in the main system is now 10^{-5} mm Hg. This pressure rises to 5×10^{-5} mm Hg when the ion-source is running.

A simple high-vacuum valve was designed and incorporated in the system to facilitate the changing of targets.

5. THE RESOLVING MAGNET.

After the deuteron beam has been accelerated through the main high voltage it passes between the poles of an electro-magnet which causes a field which is a right angles to the beam and deflects it. By adjusting the magnet current the strength of the field is arranged so that only the monatomic deuterium ions strike the target. The electro-magnet which is used is one that had been constructed previously as a model for a large electro-magnet which is used in this department for β-ray spectroscopy.

Resolved currents of up to 100 μ amps have, on occasion, been obtained. This quantity is difficult to obtain regularly and the set can only be relied upon to produce about 50 μ amps constantly.

6. THE TARGETS.

(a) Deuterium target.

A layer of heavy ice deposited on a copper tube was used as a deuterium target. This was achieved in the following manner.

A small glass sphere containing heavy-water is sealed off from the main system by a vacuum tap. The tap is opened and closed immediately. Heavy-water vapour evaporates into the main system and condenses on a copper tube let into the system and cooled by liquid oxygen. This forms a heavy-ice target which lasts for about 15 minutes before evaporating under deuterium bombardment.

With 50 μ coulombs of incident deuterons this target was estimated, from measurement of counting rates in scintillation counters, to yield about 10^7 neutrons/sec. This was in good agreement with the expected yield calculated from published data on the yield of thick deuterium targets.

(b) Tritium target.

Tritium targets were obtained from Harwell in the form of tritium absorbed on a layer of zirconium backed by molybdenum.

For deuterons of 50 kev this is a thick target.

With 50 μ coulombs of incident neutrons this target was estimated to yield about 5×10^8 deuterons/sec. This figure was also in good agreement with the expected yield calculated from published data on the cross-section for the reaction $T(d,n)He^4$.

Initially, when these targets were used for extended runs, the neutron yield was found to decrease after some time. The decrease was traced to the deposition of carbon, from the oil vapour in the system, on the target which stopped the low energy deuterons from entering the target. This was cured by placing a liquid-air jacket round the beam chamber while the target itself was held at about 30° C.

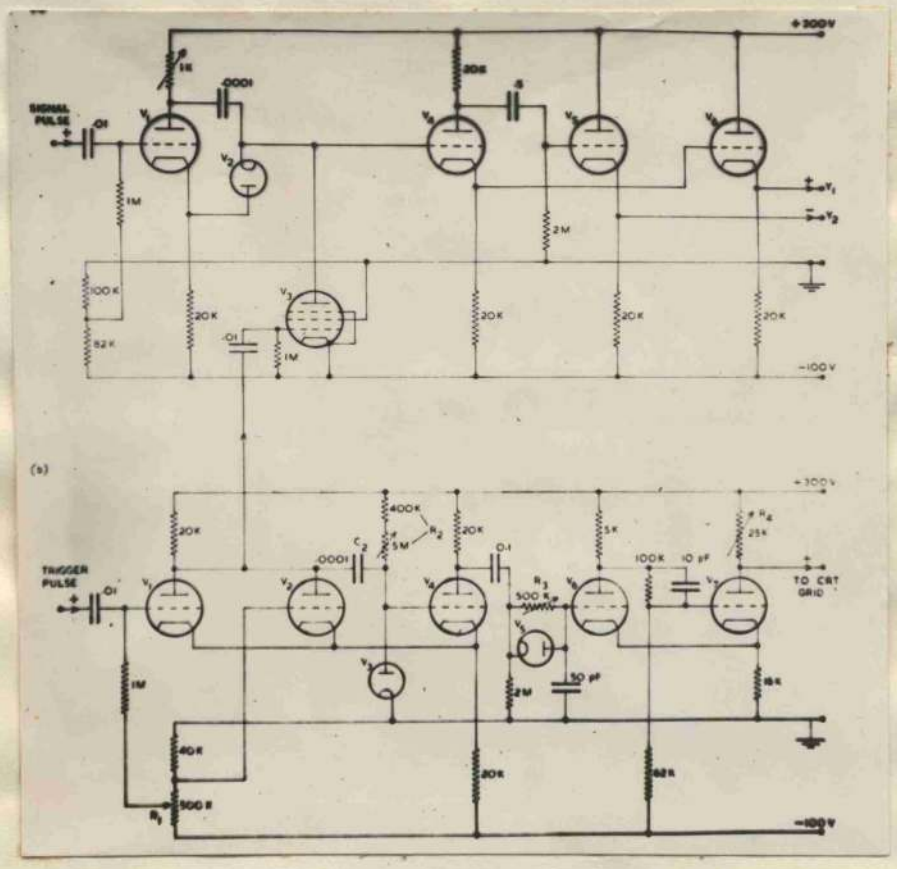

FIG.C.1.

FIG.C.2.

PULSE LENGTHENER: V_1 = EF55; V_2 = VR92; $V_{3'4'5'6}$ = EF50.

PULSE BRIGHTENER: $V_{1'2'4'6'7}$ = EF50; $V_3 + V_5$ = VR54.

APPENDIX C: SOME ELECTRONIC EQUIPMENT.

1. LENGTHENING AND BRIGHTENING CIRCUITS FOR PHOTOGRAPHIC PULSE ANALYSIS.

Some of the analyses of pulse distributions in the work described in this thesis were performed using a photographic method. The method is simple and accurate but rather laborious. It was later replaced by a single-channel electronic pulse analyser and all the later results were obtained using a 100 channel HUTCHISON and SCARROT (1951) pulse analyser.

The principle of the photographic method is straightforward. Pulses to be analysed are applied to the Y-plates of an oscilloscope while the X-plates are deflected by a slow (50 cycle) time-base. The pulses are lengthened at their maximum value whilst, during this lengthening period, the scope brightness which is normally effectively zero, is increased to a high value. The pulses then appear as small spots on the scope screen: the height of the spots above the base line being proportional to the pulse size. The spots are photographed and subsequently re-projected and analysed.

The circuits which achieve the lengthening and brightening are shown in Figs.C.1 and 2 respectively and are described below.

(a) Lengthening Circuit.

The pulse lengthening unit consists essentially of a cathode-follower input valve (V_1) and a phase-splitting valve (V_4) which provides a push-pull output via the two cathode-followers V_5 and V_6. The grid of the valve V_4 is connected to the H.T. line through the pentode V_3 which is normally just running. If now a negative pulse is applied to the grid of V_3, immediately after the arrival of a positive signal pulse on the grid of V_4, V_3 is cut off and because of the diode V_2 the grid of V_4 becomes completely isolated. The grid of V_4 remains at the maximum potential of the signal pulse just as long as the negative signal is applied to

V_3. The output pulses are, therefore, lengthened at their maximum value and the duration of the pulse is controlled by the length of the signal applied to the grid of V_3.

(b) Brightening Circuit.

In the pulse brightening unit a positive pulse of fixed height and variable length is produced by the valves V_1 to V_4. The duration of this pulse is determined by the time constant R_2C_2 and the pulse length control is provided by the 5M potentiometer making up R_2. The 400 K fixed resistor R_2 is used to safeguard the two valves V_3 and V_4. The negative lengthening signal applied to the grid of V_3 in the pulse lengthening unit is taken from the common anode load of V_1 and V_2. The output from the anode of V_4 is fed through the cathode-coupled valves V_6 and V_7 onto the grid of the C.R.O. A square positive pulse is provided with a variable delay on the front-edge provided by R_3, and variable amplitude provided by the control R_4. The delay is incorporated to ensure that the signal pulse has reached its maximum value before the brightening pulse is applied. From the above description it may be seen that the control R_2 varies the length of both the brightening and the signal pulses. The circuit is designed to cut off the brightening pulse at a fixed time interval before the back-edge of the signal pulse.

2. COINCIDENCE CIRCUIT. ($\tau \sim 10^{-7}$ SECS.)

The double-scattering pulse height spectrometer requires a coincidence unit with short resolving time. Unless time discrimination against γ-rays is desired, a resolving time $\sim 10^{-7}$ secs is sufficient to reduce the random coincidence rate, in most experiments, to negligible proportions. At the same time, such a resolving time may be obtained by careful application of conventional electronic circuitry, thus avoiding the manifold difficulties associated with units which achieve resolving times $< 10^{-8}$ secs. The circuit which was used to obtain a resolving time of

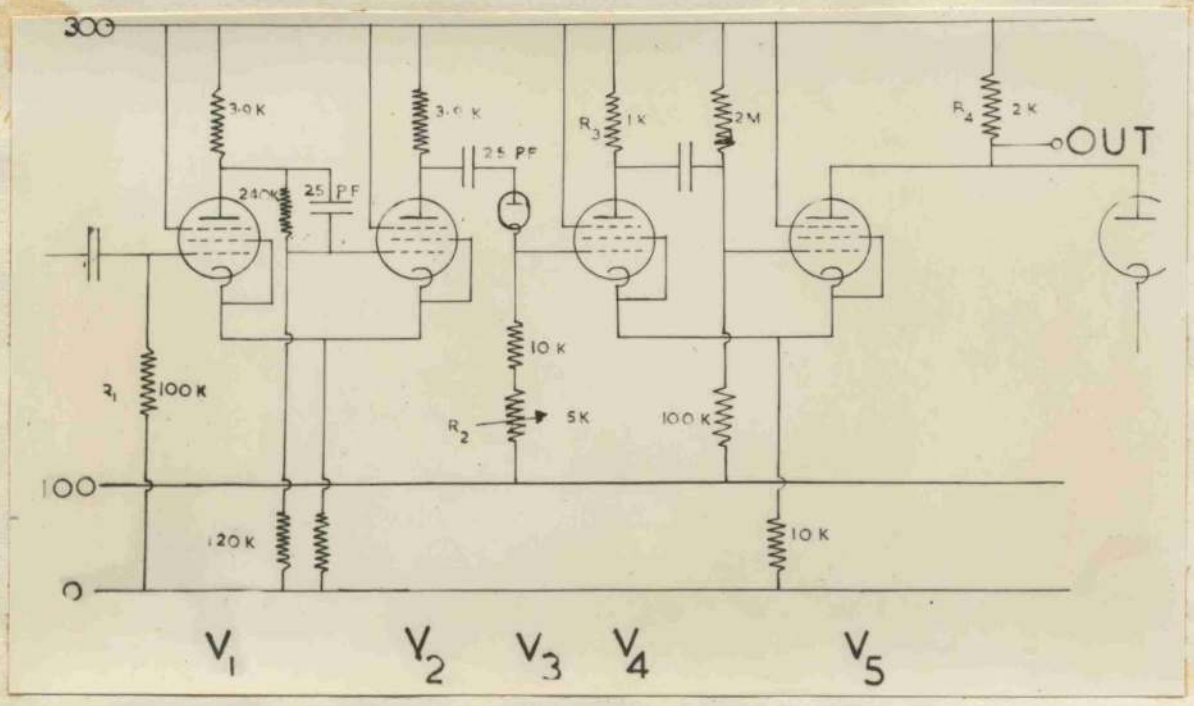

FIG.C.3. COINCIDENCE CIRCUIT ($\tau \sim 10^{-7}$ secs).

10^{-7} secs. consisted of two identical channels: a diagram of one channel is shown in Fig.C.3. Its operation is described below.

Pulses are applied to the grid of valve V_1. Valves V_1 and V_2 produce square pulses of constant amplitude but whose lengths depend on the lengths of the input pulses. These pulses are subsequently differentiated and pulses of constant amplitude and length are fed in to the grid of V_4. The length of these pulses is determined by the value given to the variable resistance R_2. V_4 and V_5 are an A.C. coupled flip-flop which produce at point A pulses of constant amplitude and length. (The length is determined by the length of the input pulse to V_4, that is, by R_2.) The arrival of two overlapping pulses at A leads to a double sized pulse at the output which may easily be distinguished from single pulses.

The resolving time of the circuit is evidently determined by the lengths of the pulses arriving at A and may be varied by means of the resistances R_2 in each channel. A resolving time not less than 10^{-7} secs was obtained in this way.

3. <u>FAST COINCIDENCE UNIT ($\tau = 2.5 \times 10^{-9}$ SECS)</u>.

The Time-of-Flight spectrometer requires a coincidence unit of the minimum possible resolving time. Various circuits have been proposed in the past few years to achieve resolving times between $\sim 10^{-8}$ and 5×10^{-8} secs, notably by BAY (1951) and by BELL et al (1952). Of these the basic design used by Bell et al seemed the most likely to give the shortest resolving time in the most straightforward manner. Accordingly an adaptation of their circuit was built and tested.

In principle, the circuit is simple in operation. The block diagram is shown earlier in Fig.IV.3.2 and a brief description is given in the accompanying text. In practice, stable resolving times of less than $\sim 5 \times 10^{-8}$ secs can only be attained with difficulty and the utmost care. The problems of this type of

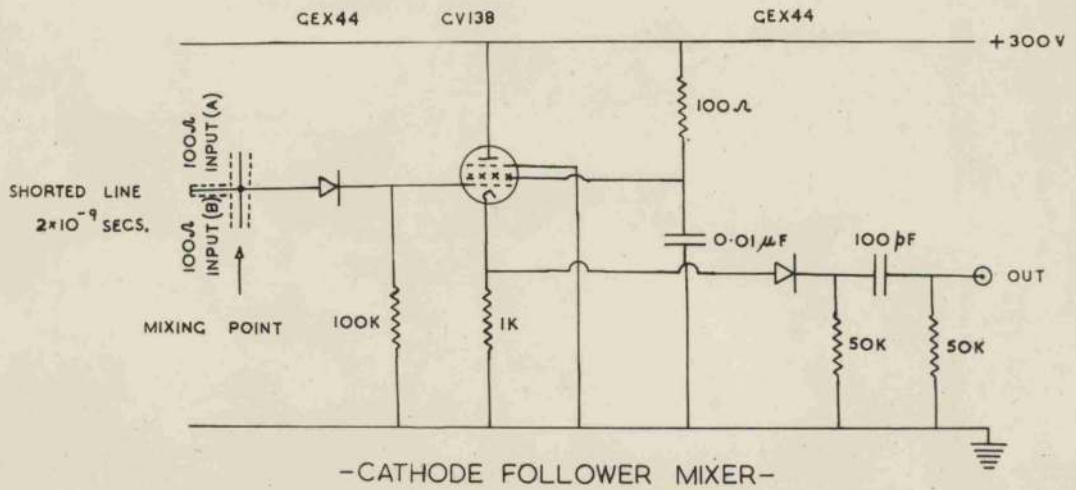

-CATHODE FOLLOWER MIXER-

FIG.C.4.

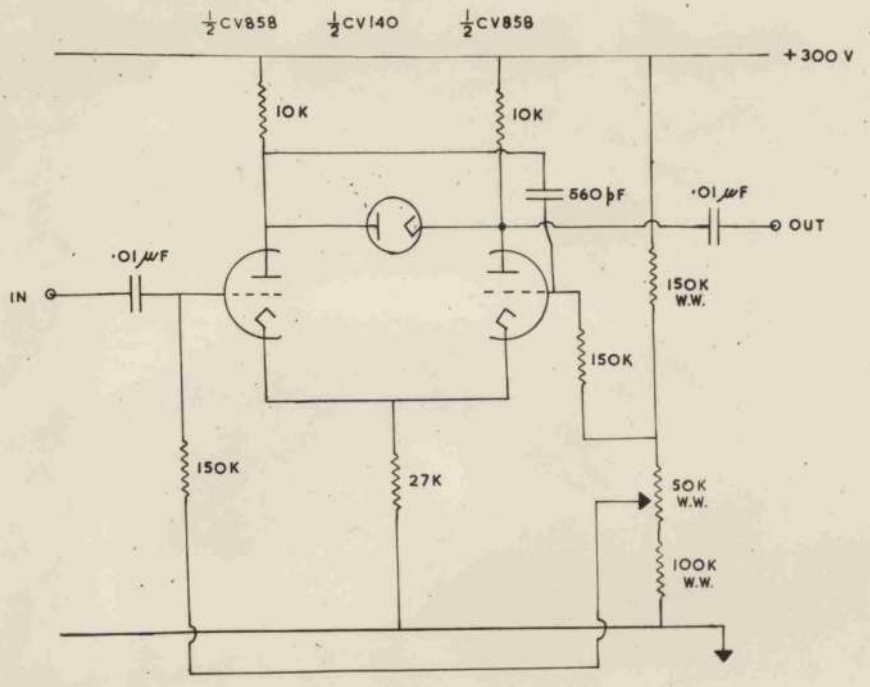

-DISCRIMINATOR-

FIG.C.5.

circuit are not treated in detail here. (A detailed discussion has been given by Bell et al.) Emphasis must be laid, however, on the basic necessity of absolute stability of all components and especially of the H.T. and heater voltages of the units before the mc/s amplifier. The resolving time (and the efficiency) at short resolving times depends essentially on the rise time of the pulses at the anode of the limiter. Slight variation in the amplification factor of this valve affects the effective rise time of these pulses seriously. It was eventually found necessary to run the heaters of the limiters from two 6v 144 ampere hr batteries in parallel largely to achieve stable short resolving times. This difficulty should be largely removed by incorporating a 100 mc/s amplifier between the photomultiplier outputs and the limiting valves. In this way all pulses from the photomultiplier should appear to the limiter to be faster than the resolving time required (1×10^{-9} secs).

Details of the cathode-follower mixer and the discriminator are shown in Figs. C.4 and 5. The discriminator is straightforward in operation and was found to be extremely stable. The cathode-follower mixer is described below.

(a) Cathode-Follower Mixer.

Pulses from the limiting valves are sent to the point A along cables of characteristic impedance 100Ω. These pulses are of equal size, effectively zero rise time and long decay time. At A the 50Ω matching cable converts these into square pulses of equal height and length.

The action of the specially selected crystal diode V_1 is twofold. Firstly, it lengthens the duration of the pulses from A to a time determined by its stray capacitance and the 100K resistor to earth. Secondly, owing to its non-linear characteristic, it effectively amplifies coincident pulses at A as compared with single pulses.

The pulses are further lengthened by the cathode follower V_2,

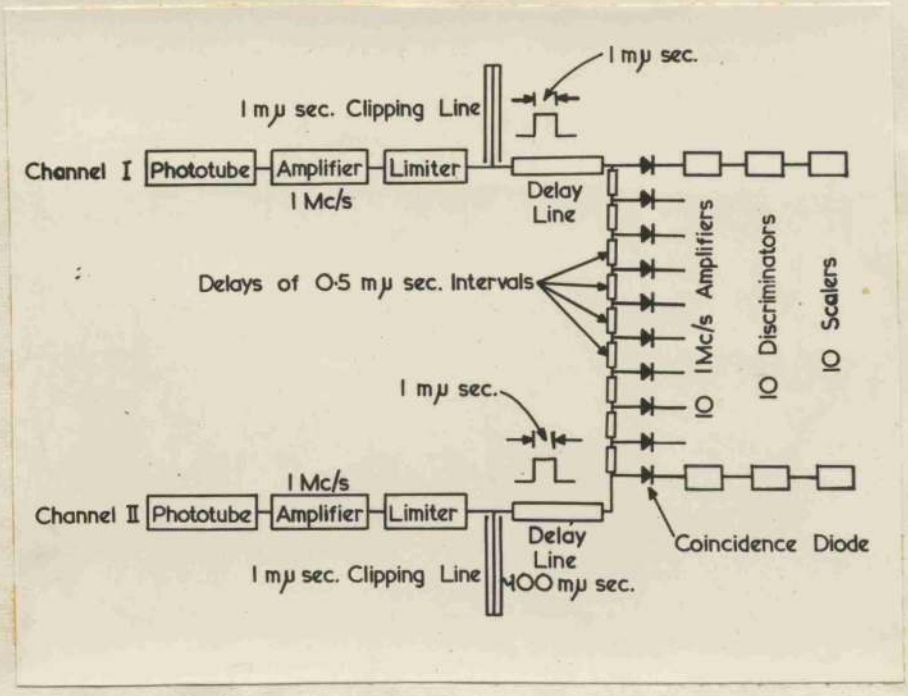

FIG.C.6. MULTICHANNEL TIME ANALYSER.

crystal V_3 and differentiating circuits so that they may be amplified by the conventional 1 Mc/s amplifier.

4. MULTICHANNEL TIME ANALYSER.

In the experiment performed with the Time-of-Flight spectrometer different delays had to be inserted in the lines from S_1 to S_2 to obtain the coincidence rate corresponding to each delay. This procedure is time wasting and may be avoided by using a time analyser which records the coincidence rates corresponding to several (in this case 10) delays simultaneously. Such a device also prevents inaccuracies which may arise from the resolving time and efficiency of the coincidence unit varying with time. The block diagram of a unit which was designed (with the assistance of Mr. J. Shields) to do this is shown in Fig.C.6. It was operated successfully (without the 100 mc/s amplifiers) over 3 channels. The operation is described below.

Effectively, the analyser consists of 10 cathode-follower mixer circuits (Fig.C.4) spaced at $\frac{1}{2}$ mμsec intervals along a delay line connecting the two limiting valves.

Pulses from each photomultiplier are fed through 100 mc/s amplifiers and limiters to separate shaping circuits. The resultant square pulses (duration 10^{-9} secs) approach the 10 mixing units from opposite directions and will record on one of the units if there is the appropriate difference between their times of origin. In this way delay times over an interval of $2 \times 10 \times \frac{1}{2} \times 10^{-9}$ sec ($= 10^{-8}$ sec) may be measured simultaneously at 1 mμsec intervals. Delay lines of the order of 100 mμsec are inserted in each channel to ensure that pulses from one channel do not return after reflection in the shorted line of the other channel in time to interfere with the original pulses.

REFERENCES.

Adair, R.K.	1950 Revs. Mod. Phys. 22, 249.
Allan, D.L.	1954 Nature, 174, 267.
Allen, R.A., Beghian, L.E. and Calvert, J.M.	1952 Proc. Phys. Soc. 65A, 295.
Amaldi, E., Bocciarelli, D., Cacciapuoti, B.N. and Trabacchi, G.C.	1947 Rep. on Int. Conf., Phys. Soc. London, Vol I, p97.
Auger, P.	1933 Comptes Rendus, 196, 170.
Baldwin, G.C. and Klaiber, G.S.	1948 Phys. Rev., 73, 1156.
Barschall, H.H., Rosen, L., Taschek, R.F. and Williams, J.H.	1952 Rev. Mod. Phys., 24, 1.
Batchelor, R.	1952 Proc. Phys. Soc., A65, 674.
Batchelor, R.	1955 Proc. Phys. Soc., A68, 452.
Bay, Z. and Cleland, M.R.	1952 Phys. Rev., 87, 901.
Beghian, L.E., Allen, R.A., Calvert, J.M. and Halban, H.	1952 Phys. Rev., 86, 1044.
Bell, P.R.	1948 Phys. Rev., 73, 1405.
Bell, R.F.	1952 Can. Jour. of Phys., 30, p35
Benford, R.	1938 J. Opt. Soc. Amer.
Birks, J.B.	1951 Proc. Phys. Soc., A64, 874.
Bohr, N.	1936 Nature, 137, 344.
Breitenberger, R.	1955 Prog. in Nuc. Phys. 4.
Butler, S.T.	1950 Phys. Rev., 80, 1095.
Chadwick, J. and Goldhaber, M.	1935 Proc. Roy. Soc., 151, 479.
Chagnon, P.R., Madansky, L. and Owen, G.E.	1953 Rev. Sci. Inst., 24, 656.
Cohen, B.L.	1951 Nucleonics, 8, No. 2, 29.
Conner, J.P.	1953 Phys. Rev. 89, 712.
Coon, J.H.	1955 Prog. in Nuc. Phys., 4,
Courant, E.D.	1948 Phys. Rev. 74, 1226.
Cross, W.G.	1951 Phys. Rev. 83, 873 (A).
Cross, W.G.	1952 Phys. Rev. 87, 223 (A).
Curran, S.C.	1953 Luminescence and the Scintillation Counter. (Butterworth)
Dee, P.I. and Gilbert.	1935 Proc. Roy. Soc., 149, 200.
Draper, J.E.	1954 Rev. Sci. Inst., 25, 558.

Feather, N.	1935 Nature, 136, 468.
Franzen, W., Pelle, R.W. and Sherr, R.	1950 Phys. Rev., 79, 742.
Frey, H.B., Grim, W.M., Preston, W.M. and Gray, T.S.	1951 Phys. Rev., 82, 372.
Fuller, E.G.	1949 Phys. Rev., 76, 576.
Fuller, E.G.	1950 Phys. Rev., 79, 303.
Garlick, G.F.J. and Wright, G.T.	1952 Proc. Phys. Soc., B65, 415.
Gibson, W.M.	1948 Proc. Phys. Soc., 60, 523.
Giles, R.	1953 Rev. Sci. Inst., 24, 986.
Graves, E.R. and Rosen, L.	1953 Phys. Rev., 89, 343.
Griffiths, G.L.	1955 Phys. Rev., 98, 579.
Hanson, A.O. and McKibben, J.L.	1947 Phys. Rev., 72, 673.
Hanson, A.O., Taschek, R.F. and Williams, J.H.	1949 Rev. Mod. Phys., 21, 635.
Harrison, F.B.	1952 Nucleonics, 10, No. 6, 40.
Harrison, F.B.	1954 Nucleonics, 12, No. 3, 24.
Harrison, F.B., Cowan, C.L. and Reines, F.	1954 Nucleonics, 12, No. 3, 44.
Hauser, W. and Feshbach, H.	1952 Phys. Rev., 87, 366.
Heitler, W.	1936 The Quantum Theory of Radiation. (O.U.P.)
Hirzel, O. and Waffler, H.	1947 Helv. Phys. Acta., 20, 373.
Hofstadter, R.	1948 Brookhaven Int. Rep., BNL-I-7.
Hofstadter, R. and McIntyre, J.	1951 Phys. Rev., 78, 242.
Holt, J.R.	1954 Proc. Glas. Nuc. Phys. Conf. p62.
Holt, J.R. and Litherland, A.E.	1954 Rev. Sci. Inst., 25, 3, 298.
Hornyak, W.F., Lauritsen, T. Morrison, P. and Fowler, W.A.	1950 Rev. Mod. Phys., 22, 291.
Huby, R.	1952 Proc. Roy. Soc., A215, 385.
Hughes, D.J. and Harvey, J.A.	1955 A.E.C. Neutron cross-sections BNL 325.
Hutchinson, G.W. and Scarrot, G.G.	1951 Phil. Mag., 42, 792.
James, D.B. and Treacy, P.B.	1951 Proc. Phys. Soc., A64, 847.
Jennings, B., Weddell, J., Alexeff, I. and Hellens, R.L.	1955 Phys. Rev., 98, 582.

Johnson, V.R.	1952 Phys. Rev., 86, 302.
Kallmann, H. and Furst, M.	1950 Phys. Rev., 79, 857.
Katz, L.	1950 Phys. Rev., 80, 1062.
Katz, L.	1951 Phys. Rev., 82, 1071.
Keepin, G.R. and Roberts, J.H.	1949 Phys. Rev., 76, 154.
Little, R.N., Long, R.W. and Mandeville, C.E.	1946 Phys. Rev., 69, 414.
Livingston, M.S. and Bethe, H.A.	1937 Rev. Mod. Phys., 9, 245.
McElhinney, J., Hanson, A.O., Becker, R.A., Duffield, R.B. and Diven, B.C.	1949 Phys. Rev., 75, 542.
McKibben, J.L.	1946 Phys. Rev., 70, 101.
Muelhause, C.O., and Thomas, G.E.	1952 Phys, Rev., 85, 926.
Muelhause, C.O. and Thomas, G.E.	1953 Nucleonics, Vol.2, 1, 44.
Oppenheimer, J.R.	1935 Phys. Rev., 47, 845.
Oppenheimer, J.R. and Phillips, M.	1935 (a) Phys. Rev., 48, 500.
Owen, G.E., Neiler, J. and Wheatley.	1951 U.S. Office of Naval Research report, Univ. of Pittsburgh, June, 1951.
Perlman, M.L. and Friedlander, G.	1948 Phys. Rev., 74, 442.
Peaslee, D.C.	1948 Phys. Rev., 47, 1001.
Philips, D.D., Davis, R.W. and Graves, E.R.	1952 Phys. Rev., 88, 600.
Poole, M.J.	1952 Phil. Mag., 43, 1060.
Poole, M.J.	1952 (a) Proc. Phys. Soc., A64, 453.
Poole, M.J.	1953 Phil. Mag., 44, 1398.
Poss, H.L.	1950 Phys. Rev., 79, 539.
Post, R.F. and Schiff, L.I.	1950 Phys. Rev., 80, 1113.
Post, R.F.	1952 Nucleonics, 10, No.6, 56.
Price, GA. and Kerst, D.W.	1950 Phys. Rev., 77, 806.
Rarita, W. and Schwinger, J.S.	1941 (a) Phys. Rev., 59, 556.
Rarita, W., Schwinger, J.S. and Nye, H.A.	1941 (b) Phys. Rev., 59, 209.
Redmund, A.E. and Ricamo, R.	1952 Helv. Phys. Acta., 25, 447.
Roberts, J.H.	1947 Phys. Rev., 72, 76.
Rosen, L.	1953 Nucleonics, 11, No.7, 32 and No.8, 38.

Rossi, B.B. and Staub, H.	1949	Ionization Chambers and Counters (McGraw Hill).
Russell, B., Sachs, D., Wattenberg, A. and Fields, R.	1948	Phys. Rev., 73, 545.
Rutherglen, J.G.	1951	Ph.D. Thesis, Univ. of Glas.
Segel, R.E., Swartz, C.D. and Owen, G.E.	1954	Rev. Sci. Inst., 25, 140.
Serber, R.	1947	Phys. Rev., 72, 1008.
Shields, J.	1953	Private communication.
Shields, J.	1954	Private communication.
Stelson, P.H. and Preston, W.M.	1952	Phys. Rev., 86, 132.
Strauch, K.	1951	Phys. Rev., 81, 973.
Swank, R.K. and Buck, W.L.	1953	Phys. Rev., 91, 927.
Swank, R.K. and Buck, W.L.	1955	Rev. Sci. Inst., 26, 15.
Taylor, C.J., Jentschke, W.K., Remley, M.E., Eby, F.S. and Kruger, P.G.	1951	Phys. Rev., 84, 1034.
Walker, R.L., McDaniel, B.D. and Stearns, M.B.	1950	Phys. Rev., 79, 242.
Walt, M. and Barschall, H.H.	1954	Phys. Rev., 93, 1062.
Ward, A.	1954	Nature, 173, 771.
Ward, A. and Grant, P.J.	1955	Proc. Phys. Soc., A68, 637.
Whitehead, W.D. and Snowdon, S.C.	1953	Phys. Rev., 92, 114.
Whitehead, W.D. and Snowdon, S.C.	1954	Phys. Rev., 94, 1267.
Wilkinson, D.H.	1949	Ionization Chambers and Counters (C.U.P.).
Wilkinson, D.H.	1954	Proc. Glas. Nuc. Phys. Conf., p161.
Worth, D.	1949	Phys. Rev., 75, 903.
Worth, D.	1950	Phys. Rev., 78, 378.